CENTRO DE INVESTIGACIÓN Y DE ESTUDIOS AVANZADOS DEL INSTITUTO POLITÉCNICO NACIONAL

UNIDAD ZACATENCO

DEPARTAMENTO DE BIOTECNOLOGÍA Y BIOINGENIERÍA

Modelado, simulación y control de un bioproceso de lixiviación usando una bacteria quimiolitoautótrofa acidofílica del orden *β-proteobacteria*

Tesis que presenta

Juan Carlos Figueroa Estrada

Para obtener el grado de

DOCTOR EN CIENCIAS

EN LA ESPECIALIDAD DE BIOTECNOLOGÍA

Directores de la Tesis: Dr. Ricardo Aguilar López / Dra. María Isabel Neria González

México, CDMX. Septiembre del 2022

AGRADECIMIENTOS

HAGO EXTENSIVO MI AGRADECIMIENTO AL CONSEJO NACIONAL DE CIENCIA Y TECNOLOGÍA (**CONACYT**), POR HABERME OTORGADO LA BECA CON NÚMERO 230859 PARA LA REALIZACIÓN DE ESTÁ INVESTIGACIÓN.

AGRADEZCO AL CENTRO DE INVESTIGACIÓN Y DE ESTUDIOS AVANZADOS DEL INSTITUTO POLITÉCNICO NACIONAL (**CINVESTAV**) POR PROPORCIONARME RECURSOS Y FACILITARME CURSOS E INSTALACIONES PARA REALIZAR LA INVESTIGACIÓN DE ESTE PROYECTO.

AGRADEZCO AL TECNOLÓGICO DE ESTUDIOS SUPERIORES DE ECATEPEC (**TESE**), POR EL AOPOYO QUE ME PROPORCIONÓ PARA LA ETAPA EXPERIMENTAL DE ESTE PROYECTO.

AGRADEZCO A MIS DIRECTORES DE TESIS, LA **DRA. MARIA ISABEL NERIA GONZALEZ Y EL DR. RICARDO AGUILAR LÓPEZ** POR EL APOYO, TIEMPO Y PACIENCIA PARA MI FORMACIÓN DESDE MIS ESTUDIOS DE POSGRADO EN MAESTRÍA. LOS DOS APORTARON A MI CRECIMIENTO ACADÉMICO Y PERSONAL, POR LO QUE LES DEBO MUCHO DE LO QUE SOY AHORA.

AGRADEZCO A MIS PADRES **ROSA ESTRADA PREZA Y JORGE FIGUEROA LUGO** POR SIEMPRE APOYARME Y REGALARME SU ESFUERZO Y CUIDADO. POR ESTAR SIEMPRE PARA MI INCONDICIONALMENTE Y ALENTARME A SUPERARME Y SER MEJOR. POR SIEMPRE DARME SU COMPRENSIÓN Y AMOR.

GRACIAS A DIOS POR DEMOSTRARME ESTAR PRESENTE EN MI VIDA.

AGRADEZCO A MI ESPOSA **JUANA LIRA PÉREZ**, POR SER LA MEJOR COMPAÑERA DE VIDA. POR BRINDARME FELICIDAD, APOYO Y AMOR. SIN SU COMPAÑÍA NINGUNA META LOGRADA SERÍA LO MISMO.

GRACIAS AL RESTO DE PERSONAS QUE DIRECTA O INDIRECTAMENTE HAN APORTADO A LA REALIZACIÓN DE ESTE TRABAJO DE TESIS.

Contenido

Índice de Tablas

Índice de Figuras

Resumen

En este trabajo se estudiaron tres sistemas de lixiviación de metales. En el primero se caracterizó una bacteria quimiolitoautotrófa (LR-1) y se estudió su capacidad para lixiviar metales a partir de minerales. Además, se estudió la capacidad de biolixiviación de 6 metales con 5 minerales diferentes en un medio acido. Los resultados se compararon con un experimento control sin el uso de la cepa LR1 y se obtuvieron en todos los casos mayores porcentajes de metales lixiviados. En el segundo sistema se propone un modelo cinético de los datos experimentales reportados en un trabajo previo (Biagiola et al., 2000). Además, se diseña una ley de control de tipo “Super-twisting sliding mode” (STSM), aplicada al sistema no lineal para fines de regulación de lixiviación de hierro. Se comparo su rendimiento con un control STSM estándar y los experimentos numéricos mostraron desempeño satisfactorio a lazo cerrado. El tercer sistema, se centra en el análisis de circuito abierto y circuito cerrado de la operación de un reactor de tanque agitado continuo para la lixiviación de zinc a partir de esfalerita (ZnS) a través del enfoque de modelado y simulación. Se realizo un análisis del proceso correspondiente con un enfoque de múltiples entradas y múltiples salidas (MIMO), un análisis de la matriz de ganancia relativa (RGA) para determinar los mejores pares de entrada de control y un análisis de bifurcación. Finalmente, se propone una ley de control STSM, para regular el oxígeno disuelto y el pH, lo que conduce a aumentar la lixiviación de esfalerita, su rendimiento se comparó con un controlador estándar STSM. Los experimentos numéricos muestran el rendimiento satisfactorio del controlador propuesto en las condiciones de operación seleccionadas.

Abstract

In this work, three metal leaching systems were studied. In the first one, a chemilitoautotrophic bacterium (LR-1) was characterized and its ability to leach metals from minerals was studied. In addition, the bioleaching capacity of 6 metals with 5 different minerals in an acid medium was studied. The results were compared with a control experiment without the use of strain LR-1 and higher percentages of leached metals were obtained in all cases. In the second system, a kinetic model of the experimental data reported in a previous work is proposed (Biagiola et al., 2000). In addition, a “Super-twisting sliding mode” (STSM) type control law is designed, applied to the nonlinear system for iron leaching regulation purposes. Their performance was compared with a standard STSM control and the numerical experiments showed satisfactory closed loop performance. The third system focuses on the open circuit and closed circuit analysis of the operation of a continuous stirred tank reactor for leaching zinc from sphalerite (ZnS) through the modeling and simulation approach. A corresponding process analysis was performed with a multi-input and multi-output (MIMO) approach, a relative gain matrix (RGA) analysis to determine the best control input pairs and a bifurcation analysis. Finally, an STSM control law is proposed, to regulate dissolved oxygen and pH, which leads to increased sphalerite leaching, its performance was compared with a standard STSM controller. The numerical experiments show the satisfactory performance of the proposed controller under the selected operating conditions.

1. Introducción

La tendencia global hacia la urbanización y la industrialización está respaldada por la creciente demanda de metales industriales. Además, las reservas mundiales de minerales de alta ley están cerca de agotarse (Anjum et al., 2012; Mahmoud et al., 2017). Los problemas relacionados con la disminución de minerales de alta ley, combinados con la contaminación ambiental, han llevado al proceso de minería convencional a implementar enfoques de biolixiviación (Gilligan & Nikoloski, 2015; Jalali et al., 2019). La biolixiviación se usa normalmente en la extracción de metales, donde los metales se solubilizan por acción microbiana y posteriormente se recuperan de la solución (Gumulya et al., 2018). En otras palabras, la biolixiviación es la solubilización oxidativa del mineral que contiene azufre y es mediada por la acción de microorganismos (Gentina & Acevedo, 2016).

La lixiviación se aplica mediante dos procesos de ingeniería. El primero es en reactores de descarga o pila, donde se riega mineral o concentrado. El segundo sucede en reactores de tanque agitado, donde el mineral es finamente molido y tratado como una suspensión agitada y aireada. Los reactores se utilizan principalmente para la recuperación de oro a través de biooxidación y para cobalto. El cobre, níquel y zinc se extraen en grandes operaciones de biolixiviación de pilas (Kutschke et al., 2015). El campo de la bioingeniería permite analizar y desarrollar sistemas que contienen catalizadores biológicos, para ser explotados en el desarrollo de tecnologías y la mejora de bioprocesos. Usualmente, los modelos cinéticos en donde intervienen sistemas biológicos suelen tener comportamientos no lineales, en algunos casos se

pueden presentar bifurcaciones y oscilaciones que conducen a comportamientos dinámicos interesantes. En los cuales es posible implementar teorías de control, las que a su vez permiten aplicar alguna estrategia para mejorar cierta respuesta del sistema o bioproceso.

Por ello, en este trabajo se propone el estudio de tres sistemas enfocados a la lixiviación de metales. En el primero se caracterizó una bacteria quimiolitoautotrófa (LR-1) y se estudió su metabolismo quimiolitoatótrofo. También se estudió la capacidad de biolixiviación de 6 metales (Ag, Cr, Cu, Fe, Pb y Zn) con 5 minerales de diferentes minas de México (Remedios, Guerrero, Bolañitos, Aldama y Ocampo). En todos los casos se obtuvieron mayores porcentajes de metales lixiviados cuando se compararon con ensayos control. En el segundo y tercer sistema, se realizaron experimentos numéricos por medio se simulaciones a computadora, estos se centran en el análisis a circuito abierto de la operación de un reactor continuo de tanque agitado para la lixiviación de hierro y zinc, de los cuales se utilizaron datos experimentales y modelos reportados previamente (Biagiola et al., 2000; Haakana et al., 2007). Se obtuvieron los datos correspondientes de los estados estacionarios y asimismo la estabilidad de los estados estacionarios se determinó por medio del cálculo de los valores propios correspondientes. En ambos casos, los resultados proporcionaron datos sobre las regiones de operación en las que se favorece la lixiviación de ambos metales. Para el caso de lixiviación de zinc, se realizó un análisis del proceso con un enfoque de múltiples entradas y múltiples salidas, por medio de la matriz de ganancia relativa y se determinaron los mejores pares de entrada-salida para utilizar enfoques de control. Finalmente, para ambos casos se proponen leyes de control “Super-twisting

sliding mode" (STSM), las cuales conducen a aumentar la lixiviación de hierro y zinc. Los rendimientos a lazo cerrado se compararon con un controlador estándar STSM. Finalmente, los resultados mostraron rendimientos satisfactorios de los controladores propuestos en las condiciones de operación seleccionadas.

1.1. Bacterias quimiolitoautótrofas y biolixiviación

La biolixiviación ocurre como un proceso natural en los minerales sulfurados los cuales también contienen hierro. Además, el dióxido de carbono y el oxígeno son nutrientes esenciales que los microorganismos usan para crecer. Estos microorganismos disuelven minerales oxidando azufre y hierro, produciendo a su vez protones de Fe^{3+} e hidrógeno. Por lo tanto, se requieren ambientes esencialmente inorgánicos, aeróbicos y moderadamente ácidos o extremadamente ácidos para este proceso. La mayoría de estos microorganismos son procariotas que comprenden una miríada de bacterias y arqueas filogenéticamente diversas. Microorganismos acidófilos de diferentes taxones pueden lixiviar minerales, incluidas las proteobacterias (*Acidithiobacillus*, *Acidiphilium*, *Acidiferrobacter*, y *Ferrovum*), Nitrospira (*Leptospirillum*), Actinobacteria (*Ferrimicrobium*, *Acidimicrobium* y *Ferrithrix*) y Firmicutes (*Alicyclobacillus* and *Sulfobacillus*). También, se han informado arqueas que pertenecen principalmente al grupo Sulfolobales, que incluye géneros como *Sulfolobus*, *Acidianus*, *Metallosphaera*, and *Sulfurisphaera* (Norris et al., 2000). Además, Thermoplasmatales contiene dos especies oxidantes de Fe^{2+}, *Ferroplasma acidiphilum* (O. V. Golyshina et al., 2000; Olga V. Golyshina & Timmis, 2005) and *Ferroplasma acidarmanus* (Edwards, 2000; Johnson, 2008).

1.1.1. Mecanismos de biolixiviación

El papel de los microorganismos en los procesos de biolixiviación es oxidar las especies de sulfuro metálico, como el hierro ferroso (Fe^{2+}) y los compuestos de azufre, para producir hierro férrico (Fe^{3+}) y protones. Estos productos de oxidación son los agentes de ataque de sulfuro metálico. La producción de protones mantiene el pH bajo y, por lo tanto, mantiene los iones Fe en solución (Brierley & Brierley, 2013; Schippers et al., 2013). Los metales se liberan de los minerales de sulfuro por mecanismos directos o indirectos. El mecanismo directo requiere oxidación bacteriana, mientras que el mecanismo indirecto está relacionado con la oxidación química, que involucra a la pareja Fe^{2+}/Fe^{3+} como portador y aceptor de electrones intermedio (Bosecker, 1997; Mahmoud et al., 2017). La figura 1, muestra una propuesta básica de estos dos mecanismos basada en estudios previos (Jia et al., 2019; Li et al., 2013).

Las siguientes ecuaciones suman los mecanismos directos e indirectos (Li et al., 2013; Mahmoud et al., 2017; Sand et al., 2001).

Mecanismo Directo:

$$MS_{(s)} + 2O_{2(g)} \xrightarrow{\text{Bacteria}} MSO_{4(aq)}, \quad (1)$$

donde MS es el metal sulfurado.

La oxidación directa de la pirita por acción de bacterias acidófilas esta descrita por las ecuaciones 2 y 3:

$$4FeS_2 + 14O_2 + 4H_2O \xrightarrow{\text{Bacteria}} 4FeSO_4 + 4H_2SO_4 \quad (2)$$

$$4FeSO_4 + O_2 + 2H_2SO_4 \xrightarrow{\text{Bacteria}} 2Fe_2(SO_4)_3 + 2H_2O. \quad (3)$$

Algunos estudios sugieren que la pirita es atacada directamente por bacterias oxidantes (Mahmoud et al., 2017; Sand et al., 2001):

$$4FeS_2 + 15O_2 + 2H_2O \xrightarrow{\text{Bacteria}} 2Fe_2(SO_4)_3 + 2H_2SO_4. \quad (4)$$

Mecanismo indirecto:

$$MS + Fe_2(SO_4)_3 \longrightarrow MSO_4 + 2FeSO_4 + 2S^0. \quad (5)$$

La pirita es oxidada químicamente por iones Fe^{3+} de acuerdo con la siguiente reacción:

$$FeS_2 + Fe_2(SO_4)_3 \longrightarrow 3FeSO_4 + 2S^0. \quad (6)$$

La generación de azufre también puede estar mediada por las bacterias oxidantes. Esta acción forma ácido sulfúrico, como se describe en la ecuación 7 (Li et al., 2013; Mahmoud et al., 2017):

$$2S^0 + O_2 + 2H_2O \xrightarrow{\text{Bacteria}} 2H_2SO_4. \quad (7)$$

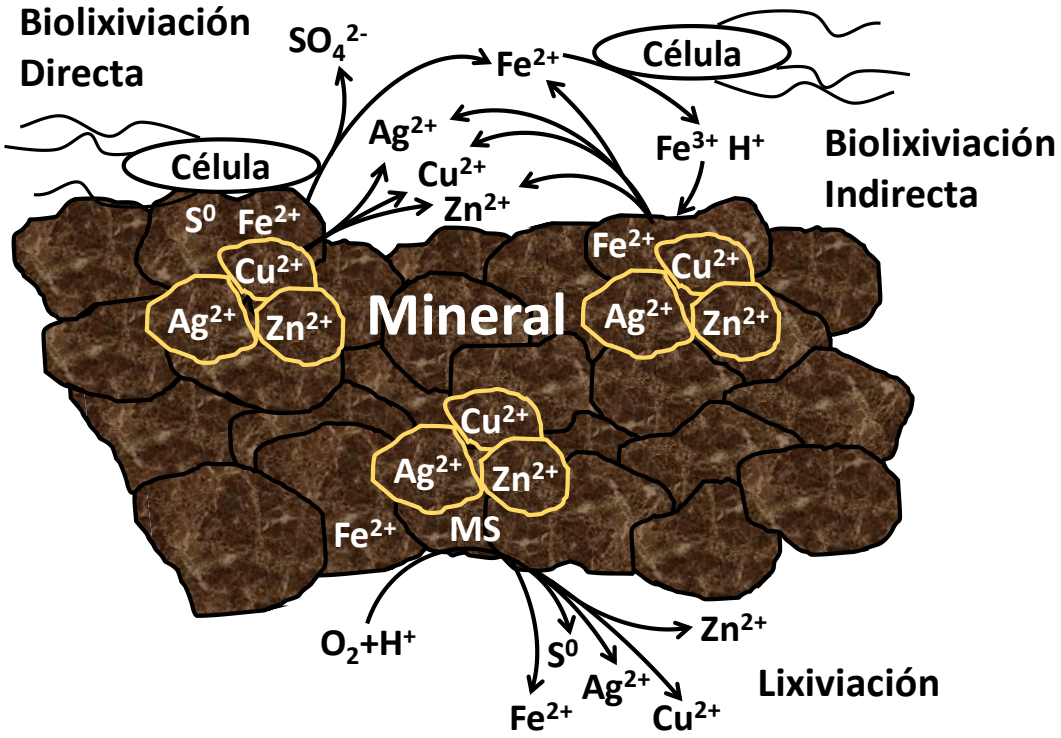

Figura 1. Ilustración de los mecanismos de biolixiviación y lixiviación mineral.

Mecanismo de biolixiviación directa: las bacterias se unen físicamente al mineral y lo oxidan, causando su disolución. Mecanismo indirecto de biolixiviación: el hierro férrico actúa como agente oxidante para solubilizar minerales. Lixiviación: en presencia de protones de oxígeno e hidrógeno, el azufre del mineral se oxida solubilizando el mineral.

1.2. Cepa LR-1 (caso de estudio).

La cepa LR-1 se aisló del mineral extraído de la mina Bolañitos del estado de Guanajuato en México (Hidalgo Rosas, 2014). Fue crecida usando el medio WAYE

diseñado para el aislamiento de bacterias quimiolitótrofas y mesofílicas oxidadoras de hierro y acidófilas heterótrofas, suplementado con $FeSO_4$ y mineral triturado como fuente de energía a un pH de 2.5. La muestra del mineral se tomó de la mina bolañitos, de cual se extrae principalmente oro y plata. La cepa LR-1 es una *β-proteobacteria*, su caracterización morfológica corresponde a bacilos gram positivos. El análisis filogenético realizado por Hidalgo en el 2014 mostró una fuerte relación con la cepa NT-26, una bacteria arsenito-oxidante identificada recientemente (Santini et al., 2000). NT-26 pertenece a la rama de *Agrobacterium* / *Rhizobium* de las *α-proteobacteria* y puede representar una nueva especie. Se ha reportado que es uno de los organismos quimiolitoautotróficos conocidos que tienen el más rápido crecimiento oxidando arsenito, (Santini et al., 2000).

1.3. Lixiviación asistida por bacterias en reactores (modelos cinéticos).

Existe un creciente interés en la investigación sobre la biolixiviación para desarrollar modelos matemáticos, (Watling, 2006). Varios modelos cinéticos han sido propuestos para la oxidación bacteriana de Fe^{2+}, en general estos pueden ser clasificados empíricamente o por su velocidad de crecimiento Michaelis-Menten/Monod (Ojumu et al., 2006). Los datos experimentales para la oxidación de Fe^{2+} con bacterias acidófilas son ajustados con velocidades de crecimiento usando el modelo de Monod (Ojumu et al., 2006); este modelo es solo aplicable para las velocidades iniciales y no considera los efectos de inhibición. Ojumu y colaboradores en el 2006, analizan trabajos previos de modelos cinéticos aplicados a la oxidación de hierro en procesos de biolixiviación, (Tabla 1).

A escala comercial para el procesamiento de ciertos minerales sulfurados, la lixiviación asistida bacteriana se aplica mediante dos procesos de ingeniería: reactores de descarga o pila, donde se riega mineral o concentrado, y reactores de tanque agitado, donde el mineral es finamente molido y tratado como una suspensión agitada/aireada. Los reactores se utilizan principalmente para la recuperación de oro a través de biooxidación y para el cobalto (1 operación), el cobre, el níquel y el zinc se extraen en grandes operaciones de biolixiviación de pilas (Kutschke et al., 2014).

Tabla 1. Modelos cinéticos publicados para biolixiviación.

Referencia	**Modelo**	**Condiciones**
(Ojumu et al., 2006)	$-rFe^{2+} = k\left(\frac{[Fe^{2+}]/[H^+]}{K_{Fe} + \frac{[Fe^{2+}]}{[H^+]} + K_i[Fe^{3+}]}\right)^{0.5}\left(\frac{[O_2]}{K_O + [O_2]}\right)^{0.5}$	**Teórico**
(Ojumu et al., 2006)	$rFe^{2+} = \frac{q_{max} - K_3\frac{[Fe^{3+}]}{[Fe^{2+}]}}{1 + \frac{K_1}{[Fe^{2+}]} + K_2\frac{[Fe^{3+}]}{[Fe^{2+}]}}$	**Teórico**
(Meruane et al., 2002)	$q_{Fe^{2+}} = \frac{K_1^* exp\left[\frac{nF}{2RT}(E^m - E_h^0)\right]\left\{1 - exp\left[\frac{nF}{RT}\right](E^m - E_h^0)\right\}}{1 + \frac{K_2^*}{[Fe^{2+}]} + K_3^* exp\left[\frac{nF}{RT}(E_h - E_h^0)\right]}$	**Célula electroquímica**, T=30 °C, pH=1.8,
(Beolchini et al., 2010)	$\frac{dY}{dt} = k(100 - Y)$	**Matraz agitado,** cultivo mixto, T= 30 °C, pH= 2.

La tabla 2, muestra información sobre algunas mineras, los modos de operación y los metales biolixioviados. Destacatacando la tecnología BIOX® operada de 40 a 45 °C, desarrollado por Gencor para la biooxidación comercial de un concentrado de oro sulfurado, consta de una alimentación continua de la suspensión de concentrado de flotación (20% a 30% de sólidos) a una serie de reactores agitados. El proceso utiliza una población mixta de *Acidithiobacillus ferrooxidans, Acidithiobacillus thiooxidans, Leptospirillum ferrooxidans, Acidithiobacillus caldus, Leptospirillum ferriphilum y Ferroplasma acidiphilum* para descomponer la matriz mineral de sulfuro, liberando así el oro ocluido para su posterior cianuración.

Tabla 2. Mineras que utilizan tecnología de biolixiviación.

Mina	**Método**	**Escala**	**Metal Lixiviado**	**Mineral (ton/día)**	**Fecha de Operación**
Zaldivar	Apilado	Industrial	Cu	20,000	Desde 1998
Agnes (BIOX)	Tanque Agitado	Industrial	Au, Ag	20	Desde 2010
Kasese (BRGM)	Tanque Agitado	Industrial	Co	250	Desde 1999
BioNic (Billiton)	Tanque Agitado	Demostración	Ni	----------	1997
Penoles (Mintek)	Tanque Agitado	Piloto	Cu	----------	2000
BioZINC (Billiton)	Tanque Agitado	Piloto	Zn	----------	1998

1.4. SISTEMAS DE CONTROL EN PROCESOS DE BIOLIXIVOACIÓN

El control avanzado de una planta de lixiviación de metales permite mantener las variables del proceso más cerca de sus valores óptimos, aumentando así la cantidad de metales lixiviados y reduciendo la cantidad de reactivos y energía consumida (Komulainen et al., 2009; Bergh et al., 2001). En la tabla 3, se muestran las variables controlables, manipulables, de perturbación y de estado más comunes en este tipo de procesos. Además, en la tabla 4, se muestra un listado de tipos de controladores que has sido utilizados para procesos de lixiviación.

Tabla 3. Modelos cinéticos publicados para biolixiviación.

Clasificación	**Modelo**	**Referencias**
Variables controlables	Concentración rica de algún metal	(Xie et al., 2018; Xie et al., 2017; Godoy et al., 2008)
Variables manipulables	Tasa de flujo de PLS pH en la solución PLS Temperatura	
Variables de perturbación	Concentración de metales pH de la solución PLS Temperatura	
Variables de estado	Concentración parcial de metales pH en la solución PLS	

Tabla 4. Modelos cinéticos publicados para biolixiviación.

Tipo de controlador	Objetivo del proceso	Referencias.
Control experto	Lixiviación de zinc	(Min Wu et al., 2002)
Control optimo	Obtención goethita	(Xie et al., 2017)
Control optimo	Obtención goethita	(Xie et al., 2018)
Control predictivo	Lixiviación de cobre	(Komulainen et al., 2009)
Control de Modelo Interno	Lixiviación de cobre	(Godoy et al., 2008).

2. JUSTIFICACIÓN

La tendencia mundial hacia la urbanización y la industrialización respalda la creciente demanda de metales industriales. La lixiviación es uno de los procesos más importantes para la extracción de estos. Además, cuando se utilizan microrganismos capaces de catalizar la oxidación de minerales, la velocidad y cantidad de la extracción de los metales puede llegar a aumentar significativamente.

Para la explotación ambiental y económica de dichos minerales, es necesario desarrollar tecnologías eficientes. En bioingeniería se utilizan herramientas como modelado, simulación y control de procesos, las cuales son capaces de permitir mantener las variables del proceso más cerca de sus valores óptimos, aumentando así la cantidad de metales extraídos y reduciendo la cantidad de químicos y energía consumida.

3. HIPÓTESIS

El uso de herramientas matemáticas como modelos fenomenológicos, simulación y control permitirán estudiar la capacidad de biolixiviación de metales usando bacterias quimiolitoautotrofas.

4. OBJETIVOS

4.1 GENERAL

Analizar la capacidad de la cepa LR1 y otras bacterias quimiolitoautótrofas para la biolixiviación de metales, a partir de minerales sulfurados utilizando técnicas de modelado, simulación y control.

4.2 PARTICULARES

1. Realizar una identificación morfológica y fisiológica de la cepa LR1.
2. Evaluar el crecimiento de la cepa LR1 con los principales donadores de electrones (Sulfato ferroso, tiosulfato de sodio y azufre).
3. Determinar experimentalmente la dinámica de las variables capaces de describir el mecanismo de la biolixiviación.
4. Proponer y validar un modelo cinético representativo del sistema de biolixiviación.
5. Proponer un modelo de planta en continuo y estudiar su estabilidad mediante simulaciones numéricas.
6. Evaluar mediante simulaciones numéricas, la propuesta de un esquema de control para el proceso de biolixiviación.

5. METODOLOGÍA

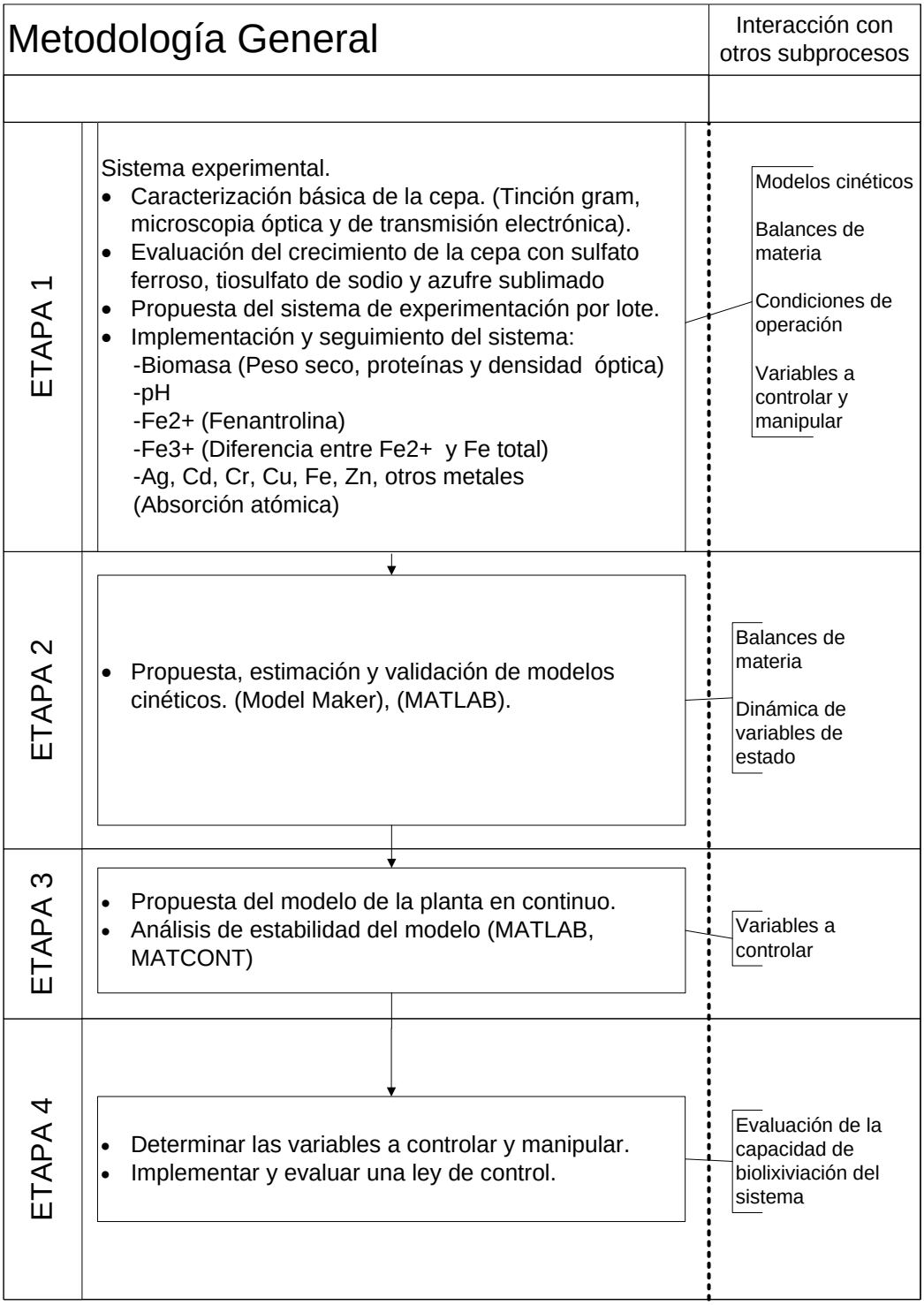

6. RESULTADOS Y DISCUSIÓN.

6.1 RESUMEN DE RESULTADOS

No. Objetivo	Objetivo Especifico	Notas
1	Identificación morfológica y fisiológica de la cepa LR1	**ARTICULO PUBLICADO:** Bioleaching for the extraction of metals from sulfide ores using a new chemolithoautotrophic bacterium.
2	Evaluación el crecimiento de la cepa LR1 con los principales donadores de electrones	
3	Determinación experimentalmente la dinámica de las variables capaces de describir el mecanismo de la biolixiviación.	
4	Propuesta y validación de un modelo cinético representativo del sistema de biolixiviación.	**Un trabajo enviado a congreso:** AMIDIQ (2017).
5	Propuesta un modelo de planta en continuo y estudio de su estabilidad mediante simulaciones numéricas.	**Dos trabajos enviados a congresos:** UJAT (2018).
6	Evaluación mediante simulaciones numéricas, la propuesta de un esquema de control para el proceso de biolixiviación	**ARTICULOS PUBLICADOS**: Design of a class of super twisting sliding-mode controller: application to bioleaching process. Controlling a continuous stirred tank reactor for zinc leaching.

6.1.1 RESULTADOS DE LOS OBJETIVOS ESPECIFICOS 1 – 3.

En esta sección se presenta el artículo correspondiente a los resultados de los objetivos específicos:

1. Identificación morfológica y fisiológica de la cepa LR1
2. Evaluación el crecimiento de la cepa LR1 con los principales donadores de electrones
3. Determinación experimentalmente la dinámica de las variables capaces de describir el mecanismo de la biolixiviación.

Los cuales se publicaron en la revista Hydrometallurgy de Elsevier con Factor de Impacto 4.217. Con el artículo titulado “Bioleaching for the extraction of metals from sulfide ores using a new chemolithoautotrophic bacterium”.

Figueroa-Estrada, J., Aguilar-López, R., Rodríguez-Vázquez, R., & Neria-González, M. (2020). Bioleaching for the extraction of metals from sulfide ores using a new chemolithoautotrophic bacterium. *Hydrometallurgy*, *197*, 105445. https://doi.org/10.1016/j.hydromet.2020.105445

Hydrometallurgy 197 (2020) 105445

Contents lists available at ScienceDirect

Hydrometallurgy

journal homepage: www.elsevier.com/locate/hydromet

Bioleaching for the extraction of metals from sulfide ores using a new chemolithoautotrophic bacterium

J.C. Figueroa-Estrada[a,b], R. Aguilar-López[a], R. Rodríguez-Vázquez[a], M.I. Neria-González[b,*]

[a] Department of Biotechnology and Bioengineering, CINVESTAV-IPN, San Pedro Zacatenco, D.F., Mexico
[b] Chemical and Biochemical Engineering Division, Tecnológico de Estudios Superiores de Ecatepec, Ecatepec, Edo. de México, Mexico

ARTICLE INFO

Keywords:
Bioleaching
Brevibacillus sp.
Chemolithotrophic
Sulfur ore
Fe^{2+} oxidation

ABSTRACT

In this work is evaluated the bioleaching capacity of a bacterium isolated from a mine in Guanajuato, México, namely LR-1. The bacterium oxidized Fe^{2+} and $S_2O_3^{2-}$ at acidic pH for its energy metabolism. This oxidant activity provided Fe^{3+} and/or protons that provoke sulfide ore dissolution. Five sulfide ore samples were obtained from different Mexican mines: Remedios, Guerrero, Bolañitos, Aldama, and Ocampo. The Ag, Cr, Cu, Fe, Pb, and Zn contents in the ores was analyzed by atomic absorption. Other physicochemical properties, including pH, electrical conductivity, and oxide-reducing potential, were also measured. Bioleaching was evaluated by metal concentration in the medium due to bacterial growth developed in basal salt medium with 2% (*w/v*) mineral in acidic conditions at 37 °C. There was an Increase in the percentage release of Ag (18.66% to 29.85%), Cu (60.90% to 73.66%), and Cr (11.71% to 15.04%), with respect to chemical leaching, mainly from the Remedios ore. A phylogenetic analysis of the 16S rRNA gene sequences revealed that bacterium LR-1 belongs to the genus *Brevibacillus*. There are no known species from this genus related with the leaching processes. This is the first report of an acidophile chemolithoautotrophic iron oxidizing bacterium from the genus *Brevibacillus* in the metal bioleaching. Therefore, these data contribute to the knowledge of the hydrometallurgical microbiology.

1. Introduction

The global trend toward urbanization and industrialization is backed for the growing commercial interest in the technology, and it demand industrial metals. These are related to ores with iron; which are used as raw materials in the steel industry to the production of different types of steel. In addition, from non-ferrous mining where metals such as Zn, Mn, Mg, and other are extracted. Parallel, global reserves of high-grade minerals are close to depletion (Anjum et al., 2012; Mahmoud et al., 2017). Further, the mining industry is seen as a source of environmental pollution. Therefore, in the last decades the mining has implemented the technology that offers the biohydrometallurgy (Gentina and Acevedo, 2016), which is divided into two conventional processes that using the action of the microorganisms: bioleaching and mineral biooxidation (Gilligan and Nikoloski, 2015; Jalali et al., 2019). Bioleaching is normally used in the extraction of metals, where the metals of interest are solubilized by microbial action and subsequently recovered from the solution (Gumulya et al., 2018), whereas mineral biooxidation is the release of metals occluded in sulfide ores such as pyrite and arsenopyrite. However, the term bioleaching can apply to both processes, since is the oxidative solubilization of the sulfide and nonsulfide ores by the microorganisms (Gentina and Acevedo, 2016).

Bioleaching occurs as a natural process on the earth's crust to the mobilization and deposition of heavy metals; although, this activity is more relationship with the iron and sulfur biogeochemical cycles. Generality, the bioleaching microorganisms are acidophiles capable of accelerate the dissolution of sulfide ores, because they gain energy from the oxidation of Fe^{2+} and sulfur. Further, the most of these acidophiles are chemolithoautotrophic, since they synthesize organic compounds from carbon dioxide and their energy derivate from oxidizing inorganic substances as H_2, Fe^{2+}, S^0, H_2S, $S_2O_3^{2-}$ and CH_4 (Valdés et al., 2010). Most of the leaching microorganisms are prokaryotes that comprise both kingdoms Bacteria and Archaea. Acidophilic bacteria belong at different taxa that including Proteobacteria (*Acidithiobacillus*, *Acidiphilium*, *Acidiferrobacter*, and *Ferrovum*), Nitrospira (*Leptospirillum*), Actinobacteria (*Ferrimicrobium*, *Acidimicrobium*, and *Ferrithrix*), and Firmicutes (*Alicyclobacillus* and *Sulfobacillus*) (Jia et al., 2019; Johnson, 2012). Reported Archaea belong mainly to the Sulfolobales group, which includes genera such as *Sulfolobus*, *Acidianus*, *Metallosphaera*, and *Sulfurisphaera* (Norris et al., 2000); and two Fe^{2+} oxidizing

* Corresponding author.
E-mail address: mineriag@tese.edu.mx (M.I. Neria-González).

https://doi.org/10.1016/j.hydromet.2020.105445
Received 14 November 2019; Received in revised form 25 May 2020; Accepted 5 August 2020
Available online 11 August 2020
0304-386X/

Thermoplasmatales species: *Ferroplasma acidiphilum* (Golyshina et al., 2000; Golyshina and Timmis, 2005) and *Ferroplasma acidarmanus* (Edwards, 2000; Johnson, 2008).

The role of the microorganisms is to oxidize the Fe^{2+} and sulfur-compounds from ores, as mentioned before. The oxidation of the Fe^{2+} allows the regeneration of Fe^{3+} from sulfide ores and promotes the direct or indirect metal releasing. The production of protons (H^+) keeps the pH low and therefore maintains the Fe ions in solution (Brierley and Brierley, 2013; Schippers et al., 2014). Then, the metals are released from sulfide ores by direct or indirect mechanisms. The direct mechanism requires bacterial oxidation, while the indirect mechanism is related to chemical oxidation, which involves the Fe^{2+}/Fe^{3+} couple as an intermediate electron carrier and acceptor (Bosecker, 1997; Hassanshahian et al., 2019; Hassanshahian and Ghoebani, 2018; Mahmoud et al., 2017). The following equations sum the direct (Eqn 1) and indirect mechanisms (Eqn 2 and 3): (Jia et al., 2019; Li et al., 2013; Mahmoud et al., 2017; Sand et al., 2001)

Direct mechanism:

$$MS_{(s)} + 2O_{2(g)} \xrightarrow{Bacteria} MSO_{4(aq)}, \quad (1)$$

where MS is the metal sulfide.

The direct oxidation of pyrite by acidophilic bacteria is described by eqs. 2 and 3:

$$4FeS_2 + 14O_2 + 4H_2O \xrightarrow{Bacteria} 4FeSO_4 + 4H_2SO_4 \quad (2)$$

and

$$4FeSO_4 + O_2 + 2H_2SO_4 \xrightarrow{Bacteria} 2Fe_2(SO_4)_3 + 2H_2O. \quad (3)$$

Some studies suggest that pyrite is directly attacked by oxidizing bacteria (Eqn 4) (Mahmoud et al., 2017; Sand et al., 2001):

$$4FeS_2 + 15O_2 + 2H_2O \xrightarrow{Bacteria} 2Fe_2(SO_4)_3 + 2H_2SO_4. \quad (4)$$

Indirect mechanism (Eqn 5 and 6):

$$MS + Fe_2(SO_4)_3 \xrightarrow{Chemical} MSO_4 + 2FeSO_4 + 2S^0. \quad (5)$$

Pyrite is chemically oxidized by Fe^{3+} ions according to the following reaction:

$$FeS_2 + Fe_2(SO_4)_3 \xrightarrow{Chemical} 3FeSO_4 + 2S^0. \quad (6)$$

Sulfur generation can also be mediated by the oxidizing bacteria. This action forms sulfuric acid, as described in Eqn 7. (Li et al., 2013; Mahmoud et al., 2017):

$$2S^0 + O_2 + 2H_2O \xrightarrow{Bacteria} 2H_2SO_4. \quad (7)$$

However in the last years, both mechanisms of bioleaching have been widely discussed, due that direct leaching is yet not clear, since it means a direct electron transfer from the metal sulfide to the cell attached to the mineral surface. Thus, the terms of direct and indirect leaching have been replaced by contact leaching and noncontact leaching for the bioleaching processes by attached and free cells, respectively. Moreover, the term "cooperative leaching" has been introduced, it describes the dissolution of sulfur colloids, sulfur intermediates, and mineral fragments by planktonic cells (Mahmoud et al., 2017; Rawlings, 2002; Rohwerder et al., 2003; Sand et al., 2001; Schippers et al., 2014; Tributsch, 2001).

Isolation and characterization of the acidophile microorganisms, and molecular techniques promote the knowledge of their metabolism, which allows the understanding of the bioleaching processes. Thus, the studies focused in the microbial leaching and the knowledge of novel bacteria are great interest in the hydrometallurgy for the metallic recovering from ores (Hassanshahian and Ghoebani, 2018; Hassanshahian et al., 2019). Currently, mining facilities are obtaining metals through bacteria-assisted leaching, for example, global production via these methods contributes 15–25% of copper, 5% of gold, and smaller percentages of cobalt, nickel, uranium and zinc (Brierley, 2008; Johnson, 2013; Kutschke et al., 2015; Puhakka et al., 2007; Schippers et al., 2014). In this work was evaluated the bioleaching capacity of a bacterium isolated from a mine in Guanajuato, México. Based on the phylogenetic position, the bacterium has not relationship with the microbial genera most studied in metallic bioleaching. Therefore, it could be a new option in the biomining for the extraction of metals from ores, and contribute in the knowledge of the hydrometallurgical and the development of engineering processes.

2. Materials and methods

2.1. Isolation and characterization of strain LR-1

Rock and waste sludge samples were obtained from a mine located in Guanajuato, México. The rock sample was collected from an inner wall of the mine at a depth of 200 m, and the sludge sample was taken from the mine's acid waste, both samples were immediately placed in a sterile 1-L bottles and transported on ice to the laboratory. The rock sample was fragmented with a hammer, pulverized in a mortar, sieved through a No. 80 mesh, and dispensed into sub-samples for subsequent analyses. Some sub-samples of pulverized rock (0.5 and 1.0 g) were autoclaved two times for 20 min each at 120 °C.

Enrichment and isolation were performed in the basal salt (BS) medium. The composition per L is: yeast extract, 0.2 g; $MgSO_4$ $7H_2O$, 5.0 g; $(NH_4)_2SO_4$, 1.5 g; KCl, 1.0 g; $Ca(NO_3)_2$, 0.1 g; 1000 mL of distilled water; pH adjusted to 2.5 with 18.3 M H_2SO_4 (Johnson, 1995). Aliquots (10 or 100 mL) of BS medium were dispensed into culture tubes or Erlenmeyer flasks and autoclaved for 15 min at 120 °C. Then, 10 mL sterile BS medium was supplemented with 1-g pulverized and sterile ore, followed by inoculation with 0.5 mL residual sludge. Further, an aliquot uninoculated-medium plus sterile ore served as negative control. The culture media were incubated at 37 °C and 130 rpm until to observe growth. The enrichment was subcultured three times into BS medium plus sterile ore. The last culture was used as inoculum (10%) for 100 mL of fresh medium supplemented with 2.5 g sterile ore, then the culture was incubated at 37 °C for 5 days. This culture was purified by serial dilutions (1:10) in BS medium and 0.5 g sterile ore and incubated at 37 °C until to observe growth. The obtained culture in the highest dilution was evaluated by microscopy and its ability to grow under chemolithoautotrophic conditions was tested.

2.2. Phenotypic characterization and electron microscopy

Morphological characterization and Gram staining were performed using a fresh culture. A preparation of the direct culture was observed under phase-contrast microscope (Axiophot Zeiss photomicroscope).

Cells from a fresh culture (incubated for 48 h) were harvested by centrifugation, the supernatant was discarded, and the cell pellet was washed with 1 mL 10% ethylenediaminetetraacetic acid (EDTA) solution. The cells collected from strain LR-1 were fixed with 2.5% glutaraldehyde, post-fixed with 2% osmium tetroxide for 1 h, dehydrated in ethanol. Then, the cells were embedded in a mix of Epon resin (Hexion Inc., USA) and Araldite 502 (Sigma-Aldrich, USA). The samples were identified and were incubate at 60 °C for 24 h to polymerize the resin. The polymerized samples were cut with a Leica Ultracut Ultramicrotome (UCT). Contrast was introduced via uranyl acetate and lead citrate, and the sections were examined under a JEOL (JEM-1010, 60 kV) transmission electron microscope. X-ray scattering analysis was performed with a JEM microscope (ARM 200F, 80 kV).

2.3. Chemolithoautotrophic growth

Chemolithoautotrophic growth of the isolated LR-1 strain was performed in the BS medium supplemented with 2% ore; the cultures were performed for triplicate. The growth was followed by the cell protein in

Fig. 1. Fig. 5 Images and micrographs of strain LR-1. a) Cells of a fresh culture under phase-contrast microscope; b) Gram stain results; c) electron micrograph of strain LR-1; d) electron micrograph of a spore formed by strain LR-1. Micrographs are from the bacterium grown in BS medium plus Bolañitos ore.

liquid phase, ferrous iron concentration, and pH. Five-mL cell culture aliquots were taken every 24 h for 5 days. The samples were centrifuged at 1800 ×*g* for 3 min, the supernatant was recovered in new tube, and the pH was measured. Protein and ferrous iron concentrations in the aqueous phase were measured using Bradford's method and the 1–10-phenanthroline technique (Kaksonen et al., 2014; Kruger, 2009), respectively, using a spectrophotometer (UV–Vis, Cole-Parmer model: 45-35-0010).

2.4. Phylogenetic analysis

The genomic DNA from strain LR-1 was extracted using a previously reported method (Cullen and Hirsch, 1998). The DNA extract was purified by Wizard DNA clean-up System (Promega, USA); and it was eluted of the column with 50 µL of 70 °C preheated deionized H_2O. Then, 2 µL dilution genomic DNA (1:10) was used as temple to amplify the 16S rDNA gene by PCR. The reaction mixture (l00 µL) contained 0.5 µM each primers; 200 µM dNTP mix (Promega,USA), 2.5 mM MgCl; and 2 U of GoTaq® DNA polymerase in the PCR buffer provided by the manufacturer (Promega, USA). The using bacterial universal primers were 46F (50-GCC TAA CAC ATG CAA GTC-30) (Yu and Morrison 2004) and 1540R (50-AAG GAG GTG ATC CAG CCGCA-30) (Edwards et al., 1989). Amplification conditions included an initial denaturation step at 94 °C for 10 min, 28 cycles of 55 °C for 1 min, 72 °C for 2 min,

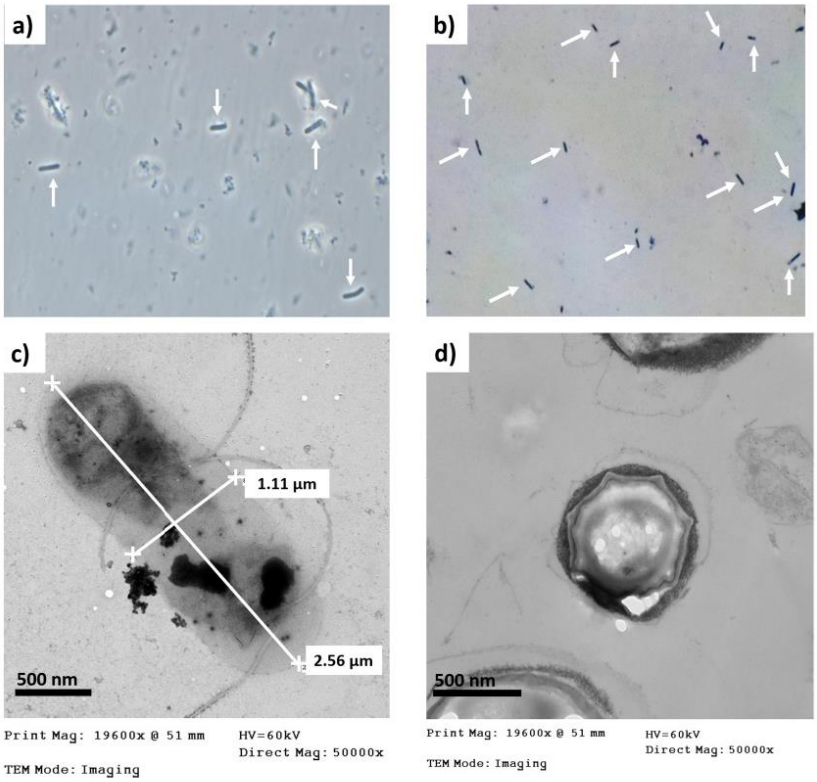

Fig. 2. Phylogenetic position of strain LR-1 among class Bacilli and leaching microorganims based on 16S rRNA gene sequence analysis. The length of the related sequences was 1453 nucleotides. The phylogenetic trees was inferred by using the maximum likelihood method and general time reversible model, and analysis and 500 bootstrap replications were assessed to support internal branches. Only values above 60% are shown. The sequences of leaching archaea act as outgroup. Nucleotide sequence accession numbers of the analyzed sequences are shown.

94 °C for 1 min, and one additional cycle at 55 °C for 1 min and 72 °C for 5 min. The amplification was done with a MultiGene OptiMax Thermal Cycler (Labnet International, Inc., USA).

PCR product was detected by electrophoresis in agarose gels 1% in 1 × TAE. DNA of *Escherichia coli* was used as a positive control in the PCR assay; negative control was carried out with reagents non-target DNA. The PCR product of 1500 pb was purified by the Promega Wizard Minipreps DNA purification system according to the manufacturer's instructions (Promega, USA). The 16S rDNA sequences were obtained with a 3730× DNA Analyzer (Applied Biosystems, Foster City, CA, USA) using 46F and 1540R primers.

16S rRNA gene sequence was analyzed for the phylogenetic characterization of the strain LR-1. The nucleotide sequence was checked for chimeras using the CHIMERA-CHECK online analysis program of the RDP-II database (Cole et al., 2003). The sequence was then subjected to a BLAST search (Altschul, 1997) and RDP Analysis Tools of Ribosomal Database Project-II Release 9 (http://rdp.cme.msu.edu/index.jsp) to determine taxonomic hierarchy of the sequence. A multiple alignment analysis was performed in CLUSTAL X using selected related sequences determined by BLAST (Thompson et al., 1997). The evolutionary history was inferred by using the maximum likelihood method and general time reversible model (Nei and Kumar, 2000). The phylogenetic tree with the highest log likelihood (−13,054.28) is shown. The percentage of trees in which the associated taxa clustered together is shown next to the branches. Initial tree(s) for the heuristic search were obtained automatically by applying the Neighbor-Join and BioNJ algorithms to a matrix of pairwise distances estimated using the maximum composite likelihood (MCL) approach, and then selecting the topology with superior log likelihood value. A discrete gamma distribution was used to model evolutionary rate differences among sites (four categories [+G, parameter = 0.5862]). The phylogenetic tree is drawn to scale, with branch lengths measured by the number of substitutions per site. This analysis involved 46 nucleotide sequences. All positions that contained gaps and missing data were eliminated (complete deletion option). There were a total of 1215 positions in the final dataset. Evolutionary analyses were conducted in MEGA X (Kumar et al., 2018).

2.5. Electron donors and statistical analysis

Ferrous sulfate (Fe^{2+}), sodium thiosulfate ($S_2O_3^{2-}$), and sublimed sulfur (S^0) were tested as electron donators for strain LR-1 energy metabolism. A volume of 200 mL BS medium was supplemented with 5, 10, or 20 mM of each chemical compound separately, and each assay was performed for triplicate. Each culture medium was inoculated with 5.0% fresh culture. The cultures were incubated at 37 °C and 120 rpm, and the cell protein and pH were measured every 24 h for 200 h, as

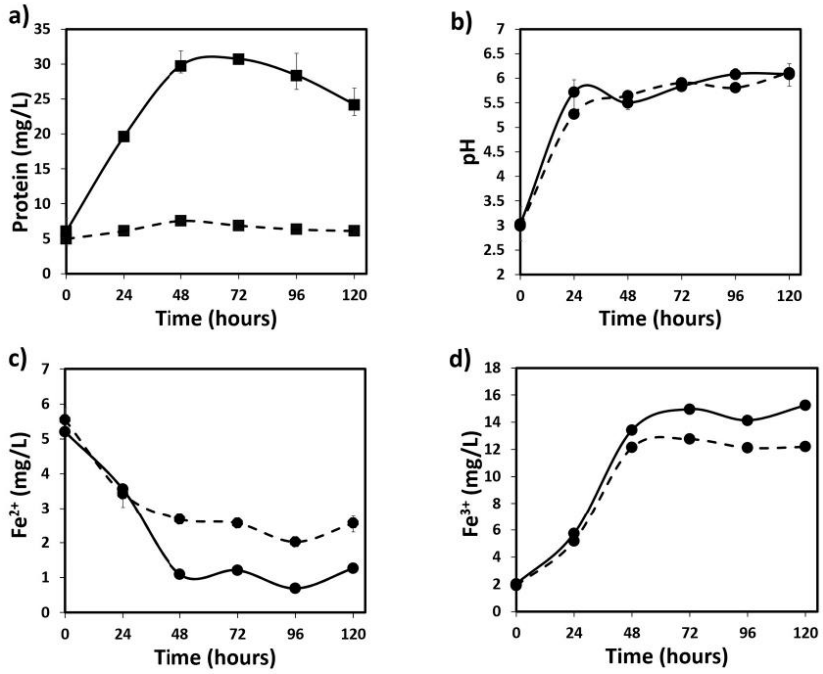

Fig. 3. Growth of strain LR-1 in BS medium with the Bolañitos ore: a) cell protein; b) pH change; c) iron consumption (Fe^{2+}); d) ferric iron production (Fe^{3+}). The solid lines correspond to the growth of LR-1, and the discontinuous lines correspond to the control culture.

described above.

To evaluate the growth and pH change, the experimental data were subjected to an analysis of variance (ANOVA), using the least significant difference (LSD) method, with $\alpha \leq 0.05$. Specifically, the maximum concentration of cellular proteins and the greatest pH change were analyzed for each treatment.

2.6. Mineral characterization for the leaching test

Five different mineral samples were used to evaluate the leaching capacity of the isolated strain. The samples were obtained from different mines located in Guanajuato, Guerrero, and Chihuahua states, Mexico. The ore samples were treated as described above, and 0.5 g of each mineral was digested with 1 mL $HNO_3/HClO_4$ (5:2) at room temperature for 96 h. The digested samples were diluted in 2% (v/v) HNO_3 to determine metal content. Metal concentrations (Ag, Cr, Cu, Fe, Pb, and Zn) were determined using atomic absorption spectrophotometry (Spectrum Thermo Scientific iCE 3000 AA). Moreover, the physicochemical properties of ores were evaluated. A 1-g sub-sample of each pulverized mineral was added to 50 mL Milli-Q water and incubated at 37 °C and 200 rpm for 5 days. Subsequently, pH, electrical conductivity, potential oxidization reduction, and the Fe^{2+} and sulfate concentrations were measured. The sulfate in solution was measured using a turbidimetric method based on the precipitation of barium (Kolmert et al., 2000). Additionally, an infrared analysis was performed to determine the presence of functional groups that indicate organic matter on the mineral samples (using a Buck Scientific Model 530 spectrophotometer).

2.7. Bioleaching capacity

The leaching capacity of strain LR-1 was measured via bacterial growth and the increase of metal concentration in solution. The treated and evaluated ores were used as the energetic substrate and CO_2 as the carbon source. The assays were performed in triplicate in BS medium with 2% of each separate ore. The control included each ore contained in the culture medium without inoculum. All cultures and analytic techniques to measure protein and the metal concentration were followed as described above.

3. Results and discussion

3.1. Isolation and characterization of strain LR-1

The strain LR-1 was isolated from waste sludge of a mine located in Guanajuato, Mexico, using BS medium supplemented with sterile ore and acidic pH, and growth temperature of 37 °C under chemolithoautotrophic conditions. This bacterial was obtained from a series of cultures carried out in the lab at different temperatures and nutrimental conditions (data not showed). The strain LR-1 was the only isolated bacterium under the conditions described in this work and with proposes of bioleaching.

Analysis of the 16S rRNA gene sequence showed that strain LR-1 belongs to the genus *Brevibacillus*; it has a strong relationship with *Brevibacillus agri* (Fig. 1). The morphological characterization of the strain LR-1 corresponds to gram-positive, motile and mesophilic rods, and the cells tend to cluster in pares (Fig. 2a-b). Electron microscopy showed that the cells measure approximately 1 to 2.6 μm, and it revealed endospores. The cellular mobility is due the presence of

Table 1
Least significant difference analysis of electron donor sources.

Response variables	Electron donor									
	Fe^{2+}			$S_2O_3^{2-}$			S^0			
	5 mM	10 mM	20 mM	5 mM	10 mM	20 mM	5 mM	10 mM	20 mM	
Protein (mg/L)	9.79 ± 2.55 d	12.42 ± 0.078 c	30.98 ± 0.08 a	8.98 ± 0.08 d	12.89 ± 0.078 c	21.56 ± 0.47 b	5.29 ± 0.16 e	6.68 ± 0.39 e	8.49 ± 0.23 d	
pH	2.43 ± 0.003 c	2.4 ± 0.006 c	2.44 ± 0.003 c	3.42 ± 0.09 a	3.12 ± 0.005 a	3.34 ± 0.01 a	2.84 ± 0.11 b	2.80 ± 0.04 b	2.92 ± 0.17 b	

Data are the averages of each variable, ±; standard error of the mean. Means followed by different letters in each column show significant differences according to Tukey test ($\alpha \leq 0.05$).

peritrichous flagella (Fig. 2c-d). These characteristics also define to *Brevibacillus* spp., since are rod shaped cells (0.7 to 0.9 by 3.0 to 5.0 μm), gram positive or variable, motile by means of peritrichous flagella, the cells form spores; and exhibit heterotrophic metabolism, but unclear if the members of genus *Brevibacillus* present a chemolithoautotrophic metabolism. The most of the species are strictly aerobic, except *Brevibacillus zaterospoius* that is facultative anaerobic (Shida et al., 1996). Thus, the strain LR-1 could be a chemolithoautotrophic acidophile bacterium of the genus *Brevibacillus*.

On the other hand, the study or application of these species in the field of the bioleaching is very poor or null. A recent research reported the isolation and identification of eight heterotrophic iron and sulfur-oxidizing bacteria from a copper mine, but only one belong *Brevibacillus formosus* (Hassanshahian et al., 2019). However, this report describe the oxidative bacterial capacity of iron and sulfur under heterotophic conditions and their possible use in the bioleaching process. Other species have been isolated from an oligotrophic environment in caves (Yasir, 2018), where described *Brevibacillus brevis* as an arsenite-oxidizing bacterium and has the capacity to bioaccumulate and biotransform arsenic when exposed to As^{3+} (Banerjee et al., 2013). Due that the main biotechnological applying of *Brevibacillus* spp. is the biological control of plant diseases (Ahmed et al., 2018), and in some case on the bioremediation of arsenic-contaminated water and soils using *B. brevis* (Bahar et al., 2013). The strain LR-1 is unconventional bacterium and the first *Brevibaccillus* sp. with a biotechnological application on the metal bioleaching.

3.2. Chemolithoautotrophic growth

The chemolithoautotrophic growth of strain LR-1 was evaluated in BS medium plus 2% sterile ore, it played as the electron source. The culture medium lacked of an organic carbon source. Bacterial growth was determined by the increase of cell protein in the aqueous phase; because of ore provoked interference in the protein measurement, and it was inversely proportional to the Fe^{2+} concentration (Fig. 3a, c). Due to the nature of the ore and aerobic condition of the culture, the pH increased at 6 for the negative control and bacterial culture (Fig. 3b). This change in the pH of medium provoked that the initial Fe^{2+} concentration decreased rapidly in 24 h, since the oxygen oxidizes Fe^{2+} at Fe^{3+}. However, the oxidation of Fe^{2+} after 24 h is slower in presence of the bacteria than in the negative control, also the concentration of Fe^{2+} increased, see Fig. 3c, d. The ore in an aqueous medium increases the pH 8.44 (Table 2), while it under an acidic aqueous medium the pH stabilizes at 6. This fact could indicate that the strain LR-1 is not acidophilic iron oxidizing bacterium because the ore is consuming acid provided by culture medium. Further, the chemical oxidation of Fe^{2+} predominates at pH $>$ 5 over bacterial oxidation, and bacterial oxidation of Fe^{2+} begins to be relevant and predominates over chemical oxidation at pH $<$ 5.0. But the bacterial oxidation of Fe^{2+} can improve in the range of pH 2.5 at 5.0 (Meruane and Vargas, 2003). Therefore, we assume that the strain LR-1 oxidized Fe^{2+} because is clear the increasing of Fe^{3+}. Besides, the alkalization of the medium and low iron containing (1.32%) on the Bolañitos ore affected the growth of bacterium.

3.3. Electron donors

LR-1 growth in BS medium was evaluated at different concentrations of ferrous sulfate (Fe^{2+}), sodium thiosulfate ($S_2O_3^{2-}$), and sublimed sulfur (S^0) as electron donors. In all cases, the bacterial growth was measured by cellular protein and pH in the aqueous phase, since the iron in the culture medium generates interferences in the methods.

The obtained data were evaluated by the LSD method as response variables to validate the electron donor that most efficaciously promoted LR-1 energy metabolism. Overall, LR-1 exhibited the highest affinity for Fe^{2+}, followed by $S_2O_3^{2-}$, while growth in the presence of

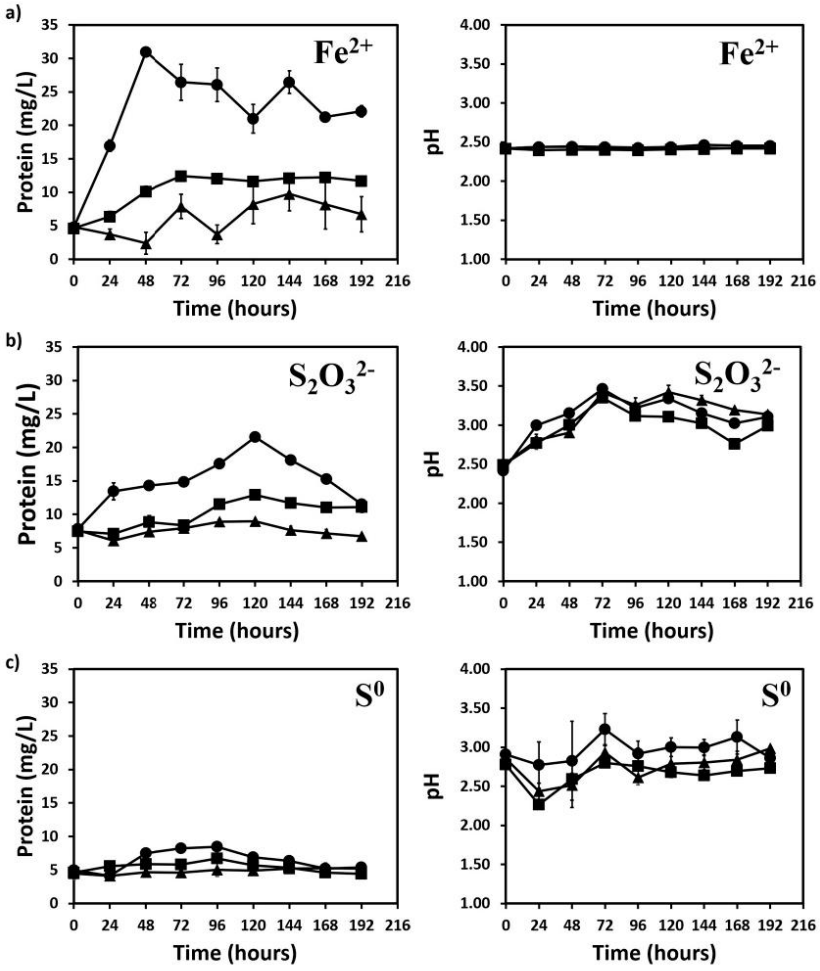

Fig. 4. Evolution of strain LR-1 growth with different electron souruces: a) cell protein and pH, BS medium plus ferrous sulfate; b) cell protein and pH, BS medium plus sodium thiosulfate; c) cell protein and pH, BS medium plus sublimated sulfur. The symbols correspond to concentrations: ▲ 5 mM; ■ 10 mM; ● 20 mM.

S^0 was not significant (Table 1). Thus, the highest growth was obtained in BS medium supplemented with ferrous iron, followed by thiosulfate; in both cases, the concentration was 20 mM (Fig. 4a-b). The culture in BS medium supplemented with sublimed sulfur did not exhibit significant growth (Fig. 4c).

The growth of the strain LR-1 to the concentration of 20 mM Fe^{2+} is clearly greater than other lower Fe^{2+} concentrations. However, once maximum growth is reached, it does not remain constant, whereas to the concentration of 10 mM Fe^{2+} the growth is constant. This could be due to the fact that Fe^{3+} in presence of oxygen forms ferric oxide, and it is deposited on the cell surface, affecting the diffusion of protons (Meruane and Vargas, 2003), despite the fact that the pH medium remains at 2.5.

The ability to oxidize Fe^{2+} and S^0 is a metabolic characteristic of chemolithotrophic microorganisms, especially for those associated with bioleaching processes (Brierley and Brierley, 2013; Johnson, 2012; Mahmoud et al., 2017; Schippers et al., 2014). While, the role of $S_2O_3^{2-}$ oxidation is not yet well documented in the bioleaching process (Brierley and Brierley, 2013; Schippers et al., 2014), but it has been studied in *Acidithiobacillus* spp. as electron donator on their chimolithotophic metabolism (Yang et al., 2019). Thus, the strain LR-1 was capable of oxidizing Fe^{2+} and $S_2O_3^{2-}$, both compounds are an electron source; and the Fe^{2+} bacterial oxidation accelerates the oxidative reactions of Fe^{2+} and sulfur-compounds from sulfide ore as pyrite, chalcopyrite, magnetite, and similar other, it favoring the leaching process.

In the process of metal leaching, acidic pH and Fe^{+3} are important for mineral solubilization. However, the Fe^{2+} oxidizing capacity of the strain LR-1 could accelerate the regeneration of Fe^{3+} and it is oxidizing agent from metal sulfide. Therefore, it is proposed to the strain LR-1 to improve the indirect leaching of sulfur ores that contain Fe^{2+} (Brierley and Brierley, 2013; Schippers et al., 2014). While, the oxidation of thiosulfate and sulfur have been studied in chemolithotrophic bacteria, the reaction mechanisms have not yet been fully elucidated (Banerjee

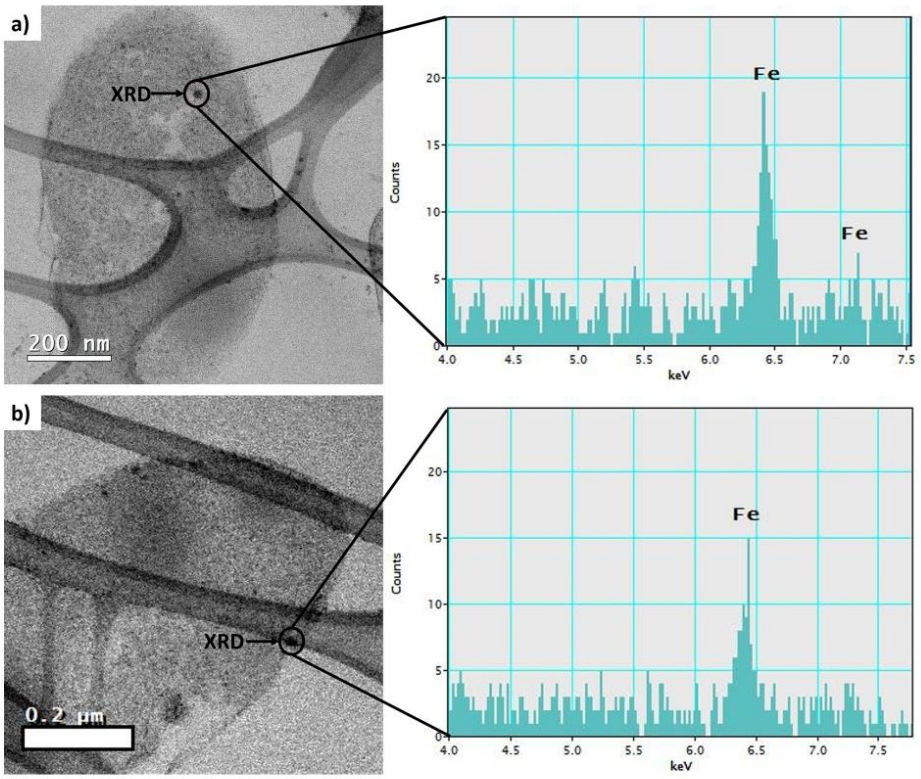

Fig. 5. Energy dispersive X-ray spectroscopy coupled to scanning electron microscopy from a cell sample. The panels show a) accumulation of iron inside the cell; b) accumulation of iron on the cell surface. The bacterium was grown in BS medium plus Bolañitos ore.

Table 2
Composition, physicochemical parameters, and concentration of mineral samples and the effect on strain LR-1 growth.

Metal	Composition of the ore (%)				
	Remedios	Guerrero	Bolañitos	Aldama	Ocampo
Ag	0.0067	0	0	0	0.00184
Cr	0.0645	0	0.01	0.0096	0.0327
Cu	0.067	1.0663	1.83057	0.0467	0.0665
Fe	43.8267	12.9463	1.32993	0.5957	2.5264
Pb	0	0.2161	0.25494	2.3315	0.1355
Zn	0.9761	1.2908	0.01407	2.4672	0.1103
Parameter	Values of physicochemical parameters and cell growth				
pH	6.51	5.44	8.44	8.38	8.6
E.C. (µS/cm)	340	457	147	89	292
ORP (mV)	144	11.9	65	85.7	237.6
Sulfates (mg/L)	357.01224	1692.29424	182.7228	281.112	1369.01544
Maximum growth (Protein mg/L)	46.406	34.099	32.556	no growth	no growth

EC = electrical conductivity; ORP = oxidation reduction potential.

et al., 2017; Li et al., 2013; Mahmoud et al., 2017; Sand et al., 2001; Schippers et al., 2014).

X-ray dispersion analysis showed that strain LR-1 can accumulate iron within the cell and in the cytoplasmic membrane (Fig. 5a-b). Some chemolithoautotrophic bacteria can form magnetosomes that comprise magnetite (Fe_3O_4) or greigite (Fe_3S_4) crystals, magnetic minerals that are key for the magnetotaxis. For example, *Acidithiobacillus ferrooxidans* synthesizes magnetite, which guides its movement through geomagnetic fields (Fang et al., 2017; Yan et al., 2013, 2016). However, iron accumulation by LR-1 is not related to the formation of magnetosomes.

3.4. Physiochemical characterization of ores

Physiochemical characterization of the ore samples was performed to evaluate the leaching potential of bacterium LR-1. The obtained results for each ore are presented in Table 2. The Remedios ore contained the highest metal contents and concentrations, including Ag, followed by the Guerrero ore (without Ag). This characteristic coincides with the high electric conductivity values in both ores. Another common characteristic between these ores was that iron had the highest concentration. This feature is important to promote the growth of the chemolithotrophic bacteria, and particularity the growth of the strain LR-1, because the iron acts as an electron source, as mentioned above (Jia et al., 2019; Li et al., 2013; Mahmoud et al., 2017; Watling, 2006). These physicochemical characteristics and an acidic pH favor the bioleaching process, and the acidity of the medium contributes to the iron solubility, its availability for the bacterium, and, in general, the solubility of metals (Mahmoud et al., 2017).

The presence of organic matter was evaluated indirectly by an

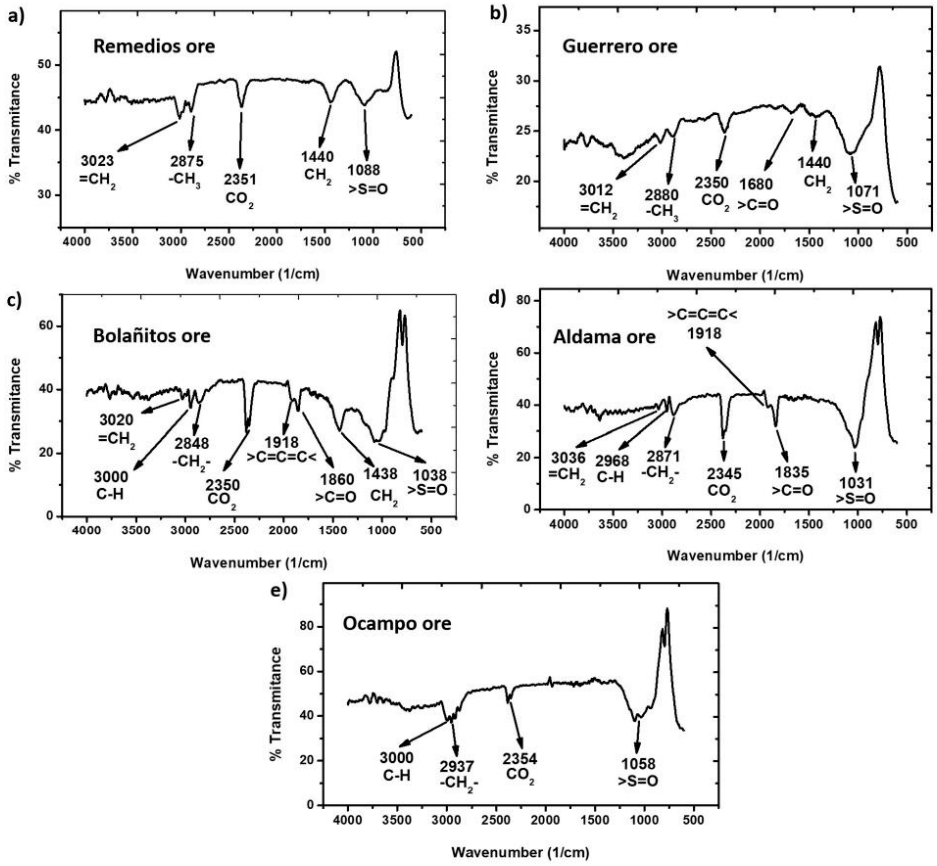

Fig. 6. Infrared analysis for the mineral simples: a) Remedios ore, b) Guerrero ore, c) Bolañitos ore, d) Aldama ore, and e) Ocampo ore.

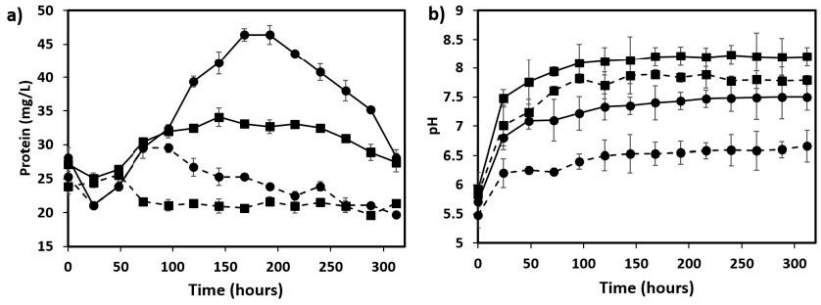

Fig. 7. Growth of strain LR-1 and pH change in BS medium supplemented with ore. The graphs show a) cell protein concentration and b) pH change. Strain LR-1 was grown in BS medium with 2% (*w/v*) Remedios or Guerrero minerals separately. ● Remedies ore; ■ Guerrero ore. The solid lines correspond to the growth of the bacterium LR1, and the discontinuous lines correspond to the control culture.

infrared spectroscopy analysis, specifically considering that the key point of the analysis is that each molecular structure and functional group has a unique spectrum that allows the identification of functional groups (Naseri et al., 2019; Panda et al., 2013). Thus, some functional groups were identified in all ores used in the present work (Fig. 6). These data show that the ores may have low organic matter content and explain why the majority leaching bacteria exhibit an autotrophic metabolism (Valdés et al., 2010). The spectrograms also detected CO_2

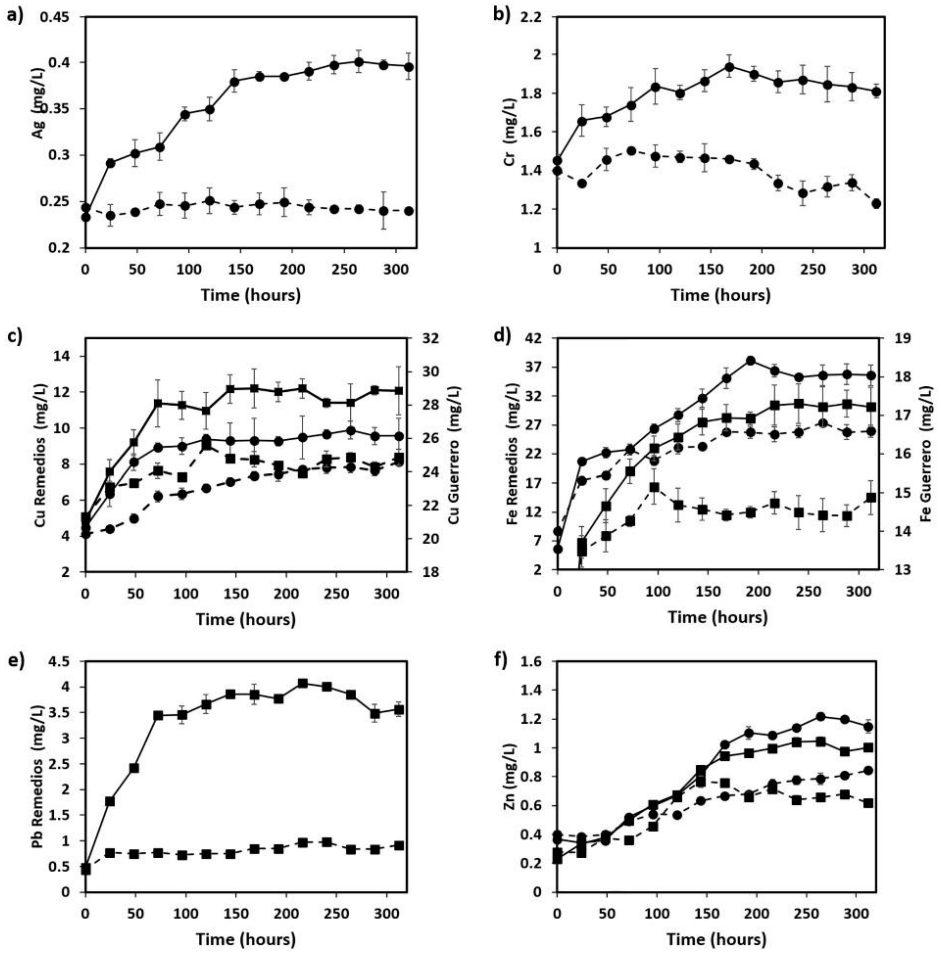

Fig. 8. Metal bioleaching of the mineral from Remedios and Guerrero ores using the strain LR-1. ● Remedies ore; ■ Guerrero ore. The solid lines correspond to the growth of the bacterium LR1, and the discontinuous lines correspond to the control culture.

Table 3
Maximum leaching concentration and percentage of metal leaching.

Metal	Maximum leach concentration (mg/L)				Total leaching (%)			
	Remedios		Guerrero		Remedios		Guerrero	
	Control	Strain LR-1	Control	Strain LR-1	Control	Strain LR-1	Control	Strain LR-1
Ag	0.25	0.40	N.D.		18.66	29.85	N.A.	
Cr	1.51	1.94	N.D.		11.71	15.04	N.A.	
Cu	8.16	9.87	25.584	28.98	60.90	73.66	12.00	13.59
Fe	27.37	38.14	16.302	17.30	0.31	0.44	0.63	0.67
Pb	N.D.		0.97	4.074	N.A.		2.26	9.43
Zn	0.84	1.22	0.76	1.04	0.43	0.62	0.29	0.40

N.A. = not aplicable; N.D. = not detected.

in all ores, which can be consumed by the bacteria. Although infrared analysis is not quantitative, the ores from the Bolañitos, Aldama, and Ocampo mines may have high CO_2 concentrations that could contribute to the alkalinity of medium by the formation of carbonates.

All ores were tested as a substrate in the BS culture medium to determine the capacity for LR-1 growth. The bacterium did not grow in presence of the Ocampo and Aldama ores; this outcome was expected due to low iron concentration and the alkalinity of the ores, Table 2. Indeed, the medium remained alkaline during the entire culture, although the initial pH of the culture medium was adjusted to 2.5. Comparatively, with the other ores the pH increased over time as the bacterium grew (Fig. 7). The bacterial growth with the Remedios and Guerrero ores were high, but the highest growth occurred in the presence of the Remedios ore (Table 2). Therefore, both ores were selected to evaluate the leaching potential of LR-1.

3.5. Bioleaching capacity of strain LR-1

A second round of the cultures in presence of Remedios and Guerrero ores were analyzed to evaluate the leaching capacity of the bacterium. In both cases, the bacterium with the ores were incubated at 37 °C for 312 h (13 days). The metal concentration in the medium was measured by atomic absorption spectrometry every 24 h. Fig. 8 shows the concentrations of the most representative metals for these ores (Ag, Cr, Cu, Fe, Pb, and Zn), considering that the Guerrero ore did not contain Ag and Cr and the Remedios ore lacked Pb (Table 2). The effect of the ore leaching by the bacterium is presented in Table 3. For both ores, the presence of strain LR-1 positively contributed to the metal leaching because the leaching percentage was higher than in the control cultures (without bacterium). In the Remedios ore, the leached copper increased from 60.9% to 73.66%. Some works reported an increase between 40 and 95% of leached Cu using mixed bacterial cultures at 4 at 43 days (Abdollahi et al., 2014; Hedrich et al. 2018; Niu et al., 2015). Comparatively, the bioleaching process in this study was examined using an axenic culture during 13 days maximum incubation. Silver leaching increased to 29.85%, a value higher than what was observed using a bacterium of the genus *Alcaligenes* (26.8%; Kanayev et al., 2016). Therefore, we can assume that the strain LR-1 may have an important application in the process of metal bioleaching, since it following an indirect or noncontact mechanism from sulfur ores that iron containing. It should be noted that the new bacterium *Brevibacillus* sp. does not require great nutritional demands, a benefit to consider for a bioleaching process.

4. Conclusions

Strain LR-1 was identified by the 16S rRNA gene sequence analysis as *Brevibacillus* sp.. The chemolithoautotrophic metabolism is not clear on the genus *Brevibacillus*. However, the strain LR-1 grows under chemolithoautotrophic conditions at low pH, it using Fe^{2+} and $S_2O_3^{2-}$ as electron donors. The iron oxidative capacity by the strain LR-1 accelerates the leaching of sulfide ores by the regeneration and oxidative power of Fe^{3+}. Thus, Fe^{3+} ions oxidize the sulfur-compounds and Fe^{2+} from ore and it provokes the releasing of metals. The Fe^{2+} oxidizing by the strain LR-1 increased the percentage of Ag (18.66% to 29.85%), Cu (60.90% to 73.66%) and Cr (11.71% to 15.04%) release from the Remedios ore. Therefore, the strain LR-1 could contribute to the process of indirect bioleaching of metals from sulfide-ores and iron. This is the first report of an acidophilic iron oxidizing bacterium from the genus *Brevibacillus* in the metal bioleaching. Therefore, these data contribute to the knowledge of the hydrometallurgical microbiology.

Declaration of Competing Interest

None.

Acknowledgements

Juan Carlos Figueroa-Estrada thanks CONACYT for support via a graduate scholarship (No. 230859, CONACYT). Partial financial support from TecNM (No. 502.17-PD) and CINVESTAV-IPN is acknowledged. The authors thank the technical support to the Center of Microscopy, Escuela Nacional de Ciencias Biológicas-IPN, Advanced electronic nanoscopy laboratory, CINVESTAV-IPN, and to M. Leandro Rodrigo González González for his cooperation in the AAS and FT-IR analysis.

References

Abdollahi, H., Shafaei, S.Z., Noaparast, M., Manafi, Z., Niemelä, S.I., Tuovinen, O.H., 2014. Mesophilic and thermophilic bioleaching of copper from a chalcopyrite-containing molybdenite concentrate. Int. J. Miner. Process. 128, 25–32. https://doi.org/10.1016/j.minpro.2014.02.003.

Ahmed, A.I., Omer, A.M., Ibrahim, A.I., Agha, M.K., 2018. Brevibacillus Spp. in agroecology: the beneficial impacts in biocontrol of plant pathogens and soil bioremediation. Fungal Genomics Biol. 08. https://doi.org/10.4172/2165-8056.1000157.

Altschul, S., 1997. Gapped BLAST and PSI-BLAST: a new generation of protein database search programs. Nucleic Acids Res. 25, 3389–3402. https://doi.org/10.1093/nar/25.17.3389.

Anjum, F., Shahid, M., Akcil, A., 2012. Biohydrometallurgy techniques of low grade ores: a review on black shale. Hydrometallurgy 117–118, 1–12. https://doi.org/10.1016/j.hydromet.2012.01.007.

Bahar, M.M., Megharaj, M., Naidu, R., 2013. Bioremediation of arsenic-contaminated water: recent advances and future prospects. Water Air Soil Pollut. 224, 1722. https://doi.org/10.1007/s11270-013-1722-y.

Banerjee, S., Majumdar, J., Samal, A.C., Bhattachariya, P., Santra, S.C., 2013. Biotransformation and bioaccumulation of arsenic by *Brevibacillus brevis* isolated from arsenic contaminated region of West Bengal. IOSR J. Environ. Sci. Toxicol. Food. Technol. 3, 1–10.

Banerjee, I., Burrell, B., Reed, C., West, A.C., Banta, S., 2017. Metals and minerals as a biotechnology feedstock: engineering biomining microbiology for bioenergy applications. Curr. Opin. Biotechnol. 45, 144–155. https://doi.org/10.1016/j.copbio.2017.03.009.

Bosecker, K., 1997. Bioleaching: metal solubilization by microorganisms. FEMS Microbiol. Rev. 20, 591–604. https://doi.org/10.1111/j.1574-6976.1997.tb00340.x.

Brierley, C.L., 2008. How will biomining be applied in future? Trans. Nonferrous Metals Soc. China 18, 1302–1310. https://doi.org/10.1016/S1003-6326(09)60002-9.

Brierley, C.L., Brierley, J.A., 2013. Progress in bioleaching: part B: applications of microbial processes by the minerals industries. Appl. Microbiol. Biotechnol. 97, 7543–7552. https://doi.org/10.1007/s00253-013-5095-3.

Cole, J.R., Chai, B., Marsh, T.L., Farris, R.J., Wang, Q., Kulam, S.A., Chandra, S., McGarrell, D.M., Schmidt, T., Garrity, G.M., Tiedje, J.M., 2003. The ribosomal database project (RDP-II): previewing a new autoaligner that allows regular updates and the new prokaryotic taxonomy. Nucleic Acids Res. 31, 442–443. https://doi.org/10.1093/nar/gkg039.

Cullen, D.W., Hirsch, P.R., 1998. Simple and rapid method for direct extraction of microbial DNA from soil for PCR. Soil Biol. Biochem. 30, 983–993.

Edwards, K.J., 2000. An archaeal iron-oxidizing extreme acidophile important in acid mine drainage. Science. 287, 1796–1799. https://doi.org/10.1126/science.287.5459.1796.

Edwards, U., Rogall, T., Blocker, H., Emde, M., Bottger, E., 1989. Isolation and direct complete nucleotide determination of entire genes. Characterization of a gene coding for 16S ribosomal RNA. Nucleic Acids Res. 17, 7843–7853. https://doi.org/10.1093/nar/17.19.7843.

Fang, J., Liu, Y., He, W., Qin, W., Qiu, G., Wang, J., 2017. Transformation of iron in pure culture process of extremely acidophilic microorganisms. Trans. Nonferrous Metals Soc. China 27, 1150–1155. https://doi.org/10.1016/S1003-6326(17)60134-1.

Gentina, J., Acevedo, F., 2016. Copper bioleaching in Chile. Minerals 6, 23. https://doi.org/10.3390/min6010023.

Gilligan, R., Nikoloski, A.N., 2015. The extraction of uranium from brannerite – a literature review. Miner. Eng. 71, 34–48. https://doi.org/10.1016/j.mineng.2014.10.007.

Golyshina, O.V., Timmis, K.N., 2005. *Ferroplasma* and relatives, recently discovered cell wall-lacking archaea making a living in extremely acid, heavy metal-rich environments. Environ. Microbiol. 7, 1277–1288. https://doi.org/10.1111/j.1462-2920.2005.00861.x.

Golyshina, O.V., Pivovarova, T.A., Karavaiko, G.I., Kondrat'eva, T.F., Moore, E., Abraham, W.R., Lunsdorf, H., Timmis, K.N., Yakimov, M.M., Golyshin, P.N., 2000. *Ferroplasma acidiphilum* gen. nov., sp. nov., an acidophilic, autotrophic, ferrous-iron-oxidizing, cell-wall-lacking, mesophilic member of the *Ferroplasmaceae* fam. nov., comprising a distinct lineage of the *Archaea*. Int. J. Syst. Evol. Microbiol. 50, 997–1006. https://doi.org/10.1099/00207713-50-3-997.

Gumulya, Y., Boxall, N., Khaleque, H., Santala, V., Carlson, R., Kaksonen, A., 2018. In a quest for engineering acidophiles for biomining applications: challenges and opportunities. Genes (Basel) 9, 116. https://doi.org/10.3390/genes9020116.

Hassanshahian, M., Ghoebani, S., 2018. Isolation and characterization of iron and sulfur oxidizing bacteria from Maiduk copper mine at Shahrbabk province in Iran.

Geomicrobiol. J. 35, 261–265. https://doi.org/10.1080/01490451.2017.1348408.
Hassanshahian, M., Toorani, S., Roghanian, R., Emtiazi, G., Genovese, M., 2019. Characterization of heterotrophic iron and sulfur-oxidizing bacteria from acid mine drainage in Sarcheshmeh copper mine Iran. Desalin. Water Treat. 147, 264–272.
Hedrich, S., Joulian, C., Graupner, T., Schippers, A., Guézennec, A.-G., 2018. Enhanced chalcopyrite dissolution in stirred tank reactors by temperature increase during bioleaching. Hydrometallurgy. 179, 125–131. https://doi.org/10.1016/j.hydromet.2018.05.018.
Jalali, F., Fakhari, J., Zolfaghari, A., 2019. Response surface modeling for lab-scale column bioleaching of low-grade uranium ore using a new isolated strain of *Acidithiobacillus Ferridurans*. Hydrometallurgy 185, 194–203. https://doi.org/10.1016/j.hydromet.2019.02.014.
Jia, Y., Tan, Q., Sun, H., Zhang, Y., Gao, H., Ruan, R., 2019. Sulfide mineral dissolution microbes: community structure and function in industrial bioleaching heaps. Green Energy Environ. 4, 29–37. https://doi.org/10.1016/j.gee.2018.04.001.
Johnson, D.B., 1995. Selective solid media for isolating and enumerating acidophilic bacteria. J. Microbiol. Methods 23, 205–218. https://doi.org/10.1016/0167-7012(95)00015-D.
Johnson, D.B., 2008. Biodiversity and interactions of acidophiles: key to understanding and optimizing microbial processing of ores and concentrates. Trans. Nonferrous Metals Soc. China 18, 1367–1373. https://doi.org/10.1016/S1003-6326(09)60010-8.
Johnson, D.B., 2012. Geomicrobiology of extremely acidic subsurface environments. FEMS Microbiol. Ecol. 81, 2–12. https://doi.org/10.1111/j.1574-6941.2011.01293.x.
Johnson, D.B., 2013. Development and application of biotechnologies in the metal mining industry. Environ. Sci. Pollut. Res. 20, 7768–7776. https://doi.org/10.1007/s11356-013-1482-7.
Kaksonen, A.H., Morris, C., Rea, S., Li, J., Wylie, J., Usher, K.M., Ginige, M.P., Cheng, K.Y., Hilario, F., du Plessis, C.A., 2014. Biohydrometallurgical iron oxidation and precipitation: part I — effect of pH on process performance. Hydrometallurgy. 147–148, 255–263. https://doi.org/10.1016/j.hydromet.2014.04.016.
Kanayev, A.T., Bulaev, A.G., Semenchenko, G.V., Kanayeva, Z.K., Shilmanova, A.A., 2016. Biooxidation of gold-bearing sulfide ore and subsequent biological treatment of cyanidation residues. Appl. Biochem. Microbiol. 52, 397–405. https://doi.org/10.1134/S0003683816040086.
Kolmert, A., Wikström, P., Hallberg, K.B., 2000. A fast and simple turbidimetric method for the determination of sulfate in sulfate-reducing bacterial cultures. J. Microbiol. Methods 41, 179–184.
Kruger, N.J., 2009. The Bradford method for protein quantitation. In: Walker, J.M. (Ed.), The Protein Protocols Handbook. Humana Press, Totowa, NJ, pp. 17–24. https://doi.org/10.1007/978-1-59745-198-7_4.
Kumar, S., Stecher, G., Li, M., Knyaz, C., Tamura, K., 2018. MEGA X: molecular evolutionary genetics analysis across computing platforms. Mol. Biol. Evol. 35, 1547–1549. https://doi.org/10.1093/molbev/msy096.
Kutschke, S., Guézennec, A.G., Hedrich, S., Schippers, A., Borg, G., Kamradt, A., Gouin, J., Giebner, F., Schopf, S., Schlömann, M., Rahfeld, A., Gutzmer, J., D'Hugues, P., Pollmann, K., Dirlich, S., Bodénan, F., 2015. Bioleaching of kupferschiefer blackshale – a review including perspectives of the Ecometals project. Miner. Eng. 75, 116–125. https://doi.org/10.1016/j.mineng.2014.09.015.
Li, Y., Kawashima, N., Li, J., Chandra, A.P., Gerson, A.R., 2013. A review of the structure, and fundamental mechanisms and kinetics of the leaching of chalcopyrite. Adv. Colloid Interf. Sci. 197–198, 1–32. https://doi.org/10.1016/j.cis.2013.03.004.
Mahmoud, A., Cézac, P., Hoadley, A.F.A., Contamine, F., D'Hugues, P., 2017. A review of sulfide minerals microbially assisted leaching in stirred tank reactors. Int. Biodeterior. Biodegradation 119, 118–146. https://doi.org/10.1016/j.ibiod.2016.09.015.
Meruane, G., Vargas, T., 2003. Bacterial oxidation of ferrous iron by *Acidithiobacillus ferrooxidans* in the pH range 2.5–7.0. https://doi.org/10.1016/S0304-386X(03)00151-8.
Naseri, T., Bahaloo-Horeh, N., Mousavi, S.M., 2019. Environmentally friendly recovery of valuable metals from spent coin cells through two-step bioleaching using *Acidithiobacillus thiooxidans*. J. Environ. Manag. 235, 357–367. https://doi.org/10.1016/j.jenvman.2019.01.086.
Nei, M., Kumar, S., 2000. Molecular Evolution and Phylogenetics. Oxford University Press, New York.
Niu, Z., Huang, Q., Wang, J., Yang, Y., Xin, B., Chen, S., 2015. Metallic ions catalysis for improving bioleaching yield of Zn and Mn from spent Zn-Mn batteries at high pulp density of 10%. J. Hazard. Mater. 298, 170–177. https://doi.org/10.1016/j.jhazmat.2015.05.038.
Norris, P.R., Burton, N.P., Foulis, N.A.M., 2000. Acidophiles in bioreactor mineral processing. Extremophiles 4, 0071–0076. https://doi.org/10.1007/s007920050139.
Panda, S., Parhi, P.K., Nayak, B.D., Pradhan, N., Mohapatra, U.B., Sukla, L.B., 2013. Two step meso-acidophilic bioleaching of chalcopyrite containing ball mill spillage and removal of the surface passivation layer. Bioresour. Technol. 130, 332–338. https://doi.org/10.1016/j.biortech.2012.12.071.
Puhakka, J.A., Kaksonen, A.H., Riekkola-Vanhanen, M., 2007. Heap Leaching of Black Schist, in: Biomining. Springer, Berlin Heidelberg, Berlin, Heidelberg, pp. 139–151. https://doi.org/10.1007/978-3-540-34911-2_7.
Rawlings, D.E., 2002. Heavy metal mining using microbes. Annu. Rev. Microbiol. 56, 65–91. https://doi.org/10.1146/annurev.micro.56.012302.161052.
Rohwerder, T., Gehrke, T., Kinzler, K., Sand, W., 2003. Bioleaching review part a: appl. microbiol. Biotechnol 63, 239–248. https://doi.org/10.1007/s00253-003-1448-7.
Sand, W., Gehrke, T., Jozsa, P.-G., Schippers, A., 2001. (Bio)chemistry of bacterial leaching—direct vs. indirect bioleaching. Hydrometallurgy 59, 159–175. https://doi.org/10.1016/S0304-386X(00)00180-8.
Schippers, A., Hedrich, S., Vasters, J., Drobe, M., Sand, W., Willscher, S., 2014. Biomining: metal recovery from ores with microorganisms. Adv. Biochem. Eng. Biotechnol. 1–47. https://doi.org/10.1007/10_2013_216.
Shida, O., Takagi, H., Kadowaki, K., Komagata, K., 1996. Proposal for two new genera, *Brevibacillus* gen. nov. and *Aneurinibacillus* gen. nov. Int. J. Syst. Bacteriol. 46, 939–946. https://doi.org/10.1099/00207713-46-4-939.
Thompson, J., Gibson, T.J., Plewniak, F., Jeanmougin, F., Higgins, D.G., 1997. The CLUSTAL_X windows interface: flexible strategies for multiple sequence alignment aided by quality analysis tools. Nucleic Acids Res. 25, 4876–4882. https://doi.org/10.1093/nar/25.24.4876.
Tributsch, H., 2001. Direct versus indirect bioleaching. Hydrometallurgy 59, 177–185. https://doi.org/10.1016/S0304-386X(00)00181-X.
Valdés, J., Cárdenas, J.P., Quatrini, R., Esparza, M., Osorio, H., Duarte, F., Lefimil, C., Sepulveda, R., Jedlicki, E., Holmes, D.S., 2010. Comparative genomics begins to unravel the ecophysiology of bioleaching. Hydrometallurgy 104, 471–476. https://doi.org/10.1016/j.hydromet.2010.03.028.
Watling, H.R., 2006. The bioleaching of sulphide minerals with emphasis on copper sulphides-a review. Hydrometallurgy 84, 81–108. https://doi.org/10.1016/j.hydromet.2006.05.001.
Yan, L., Zhang, S., Chen, P., Wang, W., Wang, Y., Li, H., 2013. Magnetic properties of *Acidithiobacillus ferrooxidans*. Mater. Sci. Eng. C 33, 4026–4031. https://doi.org/10.1016/j.msec.2013.05.046.
Yan, L., Zhang, S., Liu, H., Wang, W., Chen, P., Li, H., 2016. Optimization of magnetosome production by *Acidithiobacillus ferrooxidans* using desirability function approach. Mater. Sci. Eng. C 59, 731–739. https://doi.org/10.1016/j.msec.2015.10.060.
Yang, L., Zhao, D., Yang, J., Wang, W., Chen, P., Zhang, S., Yan, L., 2019. *Acidithiobacillus thiooxidans* and its potential application. Appl. Microbiol. Biotechnol. https://doi.org/10.1007/s00253-019-10098-5.
Yasir, M., 2018. Analysis of bacterial communities and characterization of antimicrobial strains from cave microbiota. Braz. J. Microbiol. 49, 248–257. https://doi.org/10.1016/j.bjm.2017.08.005.

6.1.2 RESULTADOS DE LOS OBJETIVOS ESPECIFICOS 4 – 6.

En esta sección se presenta el artículo correspondiente a los resultados de los objetivos específicos:

4. Propuesta y validación de un modelo cinético representativo del sistema de biolixiviación.
5. Propuesta un modelo de planta en continuo y estudio de su estabilidad mediante simulaciones numéricas.
6. Evaluación mediante simulaciones numéricas y propuesta de un esquema de control.

Parte de los resultados se presentaron en los siguientes congresos:

- XXXVIII Encuentro Nacional de la AMIDIQ del 2017 con el trabajo titulado "Influencia de rendimientos constantes y variables en la determinación de parámetros cinéticos para *Thiobacillus ferrooxidans* usando modelos no estructurados".
- 5to. Congreso Nacional de Ingeniería Química UJAT 2018 con el trabajo titulado "Sensibilidad paramétrica de modelos cinéticos no estructurados con rendimientos constantes y variables aplicados a biolixiviación".
- 5to. Congreso Nacional de Ingeniería Química UJAT 2018 con el trabajo titulado "Análisis de estabilidad en un reactor continuo bajo diversos modelos cinéticos para un proceso de biolixiviación".

Además, también se publicaron en las siguientes revistas:

- Revista Comptes rendus de l'Académie bulgare des Sciences con Factor de Impacto 0.378 Con el artículo titulado "Design of a class of super twisting sliding-mode controller: application to bioleaching process".

  Figueroa-Estrada, J., Neria-González, M., & Aguilar-López, R. (2019). Design of a Class of Super Twisting Sliding-mode Controller: Application to Bioleaching Process. *Comptes rendus de l'Académie bulgare des Sciences*, Tome 72, 7, 947. https://doi.org/10.7546/crabs.2019.07.13

- Revista Minerals Engineering de Elsevier con Factor de Impacto 5.479 Con el artículo titulado "Controlling a continuous stirred tank reactor for zinc leaching".

  Figueroa-Estrada, J., Neria-González, M., Rodríguez Vázquez, R., Tec-Caamal, E., & Aguilar-López, R. (2020). Controlling a continuous stirred tank reactor for zinc leaching. *Minerals Engineering*, *157*, 106549. ttps://doi.org/10.1016/j.mineng.2020.106549

AMIDIQ

La Academia Mexicana de Investigación y Docencia en Ingeniería Química A.C.

La Ingeniería Química en el Desarrollo Sostenible de Nuevos Procesos y Productos

Otorga el presente

RECONOCIMIENTO

A:

Juan Carlos Figueroa Estrada, Hugo Iván Velázquez Sanchez, Refugio Rodríguez Váquez, María Isabel Neria González

Por la presentación del trabajo:

INFLUENCIA DE RENDIMIENTOS CONSTANTES Y VARIABLES EN LA DETERMINACIÓN DE PARÁMETROS CINÉTICOS PARA Thiobacillus ferrooxidans USANDO MODELOS NO ESTRUCTURADOS

ID: 555

XXXVIII Encuentro Nacional de la AMIDIQ

Ixtapa Zihuatanejo, Gro., México, del 9 al 12 de mayo de 2017

Dr. Mauricio Sales Cruz
PRESIDENTE DE AMIDIQ

XXXVIII ENCUENTRO NACIONAL DE LA AMIDIQ

Dr. Jesús Alberto Ochoa Tapia
PRESIDENTE DEL COMITÉ TÉCNICO

INFLUENCIA DE RENDIMIENTOS CONSTANTES Y VARIABLES EN LA DETERMINACIÓN DE PARÁMETROS CINÉTICOS PARA *Thiobacillus ferrooxidans* USANDO MODELOS NO ESTRUCTURADOS

Juan Carlos Figueroa-Estrada[a,b], Hugo Iván Velázquez-Sanchez[a],.. Refugio Rodríguez-Vázquez[a], María Isabel Neria-González[b].
[a] Departamento de Biotecnología y Bioingeniería, CINVESTAV-IPN, D.F., 07360, México. ibineria@hotmail.com.
[b] División de Ingeniería Química y Bioquímica, TESE, Ecatepec, Edo. de México, CP 55120, México.

Resumen

En la actualidad, la biolixiviación es un campo destacado en materia de investigación y desarrollo, esto se debe a la necesidad de aumentar el rendimiento y calidad de los productos, teniendo el objetivo de reducir los costos der producción. Es un problema bien conocido que para diseñar, vigilar y controlar muchos de estos procesos biotecnológicos, es importante conocer el comportamiento cinético del sistema de estudio. Es por esta razón, que un modelo cinético que tenga la capacidad de predecir un proceso de biolixivación es un instrumento valioso. *Thiobacillus Ferrooxidans* es un microorganismo modelo en procesos de biolixiviación, se ha reportado que interviene en la liberación de metales a partir de minerales sulfurados. Los microorganismos presentan comportamientos no lineales y la aplicación de rendimientos variables son útiles para explicar este comportamiento oscilatorio. Para este trabajo se tomaron datos de crecimiento y consumo de sustrato (Fe^{2+}) con *T. Ferrooxidans* de un trabajo previo reportado. Se realizó la estimación de parámetros cinéticos para cuatro modelos no estructurados (Aiba, Luong, Monod y Tessier), y se estimaron los coeficientes para rendimientos constantes y para tres estructuras matemáticas más que corresponden a rendimientos variables. Finalmente se obtuvieron coeficientes de correlación globales que van desde 0.950 hasta 0.993.

Introducción

En general, la biolixiviación es un proceso descrito como la disolución de metales a partir de su fuente mineral por ciertos microorganismos o el uso de los mismos para transformar elementos que se pueden extraer de un material cuando el agua se filtra a través de este [11]. Como resultado, el metal oxidado permanece en los residuos sólidos en una forma más concentrada [4]. Procesos de recuperación en base a la actividad de los microorganismos ofrecen una posibilidad de obtener metales a partir de los recursos minerales que no son accesibles por la minería convencional [3, 5]. *T. ferrooxidans* es un microorganismo modelo utilizado para procesos de biolixiviación, este microorganismo puede oxidar sulfuros metálicos por un "mecanismo directo", obteniendo electrones directamente de los minerales reducidos; también puede oxidar metales reducidos a través de un "mecanismo indirecto", todo esto mediado por el hierro férrico (Fe^{3+}), procedente de la oxidación microbiana de hierro ferroso (Fe^{2+}) presente en los minerales.

El estudio del comportamiento cinético de un bioproceso es importante en la bioingeniería porque permite predecir el comportamiento de los diferentes tipos de biorreactores bajo diferentes condiciones de operación. Generalmente, se utilizan modelos no estructurados para describir el comportamiento cinético, y en la mayoría de estos, se asume que el rendimiento es constante, pero la acumulación de datos experimentales sugiere que un rendimiento constante no puede explicar comportamientos oscilatorios [7]. Por ello, algunos autores proponen modelos matemáticos de rendimientos variables, por lo general lineales o polinomiales [6, 7, 8].

ISBN-978-607-95593-5-9
SIM-143

En consecuencia, en el campo de la biotecnología resulta interesante el estudio de bacterias con capacidad de biolixiviación de metales y su comportamiento cinético por medio de modelos matemáticos. En el presente trabajo se realizó la estimación de parámetros cinéticos con cuatro modelos no estructurados (Aiba, Luong, Monod, y Tessier), para la oxidación de Fe^{2+} en un cultivo por lote de *T. ferrooxidans*, con rendimientos constantes y tres tipos de rendimientos variables. Finalmente se validaron los modelos mediante simulaciones numéricas y se obtuvieron los coeficientes de correlación global de cada modelo.

Metodología

Propuesta de modelos, rendimientos y estimación de parámetros cinéticos.- Los datos experimentales de concentraciones *vs* tiempo fueron obtenidos de un trabajo previo reportado por Biagiola [2]. Se eligieron los modelos de Aiba [1] (Ec. 1), Luong [9] (Ec. 2), Monod [12] (Ec. 3) y Tessier [10] (Ec. 4), para representar el crecimiento de *T. ferroxxidans* y la oxidación de Fe^{2+}.

$$\mu(S) = \mu_{\max} \frac{S}{(K_s + S)(1 + \frac{S}{K_i})} \tag{1}$$

$$\mu(S) = \mu_{\max} \frac{S^n}{K_s + S^n} \tag{2}$$

$$\mu(S) = \mu_{\max} \frac{S}{K_s + S} \tag{3}$$

$$\mu(S) = \mu_{\max} \left(1 - e^{\frac{-s}{Ki}} \right) \tag{4}$$

Los parámetros cinéticos (μ_{max}, K_S, K_i, n) y los coeficientes de los rendimientos, se estimaron a través de una regresión no lineal multivariable de los datos de biomasa (X), y Fe^{2+} como sustrato (S), por el método simple de mínimos cuadrados usando el programa ModelMaker 3.0.3. Las estructuras matemáticas de rendimientos constantes y variables se muestran en las ecuaciones 7-10.

Validación de los modelos.- Una vez planteados los balances de materia para concentración de biomasa (Ec. 5) y Fe^{2+} (Ec. 6), se validaron los modelos cinéticos con los datos experimentales mediante simulaciones numéricas usando MATLAB R2016a. Por último, el coeficiente de correlación global se calculó a partir de los coeficientes obtenidos de cada variable de respuesta como lo reporta Tejada [14].

$$\frac{dX}{dt} = \mu X \tag{5}$$

$$\frac{dS}{dt} = -\mu X Y_{S/X} \tag{6}$$

ISBN-978-607-95593-5-9

Resultados

Estimación de parámetros cinéticos y coeficientes de rendimientos.- En la tabla 1, se muestran los parámetros estimados para cada modelo cinético:

Tabla 1.- Parámetros cinéticos estimados.

Parámetro	Modelo			
	Aiba	Luong	Monod	Tessier
μ_{max} (t^{-1})	0.115	0.14	0.139	0.115
K_S (mg L^{-1})	1200	1980	2453.92	-------
K_i (mg L^{-1})	130000	-------	-------	3500
n	-------	0.95	-------	-------

Las estructuras matemáticas para rendimientos sustrato/biomasa ($Y_{S/X}$) constantes y variables con sus coeficientes estimados se muestran en las ecuaciones 7-10.

Rendimiento constante:

$$Y_{S/X} = 117.088 \tag{7}$$

Rendimiento variable de segundo grado:

$$Y_{S/X} = 174.76 - 3.084\times10^{-2}S + 3.335\times10^{-6}S^2 \tag{9}$$

Rendimiento variable de tercer grado:

$$Y_{S/X} = 109.175 + 0.028S - 8.564\times10^{-6}S^2 - 7.644\times10^{-10}S^3 \tag{9}$$

Estructura de rendimiento reportada por Sun [13]:

$$Y_{S/X} = \frac{46.524}{0.314 + 85152424.448\left(e^{-892S}\right)} \tag{10}$$

Simulación numérica.- En las figuras 1 y 2, se muestran las simulaciones de los cuatro modelos con rendimientos constantes y de segundo grado:

ISBN-978-607-95593-5-9

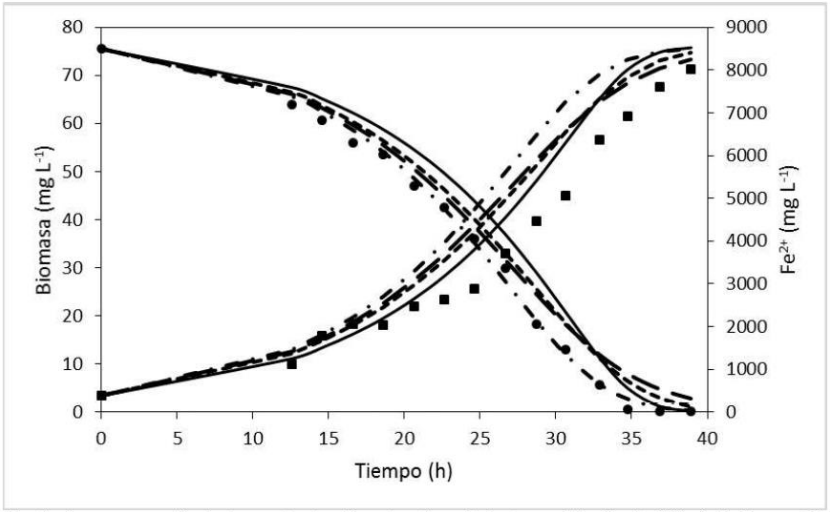

Figura 1.- Simulaciones con rendimiento constante referentes al crecimiento y oxidación de Fe^{2+} de T. Ferrooxidan. Los símbolos (▪) y (●), se refieren a los datos experimentales de biomasa y Fe^{2+} respectivamente. La líneas significan simulación con modelos de Aiba, (—);Luong, (----); Monod, (– · –) y Tessier, (– –).

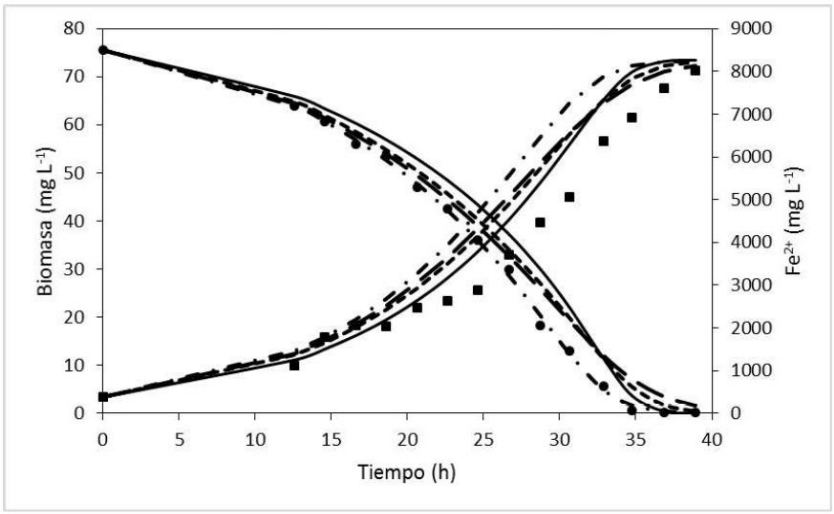

Figura 2.- Simulaciones con rendimiento de segundo grado referentes al crecimiento y oxidación de Fe^{2+} de T. Ferrooxidan. Los símbolos (▪) y (●), se refieren a los datos experimentales de biomasa y Fe^{2+} respectivamente. La líneas significan simulación con modelos de Aiba, (—);Luong, (----); Monod, (– · –) y Tessier, (– –).

ISBN-978-607-95593-5-9
SIM-146

Validación de los modelos.- En la figura 3 se muestra la regresión lineal para obtener los coeficientes de correlación con el modelo de monod con rendiento de segundo grado y Aiba con rendimiento de tercer grado. Además, en tabla 2 se muestran los resultados del cálculo de los coeficientes de correlación globales de los 4 modelos cinéticos no estructurados con rendimientos constantes y variables.

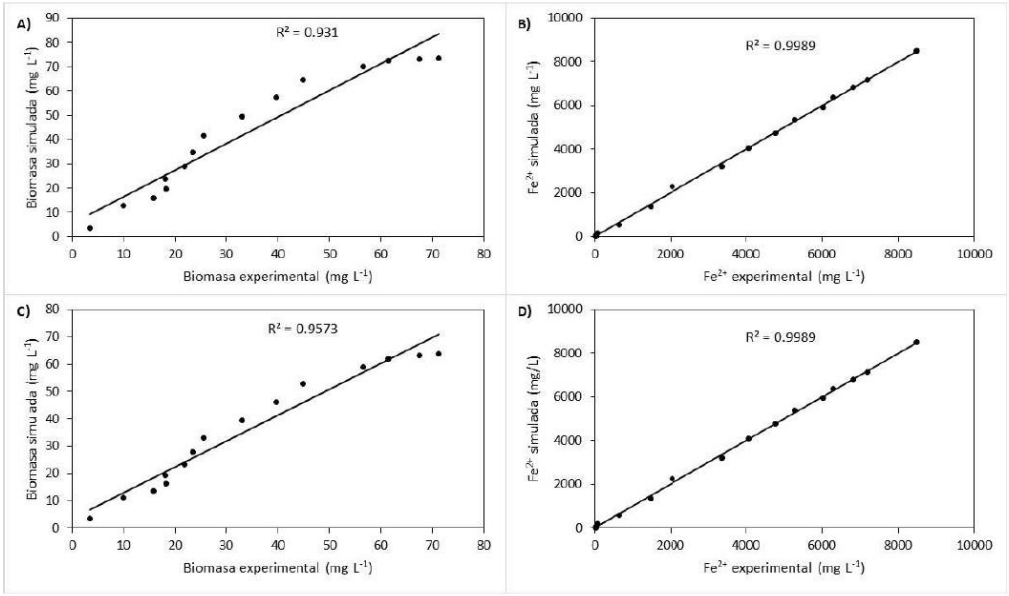

Figura 3.- Regresión lineal y coeficientes de correlación. Modelo de Monod con rendimiento de segundo grado: A) biomasa y B) Fe^{2+}. Modelo de Aiba de tercer grado: C) biomasa; D) Fe^{2+}.

Tabla 2.- Coeficientes de correlación globales.

Modelos cinéticos	Coeficientes de correlación globales			
	$Y_{S/X}$ Constante	$Y_{S/X}$ Segundo grado	$Y_{S/X}$ Tercer Grado	$Y_{S/X}$ Sun y col. (2010)
Aiba	0.984	0.980	0.993	0.988
Luong	0.987	0.983	0.984	0.981
Monod	0.987	0.991	0.960	0.950
Tessier	0.988	0.984	0.974	0.971

Los modelos cinéticos, rendimientos constantes y variables propuestos en este trabajo fueron capaces de representar la cinética de crecimiento *T. ferrooxidans*. Los mejores coeficientes de correlación globales se obtuvieron con rendimientos variables, teniendo como casos particulares el modelo de Monod con rendimiento de segundo grado y Aiba con rendimiento de tercer grado con coeficientes de correlación globales de 0.991 y 0. 993 respectivamente.

ISBN-978-607-95593-5-9

Conclusiones

Los cuatro modelos cinéticos no estructurados con los rendimientos constantes y variables propuestos en este trabajo fueron capaces de representar el crecimiento y oxidación de Fe^{2+} por parte de *T. ferrooxidans*. Los mejores coeficientes de correlación globales se obtuvieron con el modelo de Monod con rendimiento de segundo grado y Aiba con rendimiento de tercer grado, siendo estos mayores a 0.99. Además, los parámetros con sus respectivos modelos cinéticos tienen el potencial de ser aplicados en un futuro en ingeniería de diseño, control y optimización de reactores y bioprocesos con fines de reducción de costos.

Referencias

1. Aiba S., "Growth kinetics of photosynthetic microorganisms". *Advances in Biochemical Engineering*. Vol. 23, p. 85-156, 1982.
2. Biagiola, S., Solsona, J. y Milocco R., "Estimation of kinetic rates in batch *Thiobacillus ferrooxidans* cultures", *Journal of Biotechnology*, Vol. 84, p. 13-25, 2000.
3. Bosecker, K., "Bioleaching: metal solubilization by microorganisms", *FEMS Microbiology Reviews*, Vol. 20, No. 3-4, p.591-604, 1997.
4. Brandl, H., "Microbial Leaching of Metals", *Biotechnology Set*., pp.191-224, 2008
5. Brierley, C. and Le Roux, N., "Bacterial Leaching",*CRC Critical Reviews in Microbiology*, Vol. 6, No. 3, p.207-262, 1978.
6. Crooke P., Wei C.-J. y Tanner R., "The effect of the specific growth rate and yield expressions on the existence of oscillatory behavior of a continuous fermentation model" , *Chemical. Engineering*, Vol. 6, p. 333-339, 1980.
7. Dorofeev, A.G, Glagolev, M.V., Bondarenko, T.F., y Panikov, N.S., "Unusual Kinetics of Growth of Arthrobacter globiformis and Its Explanation", *Mikrobiologiya*", Vol. 61, no. 1, p. 33, 1992.
8. Huang X. y Zhu L., "A Three Dimensional Chemostat with Quadratic Yields", *Journal Mathematics Chemical*, Vol. 38, No. 4, p. 575, 2005.
9. Luong JHT, "Generalization of Monod kinetics for analysis of growth data with substrate inhibition", *Biotechnology and Bioengineering*, Vol. 29, p. 242- 248, 1987.
10. Nelson M. I. y Sidhu H. S., "Analysis of a chemostat model with variable yield coefficient: Tessier kinetics", *Journal of Mathematical Chemistry*, Vol. 46, No. 2, p. 303-321, 2009.
11. Parker, S., "Concise Encyclopedia of science & technology", *Mc Graw-Hill. New York*, 1994.
12. Robinson JA. y Tiedje JM., "Nonlinear estimation of Monod growth kinetic parameters from a single substrate depletion curve". *Applied and Environmental Microbiology*, Vol. 45, No, 5, p. 1453-1458, 1983.
13. Sun, K., Tian, Chen, Y., y Kasperski, A., "Nonlinear modelling of a synchronized chemostat with impulsive state", *Mathematical and Computer Modelling*, Vol. 52, p. 227, 2010.
14. Tejeda, A.. "Estadistica para ciencias sociales, del comportamiento y de la salud". 3ª Edición, CENGAGE Learning, Mexico., 2007.

ISBN-978-607-95593-5-9

UNIVERSIDAD JUÁREZ AUTÓNOMA DE TABASCO
"ESTUDIO EN LA DUDA. ACCIÓN EN LA FE"

División Académica de Ingeniería y Arquitectura

UJAT

IQ-UJAT

Otorga la presente

CONSTANCIA

A: JUAN CARLOS FIGUEROA ESTRADA, JUAN CARLOS FIGUEROA ESTRADA, RICARDO AGUILAR LÓPEZ, MARÍA ISABEL NERIA GONZÁLEZ

Por presentar el trabajo titulado: **"SENSIBILIDAD PARAMÉTRICA DE MODELOS CINÉTICOS NO ESTRUCTURADOS CON RENDIMIENTOS CONSTANTES Y VARIABLES APLICADOS A BIOLIXIVIACIÓN"** en modalidad **PÓSTER**, en el tópico **SIMULACIÓN Y OPTIMIZACIÓN**, en el marco del **5to. Congreso Nacional de Ingeniería Química UJAT 2018** "Avances e Impacto de la Ingeniería Química en el Entorno Social e Industrial", llevado a cabo en las instalaciones del Centro Internacional de Vinculación y Enseñanza (CIVE).

Villahermosa, Tabasco, México del 09 al 11 de octubre de 2018

Dr. Germán Pérez Hernández
Director de la DAIA

UNIVERSIDAD JUÁREZ AUTÓNOMA DE TABASCO
DIVISIÓN ACADÉMICA DE INGENIERÍA Y ARQUITECTURA
DIRECCIÓN

Dra. Mayra Agustina Pantoja Castro
Presidente del Comité Organizador

FOLIO: IQ/CDCE/2018/025/110

SENSIBILIDAD PARAMÉTRICA DE MODELOS CINÉTICOS NO ESTRUCTURADOS CON RENDIMIENTOS CONSTANTES Y VARIABLES APLICADOS A BIOLIXIVIACIÓN

PARAMETRIC SENSITIVITY OF UNSTRUCTURED KINETIC MODELS WITH CONSTANT AND VARIABLE YIELDS APPLIED TO BIOLEACHING

Juan Carlos Figueroa Estrada[1, 2], Ricardo Aguilar López[1], María Isabel Neria González[2, *]

[1] División de Ingeniería Química y Bioquímica, Tecnológico de Estudios Superiores de Ecatepec (TESE), Av. Tecnológico S/N, Valle de Anáhuac, CP. 55210, Ecatepec de Morelos, México, México.

[2] Departamento de Biotecnología y Bioingeniería, Centro de Investigación y de Estudios Avanzados del Instituto Politécnico Nacional (CINVESTAV), Av. Instituto Politécnico Nacional, Col. San Pedro Zacatenco, CP. 07360, Ciudad de México, México.

*ibineria@hotmail.com

RESUMEN

Thiobacillus Ferrooxidans es un microorganismo modelo en procesos de biolixiviación, se ha reportado que interviene en la liberación de metales a partir de minerales sulfurados. La lixiviación biológica juega un papel económico importante para la industria minera. Los modelos cinéticos has sido una herramienta importante para los procesos biotecnológicos, permiten analizar los sistemas bajo diferentes condiciones mediante simulaciones numéricas. Los parámetros de estos modelos pueden ser estudiados mas a fondo mediante un análisis de sensibilidad paramétrica. El cual permite estudiar los sistemas, cuantificando el comportamiento biológico respecto a los cambios en los parámetros del modelo, determinar los parámetros más sensibles y a su vez limitaciones experimentales. En este trabajo se realizó un análisis de sensibilidad paramétrica de cuatro modelos cinéticos no estructurados validados en un trabajo previo (Aiba, Luong, Monod y Tessier), con cuatro estructuras de rendimiento sustrato/biomasa (constante, segundo orden, tercer orden y tipo exponencial). Esto con el fin de determinar los parámetros de mayor importancia en un proceso de biolixiviación. Se realizo un análisis de sensibilidad local, basado en

la aplicación de la Matriz de Información de Fisher (FIM). Las simulaciones correspondientes se realizaron en el programa MATLAB 2017. Como resultados se obtuvo que los parámetros de mayor importancia fueron la μ_{max} (velocidad máxima de crecimiento) y los coeficientes de mayor orden de los rendimientos polinomiales.

Palabras clave: biolixiviación, modelo cinético, rendimientos variables, sensibilidad paramétrica, *T. Ferrooxidans.*

ABSTRACT

Thiobacillus Ferrooxidans is a model microorganism in bioleaching processes, it has been reported that it intervenes in the release of metals from sulphide minerals. Biological leaching plays an important economic role for the mining industry. Kinetic models have been an important tool for biotechnological processes, allowing to analyze systems under different conditions through numerical simulations. The parameters of these models can be further studied through a parametric sensitivity analysis. Which allows to study the systems, quantifying the biological behavior with respect to the changes in the parameters of the model, determining the most sensitive parameters and at the same time experimental limitations. In this work, a parametric sensitivity analysis of four unstructured kinetic models validated in previous work (Aiba, Luong, Monod and Tessier), with four substrate / biomass yield structures was performed (constant, second order, third order and exponential type). This in order to determine the most important parameters in a bioleaching process. A local sensitivity analysis was performed, based on the application of the Fisher Information Matrix (FIM). The corresponding simulations were carried out in the MATLAB R2017a program. As results, it was obtained that the parameters of greater importance were

the μ_{max} (maximum growth speed) and the coefficients of higher degree of the polynomial yields.

Keywords: bioleaching, kinetic model, variable yields, parametric sensitivity, *T. Ferrooxidans.*

INTRODUCCIÓN

En general, la biolixiviación es un proceso descrito como la disolución de metales a partir de su fuente mineral por ciertos microorganismos o el uso de estos para transformar elementos que se pueden extraer de un material cuando el agua se filtra a través de este [1]. Como resultado, el metal oxidado permanece en los residuos sólidos en una forma más concentrada [2]. Los procesos de recuperación en base a la actividad de los microorganismos ofrecen una posibilidad de obtener metales a partir de los recursos minerales que no son accesibles por la minería convencional [3]. *T. ferrooxidans* es un microorganismo modelo utilizado para procesos de biolixiviación, este microorganismo puede oxidar sulfuros metálicos por un "mecanismo directo", obteniendo electrones directamente de los minerales reducidos; también puede oxidar metales reducidos a través de un "mecanismo indirecto", todo esto mediado por el hierro férrico (Fe^{3+}), procedente de la oxidación microbiana de hierro ferroso (Fe^{2+}) presente en los minerales. El estudio del comportamiento cinético de un bioproceso es importante en la bioingeniería porque permite predecir el comportamiento de los diferentes tipos de biorreactores bajo diferentes condiciones de operación. Generalmente, se utilizan modelos no estructurados para describir el comportamiento cinético, y en la mayoría de estos, se asume que el rendimiento es constante, pero la acumulación de datos experimentales sugiere que un

rendimiento constante no puede explicar comportamientos oscilatorios [4]. Por ello, algunos autores proponen modelos matemáticos de rendimientos variables, por lo general lineales o polinomiales [4, 5, 6]. En ocasiones para un mismo sistema se realizan diversas propuestas de modelos cinéticos que son capaces de reproducir las variables de estado en estudio. Lo que genera un interés importante en tener herramientas de análisis que faciliten la discriminación y elección de un modelo en particular. Un instrumento utilizado para para caracterizar modelos y sus parámetros, es la matriz de información de Fisher [7, 8]. Esta permite cuantificar el grado de inferencia de cada variación numérica de los parámetros en cualquier momento de simulación y sus intervalos confidenciales en su determinación numérica en diferentes etapas de la fermentación. En consecuencia, en el campo de la biotecnología resulta interesante caracterizar ciertos modelos cinéticos para tener una mejor elección y guiar de mejor manera el trabajo experimental subsecuente. En el presente trabajo se realizó un de sensibilidad análisis de estabilidad local mediante la información de la matriz de Fisher, para cuatro modelos cinéticos no estructurados (Aiba, Luong, Monod, y Tessier), con cuatro estructuras de rendimiento sustrato/biomasa (constante, segundo orden, tercer orden y tipo exponencial). Los cuales fueron validados en un trabajo previo con datos experimentales para un proceso con potencial para biolixiviación de metales [9].

METODOLOGÍA

Modelos cinéticos y rendimientos. Los modelos cinéticos ecuaciones de rendimientos fueron obtenidos de un trabajo previo reportado [9]. Que corresponde a los modelos cinéticos de Aiba (Ec. 1), [10]; Luong (Ec. 2), [11]; Monod (Ec. 3), [12] y Tessier (Ec. 4), [13]. Ademas, de los rendimientos del tipo constante y variables.

$$\mu(S) = \mu_{max} \frac{S}{(K_S+S)\left(1+\frac{S}{K_i}\right)} \quad (1)$$

$$\mu(S) = \mu_{max} \frac{S^n}{K_S+S^n} \quad (2)$$

$$\mu(S) = \mu_{max} \frac{S}{K_S+S} \quad (3)$$

$$\mu(S) = \mu_{max} \left(1 - e^{\frac{-S}{Ki}}\right) \quad (4)$$

$$Y_{S/X} = 117.08 \quad (5)$$

$$Y_{S/X} = 174.76 - 3.08x10^{-2}S + 3.33x10^{-6}S^2 \quad (6)$$

$$Y_{S/X} = 109.175 + 0.028S - 8.564x10^{-6}S^2 - 7.644x10^{-6}S^3 \quad (7)$$

$$Y_{S/X} = \frac{46.524}{0.314+85152424448e^{-892S}} \quad (8)$$

Donde: K_s y K_i, son constantes de afinidad al sustrato en (mg L^{-1}); *n* es un exponente adimensional; *S* es la concentración de sustrato (mg L^{-1}); μ_{max}, es la velocidad máxima de crecimiento de *T. ferrooxidans* (h^{-1}); $\mu(S)$, velocidad especifica de crecimiento (mg L^{-1} h^{-1}); *a, b, c, d, p, r, v, y z* son los coeficientes correspondientes de las ecuaciones de rendimientos. $Y_{S/X}$, corresponde al. rendimiento sustrato/biomasa. La tabla 1 muestra los valores de los parámetros.

Tabla 1. Parámetros cinéticos.

	Modelo			
	Aiba	Luong	Monod	Tessier
μ_{max}	0.115	0.14	0.139	0.115
K_S	1200	1980	2453.92	-------
K_i	130000	-------	-------	3500
n	-------	0.95	-------	-------

Las ecuaciones 9 y 10 muestran los balances de materia para biomasa (*X*), y sustrato (*S*).

$$\frac{dX}{dt} = \mu(S)X \qquad (9)$$

$$\frac{dS}{dt} = \mu(S)XY_{S/X} \qquad (10).$$

Análisis de sensibilidad parametrica. Se realizo un análisis de sensibilidad local, basado en la aplicación de la aplicación de la Matriz de Información de. aplicación de la Matriz de Información de Fisher (FIM). Las simulaciones correspondientes se realizaron en el programa MATLAB 2017.

RESULTADOS Y DISCUSIÓN

Las figuras 1-4, muestran las gráficas de los resultados obtenidos del análisis de sensibilidad paramétrica, solo se presentan las gráficas respecto a la biomasa, ya que para el sustrato se obtienen resultados similares.

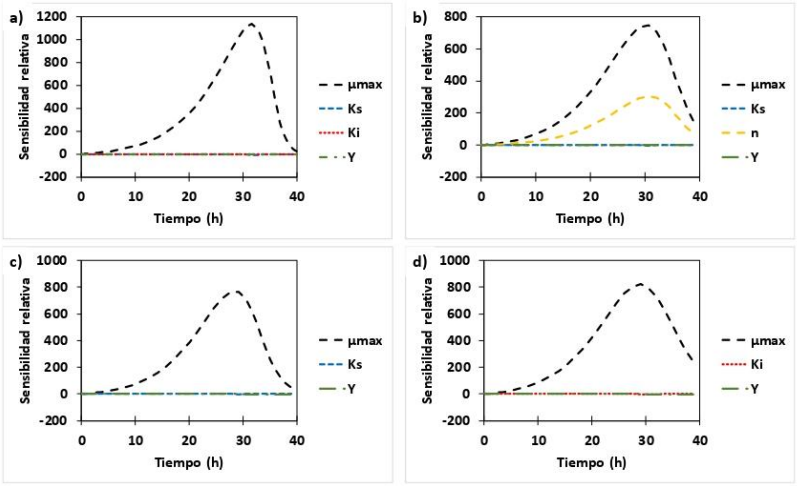

Fig 1. Análisis de sensibilidad paramétrica con rendimientos constantes. a) Aiba, b) Luong, c) Monod, d) Tessier.

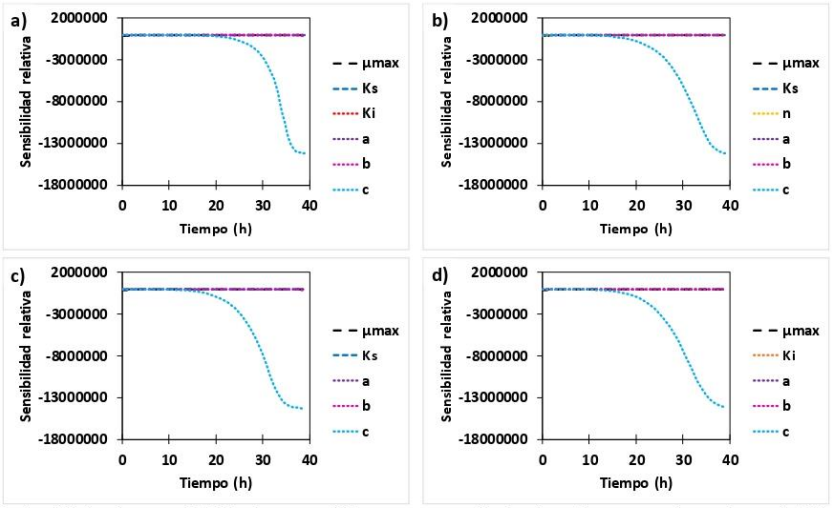

Fig 2. Análisis de sensibilidad paramétrica con rendimientos de segundo orden. a) Aiba, b) Luong, c) Monod, d) Tessier.

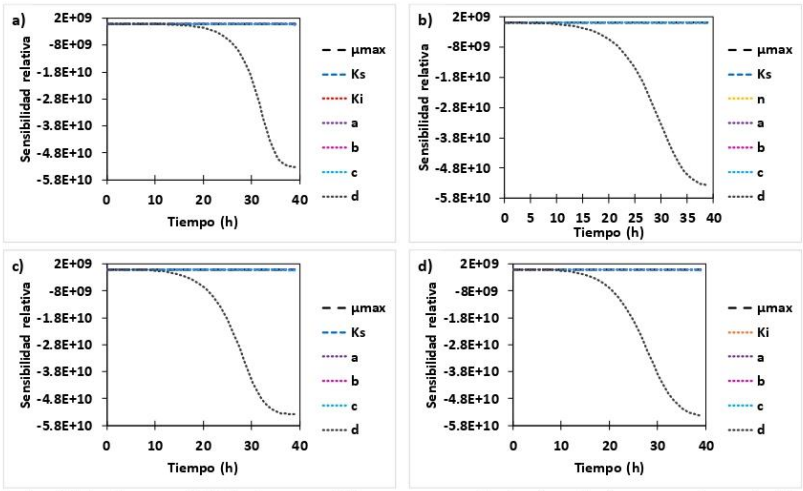

Fig 3. Análisis de sensibilidad paramétrica con rendimientos de tercer orden. a) Aiba, b) Luong, c) Monod, d) Tessier.

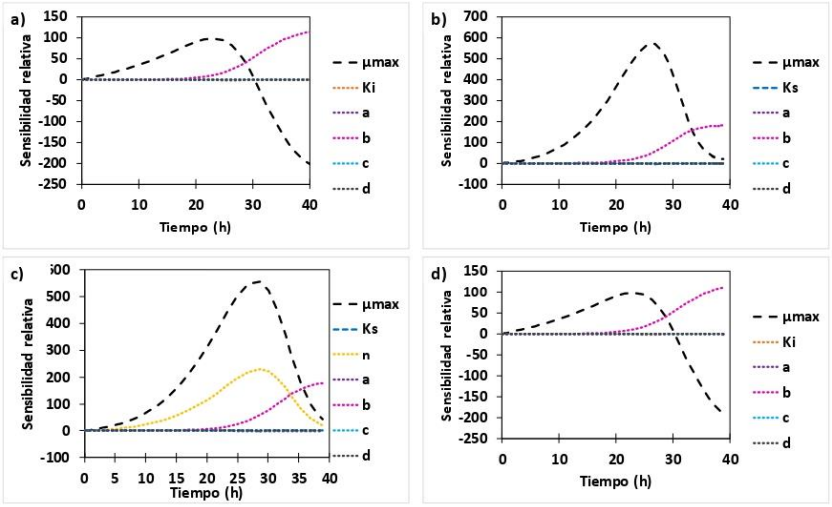

Fig 4. Análisis de sensibilidad paramétrica con rendimientos del tipo exponencial. a) Aiba, b) Luong, c) Monod, d) Tessier.

En la tabla 2, se muestran los parámetros que tuvieron mayor sensibilidad relativa, donde de manera general el parámetro más sensible es la velocidad máxima de crecimiento, excepto cuando se usan rendimientos de segundo orden siendo el parámetro más sensible el coeficiente de segundo orden.

Tabla 2. Parámetros cinéticos.

Modelos cinéticos	**Rendimientos**			
	Constante $Y_{S/X} = a$	Segundo orden $Y_{S/X} = a + b + c^2$	Tercer orden $Y_{S/X} = a + b + c^2 + d^3$	Tipo exponencial $Y_{S/X} = \frac{a}{b + c(e^{-d})}$
Aiba	μ_{max}	*c*	μ_{max}	μ_{max}, *b*
Luong	μ_{max}	*c*	μ_{max}	μ_{max}, *b*, *n*
Monod	μ_{max}	*c*	μ_{max}	μ_{max}, *b*
Tessier	μ_{max}	*c*	μ_{max}	μ_{max}, *b*

Es de esperarse que para la mayoría de los casos la μ_{max}, sea uno de los parámetros que vuelve mas sensible a los a las variables de estado en el sistema. Esto se debe a que es un coeficiente que multiplica al resto del modelo que se encuentra en ambos balances de materia. Por esa razón, se puede esperar que a valores alejados del estimado provoque un cambio drástico en las variables de estado. En el caso de con rendimientos variables de segundo orden, el coeficiente que se encuentra asociado al termino cuadrático del rendimiento, es el que provoco mayor sensibilidad al sistema. Esto se debe a que, por la naturaleza del término cuadrático con valores muy altos de su coeficiente, provoca que el valor de la ecuación aumente significativamente. Para el caso del rendimiento tipo exponencial el factor *c,* se encuentra como denominador de la ecuación y en casos de valores grandes de *c*, el valor de la ecuación de rendimiento también se vuelve grande provocando que el sistema se vuelva sensible al parámetro.

Resultados similares han sido reportados en trabajos previos [7, 14], coincidiendo en diversos parámetros como la velocidad máxima de crecimiento y los rendimientos.

CONCLUSIÓN

La industria biotecnológica involucrada en la biolixiviación de metales exige diseñar estrategias experimentales con menos interrupciones por error y una mayor eficiencia en el uso de los recursos. Por ello, es importante tener información que pueda ayudar a tener una mejor elección del modelo cinético que se utilizara para representar y estudiar los sistemas de interés. En este trabajo se logró determinar, los modelos que tienen mayor sensibilidad a sus parámetros. Lo que puede permitir a futuro, una mejor elección del modelo para estudiar este sistema y proponer condiciones que reduzcan el número de experimentos.

REFERENCIAS

[1]Parker-P S. (2012), Concise Encyclopedia of science & technology. New York.

[2]Brandl-Helmut (2008), Microbial Leaching of Metals. Biotechnology Set 191-224. doi: 10.1002/9783527620999.ch8k

[3]Bosecker Klaus (1997). Bioleaching: metal solubilization by microorganisms, FEMS Microbiology Reviews, 20 591-604.

[4]Dorofeev-A. G, Glagolev-M. V., Bondarenko-T. F. y Panikov, N.S. (1992). Unusual Kinetics of Growth of Arthrobacter globiformis and Its Explanation, Mikrobiologiya, 61 (1), p. 33.

[5]Crooke P., Wei C.-J. y Tanner R. (1980). The effect of the specific growth rate and yield expressions on the existence of oscillatory behavior of a continuous fermentation model, , Chemical. Engineering, 6, 333-339.

[6] 8. Huang X. y Zhu L. (2005), A Three Dimensional Chemostat with Quadratic Yields, Journal Mathematics Chemical, 38:4, 575-588.

[7]Velazquez-Sánchez H-I, Montes-Horcasitas M-C y Aguilar-López R. (2014). Development of a phenomenological kinetic model for butanol production using Clostridium beijerinckii, Revista Mexicana de Ingeniería Química, 13:1, 103-112.

[8]Gunawan R., Cao Y., Petzold L. y Doyle F-J. (2005). Sensitivity Analysis of Discrete Stochastic Systems, Biophysical Journal, 88, 2530-2540.

[9] Figueroa-Estrada J-C, Velázquez-Sanchez H-I, Rodríguez-Vázqueza R y l Neria-González M-A, (2017) Influencia de rendimientos constantes y variables en la determinación de parámetros cinéticos para thiobacillus ferrooxidans, XXXVIII Encuentro Nacional de la AMIDIQ, 143-148.

[10]Aiba S., (1982), Growth kinetics of photosynthetic microorganisms, Advances in Biochemical Engineering. 23, 85-156.

[11] 9. Luong J-H-T, (1987) Generalization of Monod kinetics for analysis of growth data with substrate inhibition, Biotechnology and Bioengineering, 29:. 242- 248.

[12]Robinson J-A. y Tiedje J-M., (1983) Nonlinear estimation of Monod growth kinetic parameters from a single substrate depletion curve. Applied and Environmental Microbiology, 45:5, 1453-1458.

[13]Nelson M-I. y Sidhu H-S., (2009), Analysis of a chemostat model with variable yield coefficient: Tessier kinetics, Journal of Mathematical Chemistry, 46: 2, 303-321.

[14] Grijalva-Hernández F, Velázquez-Sánchez H-I, Figueroa-Estrada J-C y Aguilar-López R. (2017), Bio-hydrogen Production by Sulphate-Reducing Bacteria: Importance of the Parametric Sensibility Analysis in the System's Modeling, Biohydrogen: Production, Applications and Technology,

UNIVERSIDAD JUÁREZ AUTÓNOMA DE TABASCO
"ESTUDIO EN LA DUDA. ACCIÓN EN LA FE"

División Académica de Ingeniería y Arquitectura

UJAT

IQ-UJAT

Otorga la presente

CONSTANCIA

A: JUAN CARLOS FIGUEROA ESTRADA, JUAN CARLOS FIGUEROA ESTRADA, RICARDO AGUILAR LÓPEZ, MARÍA ISABEL NERIA GONZÁLEZ

Por presentar el trabajo titulado: **"ANÁLISIS DE ESTABILIDAD EN UN REACTOR CONTINUO BAJO DIVERSOS MODELOS CINÉTICOS PARA UN PROCESO DE BIOLIXIVIACIÓN"** en modalidad **PÓSTER**, en el tópico **SIMULACIÓN Y OPTIMIZACIÓN**, en el marco del **5to. Congreso Nacional de Ingeniería Química UJAT 2018** "Avances e Impacto de la Ingeniería Química en el Entorno Social e Industrial", llevado a cabo en las instalaciones del Centro Internacional de Vinculación y Enseñanza (CIVE).

Villahermosa, Tabasco, México del 09 al 11 de octubre de 2018

Dr. Germán Pérez Hernández
Director de la DAIA

UNIVERSIDAD JUÁREZ AUTÓNOMA DE TABASCO
DIVISIÓN ACADÉMICA DE INGENIERÍA Y ARQUITECTURA
DIRECCIÓN

Dra. Mayra Agustina Pantoja Castro
Presidente del Comité Organizador

FOLIO: IQ/CDCE/2018/025/111

ANÁLISIS DE ESTABILIDAD EN UN REACTOR CONTINUO BAJO DIVERSOS MODELOS CINÉTICOS PARA UN PROCESO DE BIOLIXIVIACIÓN

ANALYSIS OF STABILITY IN A CONTINUOUS REACTOR UNDER VARIOUS KINETIC MODELS FOR A BIOLIXIVIATION PROCESS

Juan Carlos Figueroa Estrada[1, 2], Ricardo Aguilar López[1], María Isabel Neria González[2, *]

[1] División de Ingeniería Química y Bioquímica, Tecnológico de Estudios Superiores de Ecatepec (TESE), Av. Tecnológico S/N, Valle de Anáhuac, CP. 55210, Ecatepec de Morelos, México, México.

[2] Departamento de Biotecnología y Bioingeniería, Centro de Investigación y de Estudios Avanzados del Instituto Politécnico Nacional (CINVESTAV), Av. Instituto Politécnico Nacional, Col. San Pedro Zacatenco, CP. 07360, Ciudad de México, México.

*ibineria@hotmail.com

RESUMEN

Los reactores continuos de tanque agitado (CSTR), son equipos usados en la industria de transformación química y bioquímica. Los problemas operacionales de estas unidades se deben a la no linealidad de las variables de estado. El análisis de bifurcación es una poderosa herramienta que permite encontrar y caracterizar las regiones de operación según el parámetro de bifurcación. En aplicaciones a bioprocesos, los microorganismos suelen presentar comportamientos altamente no lineales y la aplicación de rendimientos variables en su modelado es útil para explicar el comportamiento característico en estos procesos.

La industria hidrometalúrgica, es un área especial de interés para explotar el uso de modelos cinéticos enfocados a la lixiviación de metales. *Thiobacillus Ferrooxidans* es un microorganismo modelo en procesos de biolixiviación, se ha reportado que interviene en la liberación de metales a partir de minerales sulfurados. Es por ello, que el objetivo de este trabajo es estudiar la estabilidad local y regiones optimas de operación para un proceso de biolixiviación con *T. ferrooxidans* mediante un análisis de bifurcación. Se utilizaron cuatro modelos cinéticos no estructurados (Aiba, Luong, Monod y Tessier), y cuatro estructuras de rendimiento sustrato/biomasa

(constante, segundo orden, tercer orden y tipo exponencial). En este trabajo se eligió a la tasa de dilución como parámetro de bifurcación y el análisis se realizó en MATLAB 2017 con el paquete Matcont v.2.4. Todos los casos estudiados fueron estables y principalmente los modelos con rendimientos de segundo orden presentaron regiones óptimas diferentes a las de lote que favorecen la lixiviación de metales.

Palabras clave: CSTR, *bifurcación, biolixiviación, rendimientos, T. Ferrooxidans*.

ABSTRACT

Continuous agitated tank reactors (CSTR) are equipment used in the chemical and biochemical transformation industry. The operational problems of these units are due to the non-linearity of the state variables. The bifurcation analysis is a powerful tool that allows finding and characterizing the operating regions according to the bifurcation parameter. In applications to bioprocesses, microorganisms tend to exhibit highly non-linear behavior and the application of variable yields in their modeling is useful to explain the characteristic behavior in these processes. The hydrometallurgical industry is a special area of interest to exploit the use of kinetic models focused on the leaching of metals. Thiobacillus Ferrooxidans is a model microorganism in bioleaching processes, it has been reported that it intervenes in the release of metals from sulphide minerals. That is why, the objective of this work is to study the local stability and optimal operating regions for a bioleaching process with T. ferrooxidans by means of a bifurcation analysis. Four unstructured kinetic models (Aiba, Luong, Monod and Tessier), and four substrate / biomass performance structures (constant, second degree, third degree and exponential type) were used. In this work,

the dilution rate was chosen as the bifurcation parameter and the analysis was performed in MATLAB R2007a with the Matcont package v.2.4. All the cases studied were stable and mainly the models with second grade yields presented optimal regions different from the batch ones that favor the leaching of metals.

Keywords: CSTR, bifurcation, bioleaching, yields, *T. Ferrooxidans*.

INTRODUCCIÓN

La biolixiviación es un proceso descrito como la disolución de metales a partir de su fuente mineral por ciertos microorganismos o el uso de estos para transformar elementos que se pueden extraer de un material cuando el agua se filtra a través de este [1, 2, 3, 4]. Como resultado, el metal oxidado permanece en los residuos sólidos en una forma más concentrada [2]. En general, un biorreactor se puede modelar con un sistema de ecuaciones diferenciales. Si se asume uniformidad (mezcla perfecta) dentro del biorreactor, solo ocurren variaciones respecto al tiempo, y el sistema se puede describir con un grupo de ecuaciones diferenciales ordinarias de primer orden. Según el grado de no linealidad que exhiba el sistema dinámico, se pueden observar diferentes tipos de comportamientos que son propios de estos sistemas, tales como multiplicidad de estados estacionarios (o puntos de equilibrio), periodicidad, bifurcaciones y caos [5, 6]. Una bifurcación se da cuando una pequeña variación en los valores de los parámetros de un sistema causa un brusco cambio "cualitativo" o topológico en su comportamiento. Los estados estacionarios se obtienen a partir del análisis del modelo del sistema, al igualar las derivadas a cero. Ya que generalmente el sistema está dado por

un numero de ecuaciones no lineales y puede haber más de un estado estacionario para un grupo de valores. El carácter de un estado estacionario se determina linealizando el sistema de ecuaciones diferenciales alrededor del estado estacionario, y calculando los valores propios (λ) de la matriz Jacobiana resultante, las características de los valores propios se describen en la tabla 1. Además de determinar las características de los estados estacionarios en un análisis de bifurcación, es posible determinar regiones o condiciones de operación convenientes o inconvenientes según el parámetro analizado..

Tabla 1. Clasificación de estados estaciones para un sistema bidimensional, adaptada de Paz Astudillo [5].

Valores propios	Signo	Clasificación	Descripción	Retrato fase
Ambos son reales $\boldsymbol{\lambda_1, \lambda_2 \in \Re}$	$\lambda_1, \lambda_2 < 0$	Nodo estable	Las trayectorias se dirigen al punto de equilibrio.	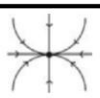
	$\lambda_1, \lambda_2 > 0$	Nodo inestable	Las trayectorias se dirigen hacia fuera del punto de equilibrio.	
	$\lambda_1 > 0,\ \lambda_2 < 0,$ $\lambda_1 < 0,\ \lambda_2 > 0$	Silla	Las trayectorias se dirigen hacia fuera del punto de equilibrio.	
Complejos conjugados $\boldsymbol{\lambda_1, \lambda_2 \in \mathbb{C}}$ $\boldsymbol{\lambda_{1,2} = \alpha \pm j\beta}$ **α:parte real** **β:parte imaginaria**	$\alpha_{1,2} < 0$	Foco estable	Las trayectorias se dirigen hacia fuera del punto de equilibrio.	
	$\alpha_{1,2} > 0$	Foco inestable	Las trayectorias se dirigen hacia fuera del punto de equilibrio.	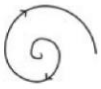

METODOLOGÍA

En consecuencia, en el campo de la biotecnología resulta interesante el estudio de bacterias con capacidad de biolixiviación de metales y su comportamiento cinético por medio de modelos matemáticos. En el presente trabajo se realizó un análisis de bifurcación utilizando a la tasa de dilución como parámetro.

Modelos cinéticos y rendimientos. Los modelos cinéticos ecuaciones de rendimientos fueron obtenidos de un trabajo previo reportado [7]. Que corresponde a los modelos cinéticos de Aiba (Ec. 1), [8]; Luong (Ec. 2), [9]; Monod (Ec. 3), [10] y Tessier (Ec. 4), [11]. Además, de los rendimientos del tipo constante y variable

$$\mu(S) = \mu_{max} \frac{S}{(K_S+S)\left(1+\frac{S}{K_i}\right)} \quad (1)$$

$$\mu(S) = \mu_{max} \frac{S^n}{K_S+S^n} \quad (2)$$

$$\mu(S) = \mu_{max} \frac{S}{K_S+S} \quad (3)$$

$$\mu(S) = \mu_{max} \left(1 - e^{\frac{-S}{Ki}}\right) \quad (4)$$

$$Y_{S/X} = 117.08 \quad (5)$$

$$Y_{S/X} = 174.76 - 3.08x10^{-2}S + 3.33x10^{-6}S^2 \quad (6)$$

$$Y_{S/X} = 109.175 + 0.028S - 8.564x10^{-6}S^2 - 7.644x10^{-6}S^3 \quad (7)$$

$$Y_{S/X} = \frac{46.524}{0.314+85152424448e^{-892S}} \quad (8)$$

s.

Donde: K_s y K_i, son constantes de afinidad al sustrato en (mg L^{-1}); n es un exponente adimensional; S es la concentración de sustrato (mg L^{-1}); μ_{max}, es la velocidad máxima de crecimiento de *T. ferrooxidans* (h^{-1}); $\mu(S)$, velocidad especifica de crecimiento (mg L^{-1} h^{-1}); *a, b, c, d, p, r, v, y z* son los coeficientes correspondientes de las ecuaciones de rendimientos. $Y_{S/X}$, corresponde al.

rendimiento sustrato/biomasa. La tabla 1 muestra los valores de los parámetros.

Tabla 1. Parámetros cinéticos.

	Modelo			
	Aiba	Luong	Monod	Tessier
μ_{max}	0.115	0.14	0.139	0.115
K_S	1200	1980	2453.92	-------
K_i	130000	-------	-------	3500
n	-------	0.95	-------	-------

Las ecuaciones 9 y 10 muestran los balances de materia para biomasa (X), y sustrato (S).

$$\frac{dX}{dt} = \mu(S)X \quad (9)$$

$$\frac{dS}{dt} = \mu(S)XY_{S/X} \quad (10).$$

Modelos cinéticos y rendimientos. En este trabajo se eligió a la tasa de dilución como parámetro de bifurcación y el análisis se realizó en MATLAB 2017 con el paquete Matcont v.2.4.

RESULTADOS Y DISCUSIÓN

Las figuras 1-4, muestran las gráficas correspondientes de los estados estacionarios más relevantes utilizando a la tasa de dilución como parámetro de bifurcación.

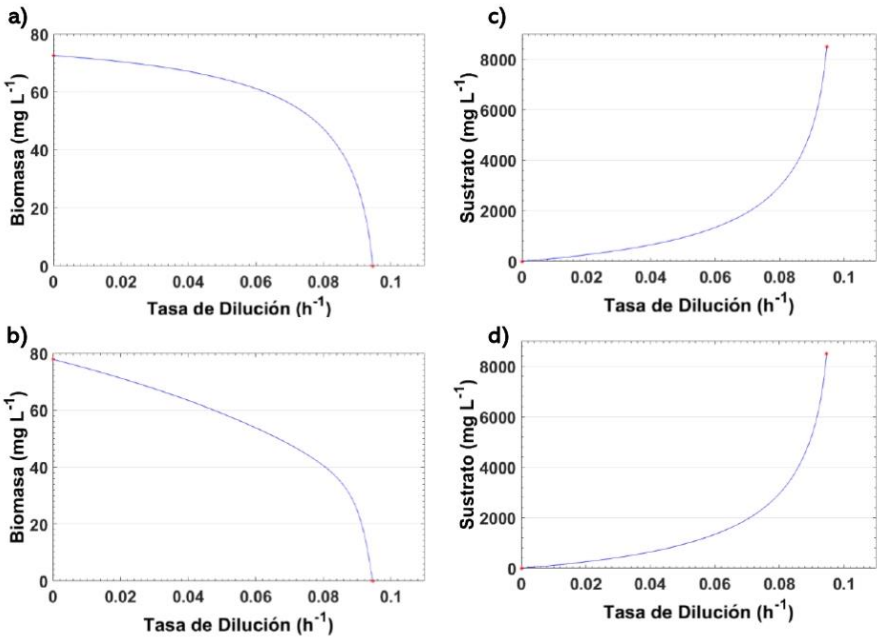

Fig 1. Estados estacionarios de la concentración de biomasa y sustrato con la tasa de dilución como parámetro de bifurcación para el modelo de Aiba. a) y b) Rendimiento constante; c) y d) Rendimiento de tercer orden.

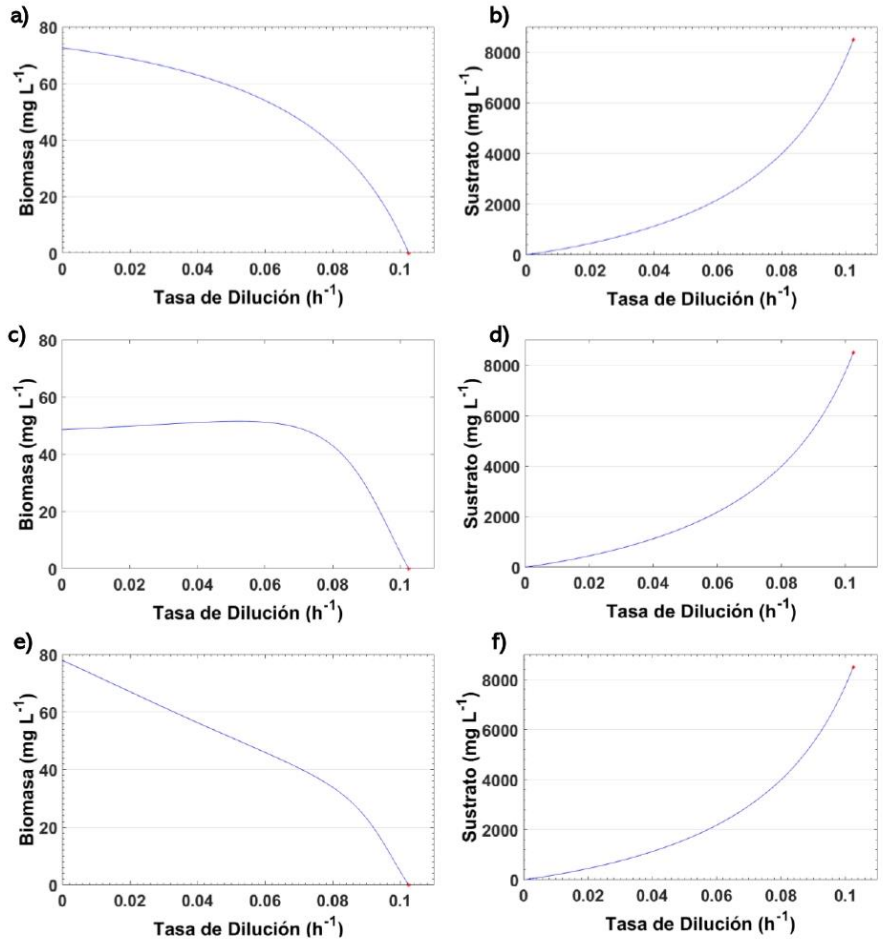

Fig 2. Estados estacionarios de la concentración de biomasa y sustrato con la tasa de dilución como parámetro de bifurcación para el modelo de Luong. a) y b) Rendimiento constante; c) y d) Rendimiento de segundo orden; e) y f) Rendimiento de tercer orden.

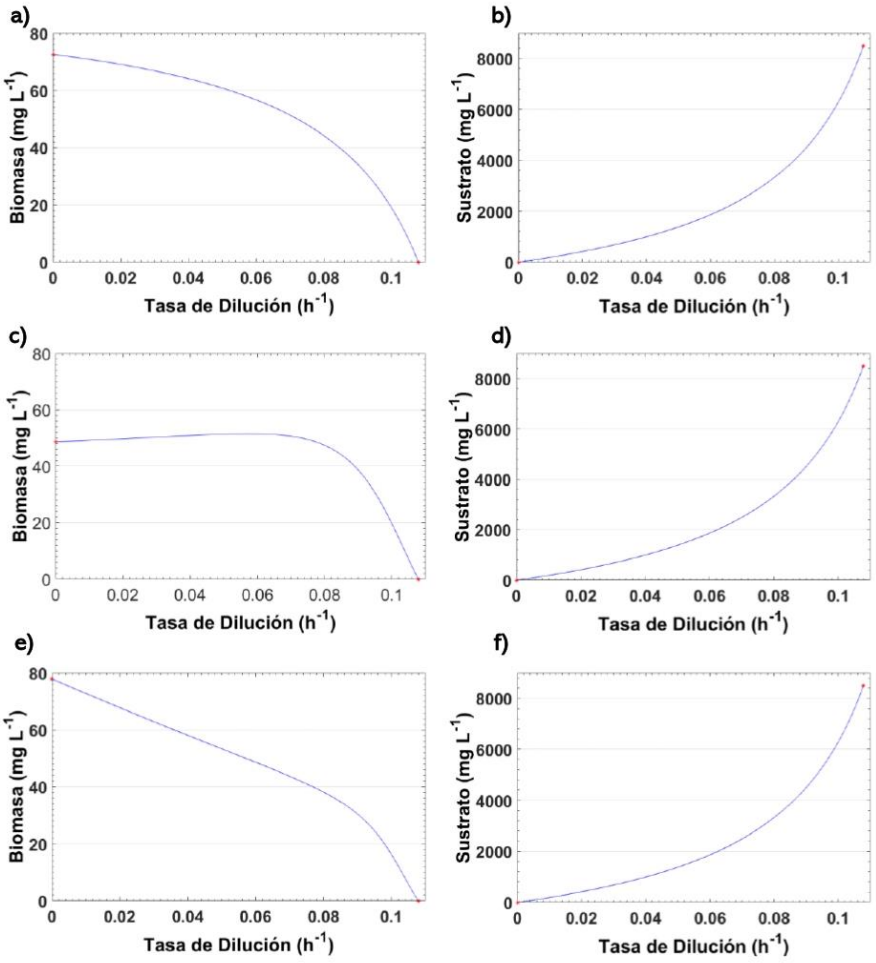

Fig 3. Estados estacionarios de la concentración de biomasa y sustrato con la tasa de dilución como parámetro de bifurcación para el modelo de Monod. a) y b) Rendimiento constante; c) y d) Rendimiento de segundo orden; e) y f) Rendimiento de tercer orden.

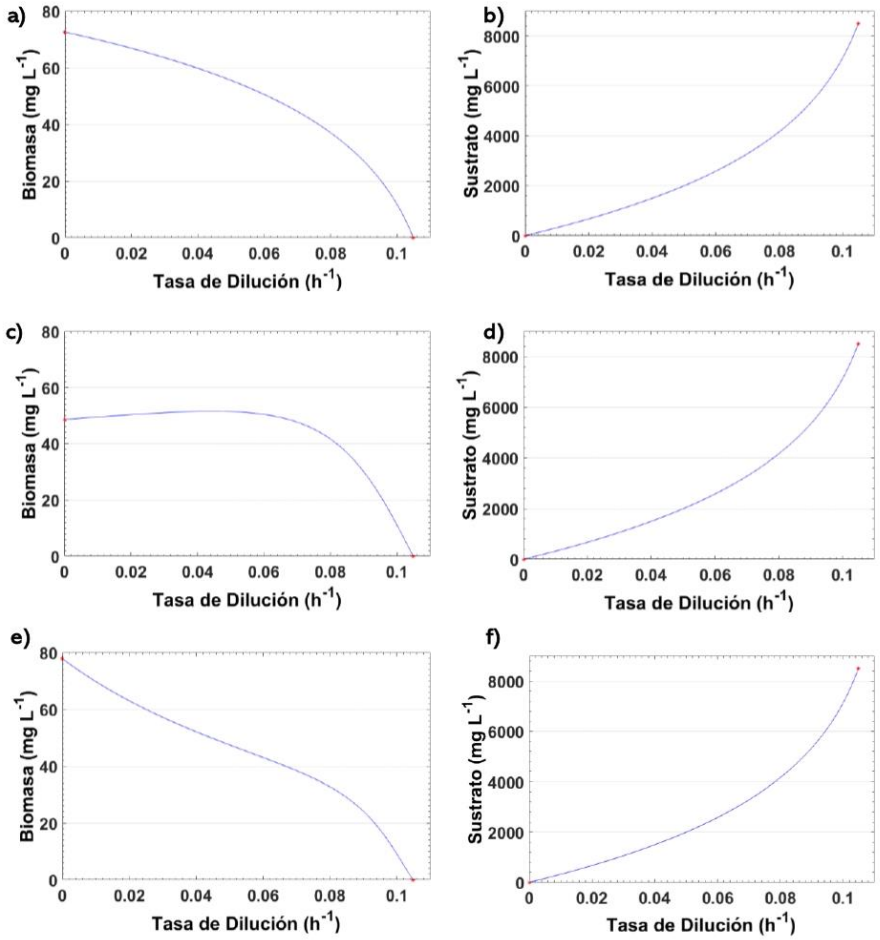

Fig 4. Estados estacionarios de la concentración de biomasa y sustrato con la tasa de dilución como parámetro de bifurcación para el modelo de Tessier. a) y b) Rendimiento constante; c) y d) Rendimiento de segundo orden; e) y f) Rendimiento de tercer orden.

Todos los valores propios calculados para los puntos estacionarios de los modelos cinéticos con los cuatro tipos de rendimientos se obtuvieron con valores negativos (Datos no mostrados). Lo que indica que todos los puntos estacionarios son estables. Respecto a las graficas de puntos estacionarios se observo que, en todos los modelos cinéticos de Luong, Monod y Tessier con rendimientos variables de segundo orden, la concentración de biomasa aumenta casi proporcionalmente respecto a la tasa de dilución, mientras que la concentración de sustrato aumenta casi de manera exponencial respecto a la tasa de dilución. Esto de alguna manera no se esperaría, ya que para que aumente la biomasa debe existir una relación indirecta que disminuya la concentración de sustrato, lo cual ya ha sido reportado con datos experimentales [12]. Con el resto de los rendimientos variables los modelos cinéticos mostraron tendencias similares de las concentraciones en estado estacionario con las concentraciones más altas de biomasa cuando la tasa de dilución se hace cero, y en todos los casos se muestra consistente la tasa de lavado del reactor cuando se tiene una tasa de dilución cercana a 0.1 h^{-1}. Los resultados reportados en este trabajo indican que al menos para el caso de estudio, el uso de ecuaciones de rendimiento de segundo orden muestras resultados inconsistentes con la naturaleza real del sistema de biolixiviación.

CONCLUSIÓN

El análisis realizado en este trabajo, aporta información importante para estudiar y elegir modelos cinéticos. También contribuye con información que puede ser interesante para proponer condiciones de operación. Esta información en conjunto permite tener una mejor elección de un modelo. Además, esta metodología puede utilizarse para otros sistemas.

REFERENCIAS

[1]Parker-P S. (2012), Concise Encyclopedia of science & technology. New York.

[2]Bosecker Klaus (1997). Bioleaching: metal solubilization by microorganisms, FEMS Microbiology Reviews, 20 591-604.

[3]Dorofeev-A. G, Glagolev-M. V., Bondarenko-T. F. y Panikov, N.S. (1992). Unusual Kinetics of Growth of Arthrobacter globiformis and Its Explanation, Mikrobiologiya, 61 (1), p. 33.

[4]Brandl-Helmut (2008), Microbial Leaching of Metals. Biotechnology Set 191-224. doi: 10.1002/9783527620999.ch8k

[5]Paz-Astudillo I-C , Carlos y Cardona-Alzate A. (2011), Influencia de las regiones de estabilidad del biorreactor en la producción eficiente de alcohol carburante, Revista Colombiana de Biotecnología, 13: 1 1-12.

[6]Crooke P., Wei C.-J. y Tanner R. (1980). The effect of the specific growth rate and yield expressions on the existence of oscillatory behavior of a continuous fermentation model, Chemical. Engineering, 6, 333-339.

[7] Figueroa-Estrada J-C, Velázquez-Sanchez H-I, Rodríguez-Vázqueza R y l Neria-González M-A, (2017) Influencia de rendimientos constantes y variables en la determinación de parámetros cinéticos para thiobacillus ferrooxidans, XXXVIII Encuentro Nacional de la AMIDIQ, 143-148.

[8]Aiba S., (1982), Growth kinetics of photosynthetic microorganisms, Advances in Biochemical Engineering. 23, 85-156.

[9]Luong J-H-T, (1987) Generalization of Monod kinetics for analysis of growth data with substrate inhibition, Biotechnology and Bioengineering, 29:. 242- 248.

[10]Robinson J-A. y Tiedje J-M., (1983) Nonlinear estimation of Monod growth kinetic parameters from a single substrate depletion curve. Applied and Environmental Microbiology, 45:5, 1453–1458.

[11]Nelson M-I. y Sidhu H-S., (2009), Analysis of a chemostat model with variable yield coefficient: Tessier kinetics, Journal of Mathematical Chemistry, 46: 2, 303-321.

[12]Biagiola, S., Solsona, J. y Milocco R., (2000), Estimation of kinetic rates in batch Thiobacillus ferrooxidans cultures, Journal of Biotechnology, 84, 13-25.

Доклади на Българската академия на науките
Comptes rendus de l'Académie bulgare des Sciences
Tome 72, No 7, 2019

ENGINEERING SCIENCES
Automatics and informatics

DESIGN OF A CLASS OF SUPER TWISTING SLIDING-MODE CONTROLLER: APPLICATION TO BIOLEACHING PROCESS

Juan Carlos Figueroa-Estrada, María Isabel Neria-González*, Ricardo Aguilar-López

(*Submitted by Academician M. Hadjiiski on May 22, 2018*)

Abstract

The main issue of this work is to propose a class of feedback controller under the framework of sliding-mode theory applied to nonlinear system for regulation purposes. This control methodology is able to regulate a class of nonlinear systems by compensating the upper bound of the main nonlinearity of the controlled system and imposing a desired dynamic behaviour, in this case to induce finite time stability. The stability of the system under the proposed controller is provided via the analysis of the regulation error dynamic. The control law is applied to a class of continuous reactor for bioleaching purposes with success, comparing its performance with a standard super twisting sliding-mode (STSM) controller. Numerical experiments show the satisfactory closed-loop performance of this proposal.

Key words: bioleaching, continuous chemical reactor, finite time stability, smooth STSM controller

Introduction. An important approach in control theory is the named sliding mode control (SMC) which has been successful in the design and application of state feedback controllers. The sliding-mode technique is able to reject bounded matched disturbances, however, its main disadvantage is chattering phenomena [1, 2]. Generally, the SMC is designed by employing a discontinuous function in

Juan Carlos Figueroa-Estrada is very grateful to Consejo Nacional de Ciencia y Tecnología for the financial support via the postgraduate scholarship No. 230859.
DOI:10.7546/CRABS.2019.07.13

the control input with an ideal infinite frequency. With this framework, the chattering appears when non modelled dynamics are not considered in the nominal model of the corresponding plant. From the above, another generation of SMC named Super-twisting sliding mode control looks as an adequate alternative to the conventional first order sliding mode control for the systems of relative degree-1 in order to avoid chattering without affecting the tracking performance, making possible to obtain an explicit relation for the controller design parameters, but the inclusion of discontinuous functions in the controllers design, leads to high demanding closed-loop performance, mainly for the high effort in the control action [3–5].

As an interesting application case, the continuous stirred tank reactors (CSTR) are process equipment used in the transformation industry with chemical and biochemical approaches. The operational issues of these units are due to the large nonlinearity and high sensitivity of the state and output variables to input variations, which are characteristic of this processes. Therefore, the process dynamic is hardly predictable and controllable by standard methods, consequently the control task requires application of advanced techniques [6–10].

Under the abovementioned framework, this work proposes a smooth version of a Super-twisting sliding mode control for regulation purposes, where the closed-loop stability analysis is relatively simple by solving the dynamic equation of the named control error.

Control design. Let us consider the following state space representation of a class of nonlinear system with affine control input:

$$\dot{x} = f(x) + g(x)u \tag{1}$$

and linear measured output:

$$y = Cx.$$

Here, $x \in \mathbb{R}^n$ is the state variable vector, $f(x) : \mathbb{R}^n \to \mathbb{R}^n$ is a nonlinear vector function, where $f(x) \subset \Sigma \in C^\infty$ and Σ is a compact set, $g(x)$ is a smooth and invertible bounded function, $u \in \mathbb{R}^p$ is the exogenous control input vector and $y \in \mathbb{R}^q$ is the measured output vector.

Now, let us propose the following feedback control:

$$u = k_1 \|\epsilon\|^{\frac{1}{i}} \frac{\epsilon}{\sqrt{1+\epsilon^2}} - k_2 u_1 \tag{2}$$

$$\dot{u}_1 = \exp(-\epsilon^2), \tag{3}$$

where, $\epsilon = x - x_{ref}$ is the control error, x_{ref} is the reference signal or set point and k_1, k_2 are the design parameters of the controller.

In order to analyze the closed-loop performance of the system (1) under the feedback (2)–(3), let us construct the dynamic equations of the control error for the regulation case, i.e. x_{ref} is a constant value, therefore:

$$\dot{\epsilon} = f(x) + g(x)\left(k_1\|\epsilon\|^{\frac{1}{\iota}}\frac{\epsilon}{\sqrt{1+\epsilon^2}} - k_2\int_0^t \exp(-\epsilon^2)d\sigma\right). \tag{4}$$

Let us consider the following assumptions:

$$\|f(x)\| \leq \mathcal{F} < \infty \;\; \forall\, x \in \mathbb{R}^n \tag{5}$$

$$\|g(x)\| \leq \wp \; < \infty \; \forall\, x \in \mathbb{R}^n \tag{6}$$

and the following properties:

$$\left\|\frac{\epsilon}{\sqrt{1+\epsilon^2}}\right\| \leq 1 \tag{7}$$

$$\left\|\int_0^t \exp(-\epsilon^2)d\sigma\right\| \leq 1. \tag{8}$$

By considering the assumptions (5)–(6) and properties (7)–(8) to equation (4) and applying the Cauchy–Schwarz inequality, the inequality (9) is obtained as follows:

$$\|\dot{\epsilon}\| \leq \mathcal{F} - k_2\wp + k_1\wp\|\epsilon\|^{\frac{1}{\iota}}. \tag{9}$$

Now, considering that the parameter k_2 is selected as:

$$k_2 \cong \wp^{-1}\mathcal{F}. \tag{10}$$

Then:

$$\|\dot{\epsilon}\| \leq k_1\wp\|\epsilon\|^{\frac{1}{\iota}}. \tag{11}$$

The above inequality induces a finite time convergence of the regulation error, where parameter $\iota > 1$ is considered an odd integer. Then the solution of inequality (11) is,

$$\|\epsilon\| \leq \text{sign}(\epsilon_0)\left(\|\epsilon_0\| - \wp k_1\frac{t}{\iota}\right)^{\iota}.$$

At steady state ($\epsilon(t) = 0$),

$$t \geq \iota\frac{\|\epsilon_0\|^{\frac{1}{\iota}}}{\wp k_1}.$$

Then finite-time convergence is given by

$$t_{ft} = \iota \frac{\|\epsilon_0\|^{\frac{1}{\iota}}}{\wp k_1}, \tag{12}$$

where ϵ_0 is the initial condition of equation (11), l is an odd number, $\mathcal{F}$ and $\wp$ are the upper bounds of the nonlinear terms of the state equation (1), t_{ft} is the finite time convergence and $\|\cdot\|$ is the standard Euclidian norm. The performance of the proposed control was compared with a standard Super Twisting Sliding-Mode (STSM) controller (Equations (13)–(14)):

$$u = \; k_1 \|\epsilon\|^{\frac{1}{\iota}} \operatorname{sign}(\epsilon) + k_2 u_1 \tag{13}$$

$$\dot{u}_1 = \operatorname{sign}(\epsilon). \tag{14}$$

Bioleaching process modelling. Several kinetic models have been proposed for the bacterial oxidation of Fe^{2+} [11–16]. For this work, the biomass and Fe^{2+} concentration data were used for a batch culture with *Thiobacillus ferrooxidans* reported by Biagiola et al. [17]. The Monod model was considered to represent the growth of *T. ferrooxidans* and the oxidation of Fe^{2+}.

$$\mu = \mu_{\max} \frac{[Fe^{2+}]}{K_{Fe^{2+}} + [Fe^{2+}]},$$

where, $\mu_{\max}$ is the maximum speed of growth and $K_{Fe^{2+}}$ is the affinity constant of Fe^{2+}.

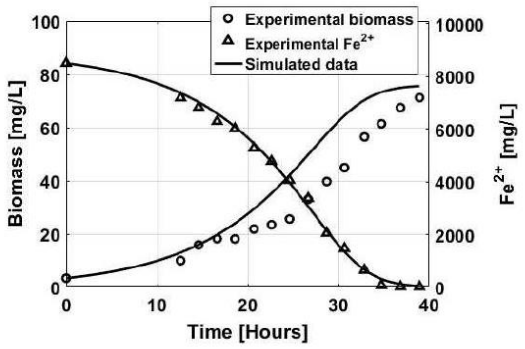

Fig. 1. Simulation of the growth of *T. ferrooxidans* and oxidation of Fe^{2+}

The values of the kinetic parameters were estimated as, $\mu_{\max} = 0.139$ 1/h, $K_{\mathrm{Fe^{2+}}} = 2453.92$ mg/L and $Y_{S/B} = 117.088$ $\mathrm{mg_{Fe^{2+}}/mg_{Biomass}}$. Subsequently, the kinetic parameters were validated by comparing the simulated values with the experimental ones. Figure 1 shows the performance of the model. For biomass, an increase in the deviation of the simulated data was observed after 18 hours, which is reflected in its correlation coefficient ($r_B^2 = 0.938$). The sensors that perform biomass measurements in line regularly do not have high precision, so the correlation coefficient is considered sufficient for this case. On the other hand, the correlation coefficient of Fe^{2+} ($r^2_{\mathrm{Fe^{2+}}} = 0.997$) indicates that the model adequately represents this variable. Finally, the overall correlation coefficient ($r_G^2 = 0.987$) was calculated by Fisher's z transformation method [18]. This value indicates that there is a strong relationship of the model simulations with the experimental data.

The controller was implemented in a stirred tank continuous reactor system (CSTR), which is described by equations (15)–(17):

$$\dot{x}_B = f(x_B) + g(x_B)u = \mu x_B - x_B u \tag{15}$$

$$\dot{x}_{\mathrm{Fe^{2+}}} = f(x_{\mathrm{Fe^{2+}}}) + g(x_{\mathrm{Fe^{2+}}})u = -\mu x_B Y_{S/B} + \left([\mathrm{Fe^{2+}}]_{in} - [\mathrm{Fe^{2+}}]\right) u \tag{16}$$

$$y = x_B, \tag{17}$$

where: $u = 0.07$ 1/h is the nominal value of the control input; $[\mathrm{Fe^{2+}}]_{in} = 8500$ mg/L is the concentration of Fe^{2+} at the reactor inlet, and y is the measured output of the reactor, in this case, the biomass concentration.

Results and discussion. In this work, the proposed controller considers a single-input single output (SISO) configuration, also it is considered the controlled variable of the biomass concentration, due to its on-line measurement capability, taking into account only regulation task, i.e. the system's trajectories are forced via the proposed controller to reach a specific set point value; which is a common closed-loop operation for chemical reactors. In order to reach an adequate closed-loop operation and improve the quantitative results, a simple bifurcation analysis is realized considering the state variables response with the corresponding control input (dilution rate) as the bifurcation parameter and selecting the operational regions, where the biomass concentration led to a minimum Fe^{2+}concentration, which is the main process objective. The above allows to select a specific set point of the biomass concentration. The operating regions were characterized under a continuous regime using the MATCONT version 5p0 program, the corresponding bifurcation diagrams were elaborated, considering the dilution rate as a bifurcation parameter. Figure 2a shows that dilution rates (u) less than 0.016 1/h are desirable to leach at least 95% of Fe^{2+}, which corresponds to a biomass concentration of $x_{ref} = 70$ mg/L which will be used as controller's set point.

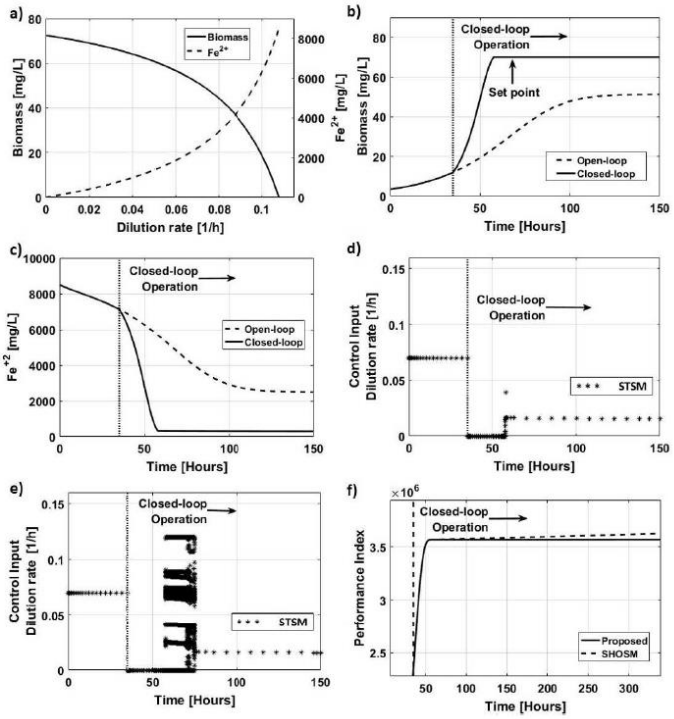

Fig. 2. a) Bifurcation diagram using the dilution rate as a bifurcation parameter. b) Dynamics of biomass with open loop and closed loop. c) Dynamics of Fe^{2+} with open loop and closed loop. d) Control action with the proposed control law. e) Control action with the standard control law. f) Dynamic behaviour of the performance index

The tuning of the controller's parameters k_1 and k_2 is based on the assumptions (5)–(6) which are adequate for a nonlinear system with bounded dynamics, in particular for the application example of the chemical reactor. From the above and by applying the Cauchy–Schwarz inequality to equation (8), the inequality (9) is obtained. It can be observed that the upper bound of the nonlinear term $\mathcal{F}$ can be compensated by choosing k_2 via equation (10), the gain $k_2 = 0.000016$ was estimated with $\mathcal{F} = 0.14$ and $\wp = 8500$. On the other hand, from equation (12) the control's gain k_1 can be selected heuristically to diminish the convergence time, it was determined as $k_1 = 0.85$.

Figure 2 (b, c) shows the difference between the operation of the bioreactor with open loop and closed loop, the set point value is reached in less than 22 hours

since the control law is activated, increasing by 26% more the Fe^{2+} concentration leached. In addition, Fig. 2 (d, e) shows that the proposed control law has a smooth and less control effort compared to the control law STSM, which suffer the chattering for the inclusion of the discontinuous *sign* function. This is an advantage of the proposed control law, since excessive control actions tend to increase operating costs and reduce the life time of the actuators used in these operations. Finally, a comparison was made with the standard STSM controller under the same closed-loop gains using the Integral Time Square Error (ITSE) performance index, which penalizes control errors at long times. Figure 2f shows the better performance of the proposed controller.

Conclusions. In this work smooth functions in a class of STSM controller are proposed in order to diminish the chattering phenomena, which are present in the standard version of the STSM structure due the discontinuous nature of the *sign* function. Via the analysis of the dynamic of the control error and considering its upper bound behaviour by applying the Cauchy–Swartz inequality the closed-loop stability is assured in a finite time. As an application case, the proposed controller is implemented via numerical simulation to a class of continuous bioreactor for the Fe^{2+} oxidation with metal leaching potential, considering a kinetic model corroborated with experimental data. The implementation of the proposed controller showed that it is possible to stabilize the system in the chosen set point with less control effort. The proposed controller has a good performance compared to the classic version of STSM control.

Acknowledgements. Juan Carlos Figueroa-Estrada is very grateful to CINVESTAV-IPN and TESE for providing the research facilities to develop this work.

REFERENCES

[1] Kamal S., J. A. Moreno, A. Chalanga, B. Bandyopadhyay, L. M. Fridman (2016) Continuous terminal sliding-mode controller, Automatica, **69**, C, 308–314.

[2] Sundarapandian V., L. Chang-Hua (2017) Applications of Sliding Mode Control in Science and Engineering (ed. Vaidyanathan, Sundarapandian, Lien, Chang-Hua), Springer International Publishing, 435–470.

[3] Rivera J., L. Garcia, C. Mora, J. J. Raygoza, S. Ortega (2011) Supertwisting Sliding Mode in Motion Control Systems (ed. Andrzej Bartoszewicz), In-Tech, 237–254.

[4] Levant A. (2005) Homogeneity approach to high-order sliding mode design, Automatica, **41**(5), 823–830.

[5] Levant A. (1993) Sliding order and sliding accuracy in sliding mode control, Int. J. Control, **58**(6), 1247–1263.

[6] Wallama F., A. Y. Memon (2017) A robust control scheme for nonlinear non-isothermal uncertain jacketed continuous stirred tank reactor, Journal of Process Control, **51**, 55–67.
[7] Hashemi M., J. Askari, J. Ghaisari (2016) Adaptive control of uncertain nonlinear time delay systems in the presence of actuator failures and applications to chemical reactor systems, European Journal of Control, **29**, 62–73.
[8] Saini P., R. Kumar, P. Sharma, N. Rajput (2016) Design and Comparative Analysis of Controllers for Continuous Stirred Tank Reactor (CSTR), Proceedings of International Conference on Intelligent Communication, Control and Devices. (eds Rajesh Singh, Sushabhan Choudhury), Singapore, Springer, 351–365.
[9] Pellegrini L., G. Biardi (2001) Chaotic behaviour of a controlled CSTR, Computers & Chemical Engineering, **14**(11), 1237–1247.
[10] Bandyopadhyay B., A. Upadhye, O. Ismail (1997) $\gamma - \delta$ Routh Approximation for Interval Systems, IEEE Transactions on Automatic Control, **42**(8), 1127–1130.
[11] Watling H. R. (2006) The bioleaching of sulphide minerals with emphasis on copper sulphides – A review, Hydrometallurgy, **84**(1–2) 81–108.
[12] Meruane, G., C. Salhe, J. Wiertz, T. Vargas (2002) Novel electrochemical-enzymatic model which quantifies the effect of the solution Eh on the kinetics of ferrous iron oxidation with *Acidithiobacillus ferrooxidans*, Biotechnology and Bioengineering, **80**(3), 280–288.
[13] Boon M., C. Ras, J. Heijnen (1999) The ferrous iron oxidation kinetics of *Thiobacillus ferrooxidans* in batch cultures, Applied Microbiology and Biotechnology, **51**(6), 813–819.
[14] Nemati M., C. Webb (1998) Inhibition effect of ferric iron on the kinetics of ferrous iron, Biotechnology Letters, **20**(9), 873–877.
[15] Crundwell F. (1997) The kinetics of the chemiosmotic proton circuit of the iron-oxidizing bacterium *Thiobacillus ferrooxidans*, Bioelectrochemistry and Bioenergetics, **43**(1), 115–122.
[16] Hansford G. S. (1997) Recent development in modelling the kinetics of bioleaching (ed. Rawlings), Berlin, Springer, 153–176.
[17] Biagiola S., J. Solsona, R. Milocco (2000) Estimation of kinetic rates in batch *Thiobacillus ferrooxidans* cultures, Journal of Biotechnology, **84**(17), 13–25.
[18] Zar J. (2014) Spearman Rank Correlation: Overview, Wiley Statsref: Statistics Reference Online, 1–9.

Biotechnology and
Bioengineering Department
Center of Research and
Advances Studies
of the National Polytechnic
Institute (CINVESTAV)
Av. National Polytechnic Institute
2508 Col. San Pedro Zacatenco
07360 México City, México
e-mail: raguilar@cinvestav.mx

**Chemical and Biochemical*
Engineering Division
Tecnológico de Estudios
Superiores de Ecatepec (TESE)
Av. Tecnológico S/N,Valle de Anahuac
55210 Ecatepec de Morelos, México

Minerals Engineering 157 (2020) 106549

Contents lists available at ScienceDirect

Minerals Engineering

journal homepage: www.elsevier.com/locate/mineng

Controlling a continuous stirred tank reactor for zinc leaching

J.C. Figueroa-Estrada[a], M.I. Neria-González[b], R. Rodríguez Vázquez[a], E.N. Tec-Caamal[a], R. Aguilar-López[a,*]

[a] Department of Biotechnology and Bioengineering, CINVESTAV-IPN, San Pedro Zacatenco, Mexico City, Mexico
[b] Chemical and Biochemical Engineering Division, Tecnológico de Estudios Superiores de Ecatepec, Ecatepec, Edo. de México, Mexico

ARTICLE INFO

Keywords:
Smooth STSM controller
Continuous chemical reactor
Zinc leaching
Oxidation

ABSTRACT

This work focuses on the open-loop and closed-loop analysis of a continuous stirred tank reactor for zinc leaching from sphalerite (ZnS) via modeling and simulation approaches. The corresponding process analysis is based on a multi-input multi-output, approach by considering the inlet flows of minerals, acid solution, and aeration as process inputs and dissolved oxygen, ZnS concentrations, and pH as process outputs. An analysis of the relative gain array matrix was performed to determine the best control input pairs. In addition, a bifurcation analysis was carried out considering the process inputs as bifurcation parameters to show adequate operating regions. A local stability analysis of the selected equilibrium points in the chemical reactor under the previously selected operating conditions is presented, employing an eigenvalue analysis. Finally, a class of smooth super twisting sliding-mode controller is proposed to regulate the corresponding dissolved oxygen and pH in the reactor, which leads to increased sphalerite leaching; its performance was compared with a standard super twisting sliding-mode controller. The controllability of the reactor was analyzed via the dynamic behavior of the uncontrolled variables (zero dynamics). Numerical experiments show the satisfactory performance of the proposed controller under the selected operating conditions.

1. Introduction

Chemical reactors are process equipment with highly non-linear behavior due to the complex nature of the reactions. Therefore, the basic aspects of operation are complicated, such as selecting the input/output pairs, the local control capacity characteristics, the stability of the open and closed-loop operation, and the selection of regions of operation. For this reason, it is important to use optimization and/or control strategies that allow improving the process performance. Unfortunately, whole operation analyses for leaching systems are not frequent in the open literature. There are tools that can help improve the design and operation of reactors. The relative gain matrix (RGA) is an analysis that allows obtaining parameters to select the best input/output pairs (Jain and Babu, 2015; Valverde-Pérez et al., 2016; Yin and Liu, 2017). Bifurcation analysis allows the identification of possible operating regions with high performance, determining the responses of variables at steady-state under selected variations of some parameter (Velázquez-Sánchez et al., 2019; Velázquez-Sánchez and Aguilar-López, 2018). In addition, for control purposes, the local stability of the operating regions can be determined through the analysis of their eigenvalues (Lyapunov's first method). The objective and control strategies are oriented to reach and maintain the mass concentrations of the selected chemical species at the reactor outlet conditions by manipulating some reactor control input (Liu and Granata, 2018; Zhou et al., 2018). The regulation tasks for chemical reactors have been achieved with linear PID, predictive, adaptive, fuzzy, neural, and I/O linearizing controllers, among others that have been successful in the design and application of state feedback controllers (Ali Reza and Mehdi, 2017; Flores-Hernández et al., 2018).

In particular, the named sliding-mode systems are designed to bring the process states onto a specific and stable surface in the state space, named sliding surface (SS). When the process reaches the SS, the sliding mode control keeps the states on the neighborhood of the SS. The standard design of the sliding mode control has two main steps. The first step is related with the design of a SS so that the sliding motion satisfies design specifications. The second is concerned with the selection of a discontinuous control law that will make the switching surface attractive to the system state in finite time (Kravaris and Savoglidis, 2012; Musmade and Patre, 2015; Zhao et al., 2015). There are two main advantages of sliding mode control. First is that the dynamic behavior of the system may be tailored by the particular choice of the sliding function. Secondly, the closed loop response becomes totally insensitive

* Corresponding author.
E-mail address: raguilar@cinvestav.mx (R. Aguilar-López).

https://doi.org/10.1016/j.mineng.2020.106549
Received 16 January 2020; Received in revised form 5 June 2020; Accepted 6 July 2020
Available online 16 July 2020

to some bounded uncertainties and/or disturbances when the stable SS is reached in a finite time. However, its main disadvantage is the chattering phenomenon due the presence of discontinuous function in the classic sliding-mode control design which originate high frequency oscillations in the input/output dynamics, this is the origin of the named chattering which is a harmful phenomenon because it leads to low control accuracy in the first generation Sliding-mode control (SMC) designs. Further generations of SMC have been considered in order to improve the controller performance by diminish or eliminate the chattering, such as, high-order sliding modes (HOSM), which the same finite time remove the chattering effect and provide for even higher accuracy in realization, fast terminal sliding mode control that eliminates also chatter and solves the system in a finite-time, Quasi-Continuous High-Order Sliding-Mode controller with a universal finite-time-convergence, it is able to control the output of any uncertain single-input-single-output process. (Lara-Cisneros et al., 2017; Nemati et al., 2017; Rivera et al., 2011; Vaidyanathan and Lien, 2017). HOSM includes additional terms to reach a smooth performance, eliminating the chattering problem due to the continuous-time nature of the control action (Levant, 2005). Unfortunately, the main disadvantage of this proposal is that the stability analysis is a complex task, (Moreno and Osorio, 2008). From the above, another generation of SMC named super-twisting sliding mode (STSM) control, looks like an adequate alternative to the conventional first-order SMC for systems of relative degree-1 to avoid chattering without affecting the tracking performance, making it possible to obtain an explicit relationship for the controller design parameters. In this proposal it is considered a class of smooth Super-Twisting Sliding-mode, which include continuous sigmoid functions in the control design, which helps to diminish the corresponding chattering. Also, in the control structure the integral term is able to compensate the main non-linearities of the process (reaction rates), inducing a finite time convergence.

In this document, the kinetic model for zinc leaching previously reported in the literature was used as a reference system to analyze the performance of a reactor in CSTR operation. An analysis of the RGA was performed to determine the best control input pairs and measurable variables. In addition, a bifurcation analysis was carried out with the reactor inputs as parameters to select operating regions. Finally, a smooth super-twisting sliding mode (SSTSM) controller proposed in this work was implemented and its performance was compared with an STSM controller (Fig. 1).

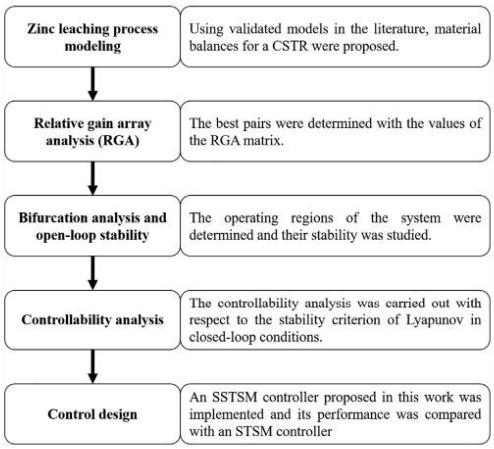

Fig. 1. Methodology flow chart.

2. Zinc leaching process modeling

The leaching of zinc concentrates is based on the oxidation of zinc sulfide in the presence of sulfured iron minerals in an acidic environment. Oxidation by molecular oxygen takes place very slowly and, therefore, the oxidation-reduction cycle of iron plays an important role. In this cycle, ferric iron is reduced with zinc sulfide to ferrous iron, which is oxidized back to the ferric form. It has been reported that for this system of reactions, copper acts as a catalyst, (Haakana et al., 2007; Lampinen et al., 2015; Ozberk et al., 1995; Sadegui et al., 2017a, 2017b). This work considered an experimentally validated kinetic model previously published by Haakana et al. (2007), where the following three main reactions for zinc leaching are considered: the reduction of ferric iron by zinc sulfide (Eq. (1)), the oxidation of ferrous iron by molecular oxygen (Eq. (2)), and the participation of molecular oxygen for direct oxidation (Eq. (3)).

$$ZnS_{(S)} + Fe_2(SO_4)_3 \rightarrow ZnSO_4 + 2FeSO_4 + S^0 \tag{1}$$

$$2FeSO_4 + H_2SO_4 + 0.5O_2 \rightarrow Fe_2(SO_4)_3 + H_2O \tag{2}$$

$$ZnS_{(S)} + H_2SO_4 + 0.5O_2 \rightarrow ZnSO_4 + H_2O + S^0 \tag{3}$$

Eqs. (4)–(6) were tested in various conditions, corresponding to the reactions of the Eqs. (1)–(3).

$$r_1 = k_1 e^{[-(E_{a1}/R)(1/T-1/T_{ref1})]} \left(\frac{C_{ZnS}}{C_{ZnS,0}}\right)^{\alpha_1} C_{H_2SO_4}^{\alpha_2} C_{Fe^{3+}}^{\alpha_3} \tag{4}$$

$$r_2 = k_2 e^{-E_{a2}/RT} (1 + 5C_{CuSO_4}^{0.5}) C_{Fe^{2+}}^2 C_{O_2} C_{H^+}^{-0.35} \tag{5}$$

$$r_3 = k_3 e^{[-(E_{a3}/R)(1/T-1/T_{ref3})]} \left(\frac{C_{ZnS}}{C_{ZnS,0}}\right)^{\alpha_4} C_{O_2}^{\alpha_5} C_{H_2SO_4}^{\alpha_6} \tag{6}$$

The above kinetic model was included in a continuous stirred tank reactor (CSTR) model based on a standard mass balance approach. The considered leaching system in this work consists of a CSTR with three inlet mass flows (Fig. 2). The corresponding process inputs are F_1, which corresponds to the acidified solution flow containing sphalerite minerals as zinc source, F_2 is the sulfuric acid solution flow and Q_{air} is the airflow. The selected process outputs are the dissolved oxygen (DO) and sphalerite (ZnS) concentrations, and the pH measurements. Note that the dissolved oxygen concentration and pH are variables with easy on-line measurements, while the sphalerite (ZnS) concentration is the control objective. The decrease of ZnS concentration implies the leaching of zinc as $ZnSO_4$. Based on the reaction rates (Eqs. (4)–(6)), the mass balances for the ferric ion (Eq. (7)), ferrous ion (Eq. (8)), sphalerite (Eq. (9)), oxygen (Eq. (10)), and sulfuric acid (Eq. (11)) as considered as follows:

$$\frac{dC_{Fe^{3+}}}{dt} = \frac{F_1}{V}(C_{Fe^{3+}{}_{Input1}}) - \frac{F_3}{V}(C_{Fe^{3+}}) - 2r_1 + r_2 \tag{7}$$

$$\frac{dC_{Fe^{2+}}}{dt} = \frac{F_1}{V}(C_{Fe^{2+}{}_{Input1}}) - \frac{F_3}{V}(C_{Fe^{2+}}) + 2r_1 - r_2 \tag{8}$$

$$\frac{dC_{ZnS}}{dt} = \frac{F_1}{V}(C_{ZnS_{Input1}}) - \frac{F_3}{V}(C_{ZnS}) - r_1 - r_3 \tag{9}$$

$$\frac{dC_{O_2}}{dt} = \frac{F_1}{V}(C_{O_2Input1}) + K_L a * \left(C_{0_{2sat}} - C_{O_2}\right) - \frac{F_3}{V}(C_{O_2}) - 0.25r_2 - 0.5r_3 \tag{10}$$

$$\frac{dC_{H_2SO_4}}{dt} = \frac{F_1}{V}(C_{H_2SO_4Input1}) + \frac{F_2}{V}(C_{H_2SO_4Input2}) - \frac{F_3}{V}(C_{H_2SO_4}) - r_2 - r_3 \tag{11}$$

As usual, perfect mixing was assumed in the reactor and a linear representation of the oxygen mass transfer coefficient, was considered as a function of the airflow velocity (Eq. (12), Aguilar-Lopez et al., 2010a).

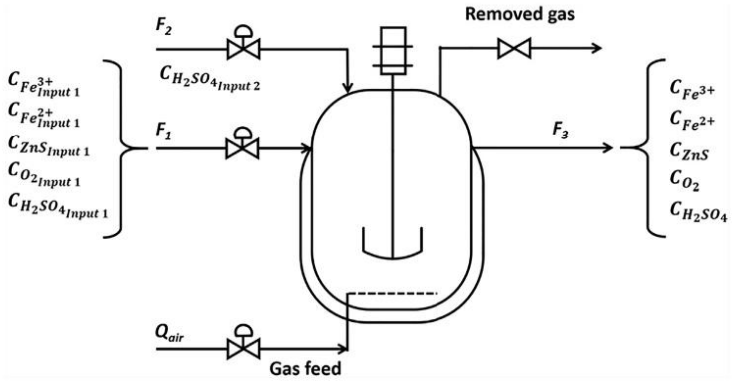

Fig. 2. Open-loop continuous process scheme for zinc leaching.

$$K_L a = K_{O_2} Q_{air} \tag{12}$$

For this work, is proposed $K_{O_2} = 4333.331/m^3$, which is a standard valued for the mass transfer coefficient.

The *pH* calculation, it is assumed that the dissociation of hydrogen protons is complete since sulfuric acid is a strong acid. Eq. (13), is used to calculate the *pH*:

$$pH = -\log(2C_{H_2SO_4(mol/L)}) \tag{13}$$

The kinetic parameters that appear in the reaction system and the operating conditions are shown in Tables 1 and 2, respectively.

3. Control analysis

This section includes a brief theoretical framework to justify the concepts and the corresponding analytical tools employed in the open-loop and closed-loop operation of the leaching process.

3.1. Relative gain array analysis (RGA)

RGA analysis provides a measure of interactions within multiple-input multiple-output (MIMO) systems under selected operation conditions around a steady state point, which is a standard tool from linear control theory. The RGA can be applied in operating regions where the input-output response of the process is step-type and the steady state gain can be determinate for all the selected input-output pairings. It is represented by a matrix with one column for each input variable and one row for each output variable (Muntean et al., 2015). Standard analysis suggests that RGA elements corresponding to input-output pairings close to 1 should be preferred (Goodwin et al., 2005; Muntean et al., 2015). The RGA matrix can be written in terms of the steady-state gain matrix:

$$\Lambda = \bar{K} \otimes [\bar{K}^{-1}]^T \tag{14}$$

where, $\bar{K}$ is a MIMO transfer matrix.

In this application case, the manipulated inputs and the measurable outputs were chosen for their viability, ease of handling, and online measurement. The manipulated control inputs correspond to F_1, Q_{air}, and F_2 flows and the measurable variables correspond to C_{O_2} and *pH*. Although the measurement of C_{ZnS} is not feasible to perform online, then RGA analysis is included to know the effect that Q_{air} and F_2 flows have on the concentration's response. Then, the matrix $\bar{K}$ is written in terms of the corresponding steady-state gains:

$$\bar{K} = \begin{bmatrix} K_{ZnS,F_1} & K_{ZnS,Q_{air}} & K_{ZnS,F_2} \\ K_{O_2,F_1} & K_{O_2,Q_{air}} & K_{O_2,F_2} \\ K_{pH,F_1} & K_{pH,Q_{air}} & K_{pH,F_2} \end{bmatrix} = \begin{bmatrix} \frac{\Delta C_{ZnS}}{\Delta F_1} & \frac{\Delta C_{ZnS}}{\Delta Q_{air}} & \frac{\Delta C_{ZnS}}{\Delta F_2} \\ \frac{\Delta C_{O_2}}{\Delta F_1} & \frac{\Delta C_{O_2}}{\Delta Q_{air}} & \frac{\Delta C_{O_2}}{\Delta F_2} \\ \frac{\Delta pH}{\Delta F_1} & \frac{\Delta pH}{\Delta Q_{air}} & \frac{\Delta pH}{\Delta F_2} \end{bmatrix} \tag{15}$$

The RGA is applied in an adequate operational steady-state point which is selected via the bifurcation analysis (mentioned below), where it is observed the steady-state response of the state variables under variation of bifurcation parameters.

Table 1
Summary of kinetic parameters.

Parameter	Value	Unit
Ea_1*	45,000	J/mol
Ea_2*	68,000	J/mol
Ea_3*	37,200	J/mol
k_1*	0.0141	$l^{(\alpha_9+\alpha_{10}+\alpha_{11})-1} mol^{l-(\alpha_9+\alpha_{10}+\alpha_{11})}/min$
k_2*	$124.8x10^9$	$l^{1.65} mol^{-1.65}/min$
k_3*	0.71	$l^{(\alpha_9+\alpha_{10}+\alpha_{11})-1} mol^{l-(\alpha_9+\alpha_{10}+\alpha_{11})}/min$
K_{air}†	4333.33	$1/m^3$
R	8.314472	J/(mol K)
T_{ref1}†	368.15	K
T_{ref3}†	368.15	K
α_1*	1.33	Dimensionless
α_2*	1.5	Dimensionless
α_3*	1.1	Dimensionless
α_4*	1	Dimensionless
α_5*	1.1	Dimensionless
α_6*	1.5	Dimensionless

* Parameters taken from Haakana et al. (2007).
† Parameters proposed in this work.

Table 2
Summary of operating conditions used in this work.

Condition	Value	Unit
$C_{Fe^{3+}0}$, $C_{Fe^{3+}Input1}$	750.26	mol/m^3
$C_{Fe^{2+}0}$, $C_{Fe^{2+}Input1}$	537.20	mol/m^3
C_{ZnS0}, $C_{ZnSInput1}$	410.5	mol/m^3
C_{O_20}, $C_{O_2Input1}$	0.113	mol/m^3
$C_{O_{2sat}}$	0.113	mol/m^3
$C_{H_2SO_40}$, $C_{H_2SO_4Input1}$	15.8	mol/m^3
$C_{H_2SO_4Input2}$	158.11	mol/m^3
C_{CuSO_4}	15.736	mol/m^3
$C_{ZnS,0}$	410.5	mol/m^3
T	373.15	K

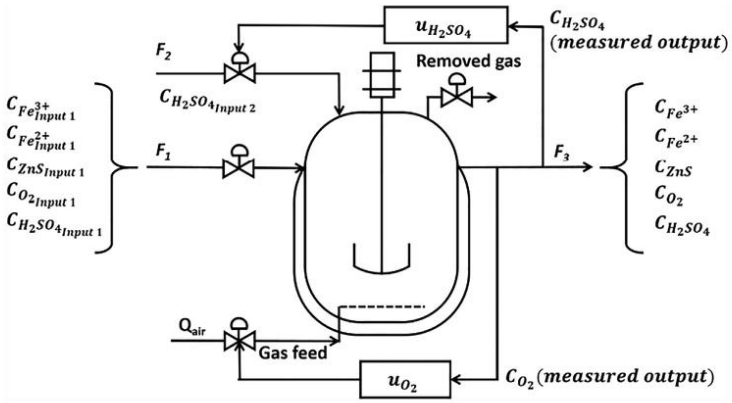

Fig. 3. Closed-loop continuous process scheme for zinc leaching.

3.2. Bifurcation analysis and open-loop stability

Bifurcation theory is an important branch of qualitative differential equation theory. The qualitative changes are analyzed in phase portraits. A particular steady state contained in the phase space corresponds to a possible state for the process. In the case of a differential equation, the solution with initial conditions defines a curve in the phase space that passes through the corresponding steady state. The global representation of these curves for all points in phase space comprises the phase portrait, which provides a global qualitative picture of the dynamic behavior of the process, this picture depends generally of the set of parameters that enter the equations of motion or boundary conditions. If one varies these parameters, the phase portrait may deform slightly without altering its qualitative features. Sometimes the dynamics may be modified significantly, producing a qualitative change in the phase portrait, where the appearance or disappearance of equilibriums, periodic orbits, or more complicated features such as strange attractors can be observed (Crawford, 1991). An important application of bifurcation analysis to process engineering is to find adequate operating conditions, avoiding dangerous (unstable) regions for the process, and determining the qualitative behavior of the process given its mathematical model by varying key operational parameters (Garhyan et al., 2003; Gomez-Acata et al., 2012; Zhang and Henson, 2001).

Generally, the stability analysis of a nonlinear process is performed via a local analysis applied to a linearized version of the nonlinear process model via first order Taylor series approximation and applying an eigenvalues test. The linearized representation of a process contained mainly in the Jacobian matrix of the process, defines three main subspaces in the state space of the process; the stable subspace, which is spanned by the generalized eigenvectors corresponding to the eigenvalues λ with $Real(\lambda) < 0$; the unstable subspace, which is spanned by the generalized eigenvectors corresponding to the eigenvalues with $Real(\lambda) > 0$ and the center subspace, which is spanned by the generalized eigenvectors corresponding to the eigenvalues $\lambda = 0$. Depending on the application, other subspaces of interest include center-stable, center-unstable, sub-center, slow, and fast subspaces (Çelik, 2012).

In particular, the Hartman-Grobman Theorem (Perko, 2001) states that in a neighborhood of a hyperbolic steady-state point (i.e. eigenvalues with $Real(\lambda) \neq 0$), the nonlinear processes are topologically equivalent to the linearized version of the process. The Hartman-Grobman theorem therefore completely solves the problem of determining the stability and qualitative behavior in a neighborhood of a hyperbolic steady-state point. In case of non-hyperbolic critical point, the Hartman-Grobman Theorem is not applicable, and its role is played by the central manifold theorem.

The central manifold theorem indicates that the qualitative behavior in a neighborhood of a non-hyperbolic critical point of the nonlinear process is determined by its behavior on the center manifold. This theorem is a model reduction technique used for determining the local asymptotic stability of an equilibrium point of a dynamical system when its linear part is not hyperbolic. It is considered that the overall system is asymptotically stable if and only if the center manifold dynamics is asymptotically stable. In this sense, this allows a reduction in the dimension of the system. Since the center manifold is generally of smaller dimension than the original process, this simplifies the problem of determining the stability and qualitative behavior of the dynamic flow trajectory near a non-hyperbolic steady-state point (Hassard and Wan, 1978; Luís and Rodrigues, 2017).

Physically, the state variables with zero eigenvalues can be related with a local steady-state behavior, therefore they remain in a constant value, becoming in a parameter of the process model. In consequence the order of the process, i.e., the number of differential equations (state equations) is diminished.

3.3. Controllability analysis

The controllability analysis was carried out with respect to the stability criterion of Lyapunov in closed-loop conditions, in which it is established that uncontrolled states must reach a point of equilibrium to guarantee the complete stability of the zero dynamics, i.e. the uncontrolled state equations. Then, to ensure the stability of the system, the derivative of the uncontrolled states must have a negative sign or zero value (decreasing trend) at the operational adjustment point (Aguilar-López et al., 2010b).

3.4. Control design

From the RGA analysis, it is selected the inflows (F_1, F_2, and Q_{air}) as the manipulated control variables and the variables to be controlled, such as the *pH* and the concentrations of *ZnS* and O_2. In this case, there are no sensors with the ability to measure the *ZnS* concentration online, so for the purposes of implementing the control law, only the *pH* and the O_2 concentration were considered as controlled variables (Fig. 3).

The general representation of vector state equation, which is based on the corresponding mass balances, is defined as follows:

$$\dot{x} = f(x) + g(x)u \tag{16}$$

where,

$$\dot{x} = \begin{bmatrix} \frac{dC_{Fe^{3+}}}{dt} \\ \frac{dC_{Fe^{2+}}}{dt} \\ \frac{dC_{ZnS}}{dt} \\ \frac{dC_{O_2}}{dt} \\ \frac{dC_{H_2SO_4}}{dt} \end{bmatrix} = \begin{bmatrix} \frac{F_1}{V}(C_{Fe^{3+}{}_{Input1}}) - \frac{F_3}{V}(C_{Fe^{3+}}) - 2r_1 + r_2 \\ \frac{F_1}{V}(C_{Fe^{2+}{}_{Input1}}) - \frac{F_3}{V}(C_{Fe^{2+}}) + 2r_1 - r_2 \\ \frac{F_1}{V}(C_{ZnS_{Input1}}) - \frac{F_3}{V}(C_{ZnS}) - r_1 - r_3 \\ \frac{F_1}{V}(C_{O_2{}_{Input1}}) - \frac{F_3}{V}(C_{O_2}) - 0.25r_2 - 0.5r_3 + Q_{air}K_{O_2} \\ (C_{0_{2_{sat}}} - C_{O_2}) \\ \frac{F_1}{V}(C_{H_2SO_4{}_{Input1}}) - \frac{F_3}{V}(C_{H_2SO_4}) - r_2 - r_3 + F_2\frac{(C_{H_2SO_4{}_{Input2}})}{V} \end{bmatrix} \tag{17}$$

In this case:

$$f(x) = \begin{bmatrix} \frac{F_1}{V}(C_{Fe^{3+}{}_{Input1}}) - \frac{F_3}{V}(C_{Fe^{3+}}) - 2r_1 + r_2 \\ \frac{F_1}{V}(C_{Fe^{2+}{}_{Input1}}) - \frac{F_3}{V}(C_{Fe^{2+}}) + 2r_1 - r_2 \\ \frac{F_1}{V}(C_{ZnS_{Input1}}) - \frac{F_3}{V}(C_{ZnS}) - r_1 - r_3 \\ \frac{F_1}{V}(C_{O_2{}_{Input1}}) - \frac{F_3}{V}(C_{O_2}) - 0.25r_2 - 0.5r_3 \\ \frac{F_1}{V}(C_{H_2SO_4{}_{Input1}}) - \frac{F_3}{V}(C_{H_2SO_4}) - r_2 - r_3 \end{bmatrix} \tag{18}$$

$$g(x) = \begin{bmatrix} 0 \\ 0 \\ 0 \\ K_{O_2} * (C_{0_{2_{sat}}} - C_{O_2}) \\ \frac{C_{H_2SO_4{}_{Input2}}}{V} \end{bmatrix} \tag{19}$$

$$u = \begin{bmatrix} 0 \\ 0 \\ 0 \\ u_{O_2} \\ u_{H_2SO_4} \end{bmatrix} = \begin{bmatrix} 0 \\ 0 \\ 0 \\ Q_{air} \\ F_2 \end{bmatrix} \tag{20}$$

Now, let us propose the following feedback control:

$$u = g_1\|e\|^{\frac{1}{m}}\tanh(e) + g_2u_1 = \begin{bmatrix} 0 \\ 0 \\ 0 \\ g_{1_{O_2}}\|e\|^{\frac{1}{m}}\tanh(e_{O_2}) + g_{2_{O_2}}u_{1_{O_2}} \\ g_{1_{H_2SO_4}}\|e\|^{\frac{1}{m}}\tanh(e_{H_2SO_4}) + g_{2_{H_2SO_4}}u_{1_{H_2SO_4}} \end{bmatrix} \tag{21}$$

$$\dot{u}_1 = -\frac{1}{e^2+1} \tag{22}$$

where, e is the regulation error and g_1, g_2, and m are the design parameters of the controller or control's gains.

Then:

$$\dot{u}_1 = \begin{bmatrix} 0 \\ 0 \\ 0 \\ \dot{u}_{1_{O_2}} \\ \dot{u}_{1_{H_2SO_4}} \end{bmatrix} = \begin{bmatrix} 0 \\ 0 \\ 0 \\ -\frac{1}{e_{O_2}^2+1} \\ -\frac{1}{e_{H_2SO_4}^2+1} \end{bmatrix} \tag{23}$$

and

$$e = \begin{bmatrix} 0 \\ 0 \\ 0 \\ e_{O_2} \\ e_{H_2SO_4} \end{bmatrix} = \begin{bmatrix} 0 \\ 0 \\ 0 \\ C_{O_2} - C_{O_2\,ref} \\ C_{H_2SO_4} - C_{H_2SO_4\,ref} \end{bmatrix} \tag{24}$$

A proof for the closed-loop stability of the proposed controller is included in Appendix A.

The performance of the proposed control law (SSTSM) was compared with a standard STSM controller (Eqs. (25) and (26)):

$$\bar{u} = g_1\|e\|^{\frac{1}{m}}\text{sign(e)} + g_2u_1 \tag{25}$$

$$\dot{u}_1 = sign(e) \tag{26}$$

The integral of the Time-weighted Squared Error (ITSE), was used as the comparison criterion for the two control laws. The performance index was calculated with the ITSE as:

$$ITSE = \int_0^\infty te^2(t)dt \tag{27}$$

4. Results and discussion

4.1. Bifurcation steady-state analysis and open-loop stability

For this work the input flows F_1, Q_{air}, and F_2 were chosen as bifurcation parameters. From the bifurcation analysis (see Figs. 4 and 5), the following operational intervals were chosen, $F_1 \in [0, 0.01]$, $Q_{air} \in [0, 0.005]$, and $F_2 \in [0, 0.002]$, which were selected considering that in those regions, the process trajectories behaves asymptotically, and higher values only represent higher operational costs, obtaining similar yields. In each analysis, the rest of the bifurcation parameters remained constant with the values $F_1 = 0.001$ m^3/min, $Q_{air} = 0.0003$ m^3/min, and $F_2 = 0.00005$ m^3/min. The bifurcation analysis was carried out using the software package MATCONT 5.3 that works within the MATLAB® environment and is commonly used for the interactive numerical study of dynamic systems.

Fig. 4 shows the stationary states of each state variable ($C_{Fe^{3+}}$, $C_{Fe^{2+}}$, C_{ZnS}, C_{O_2}, $C_{H_2SO_4}$, pH), applying each bifurcation parameter correspondingly (F_1, Q_{air}, F_2), for the three cases. The figure show that there is no multiplicity of stationary states. For the case of zinc leaching, the analysis with parameter F_1 showed that with values close to zero, higher zinc leaching is achieved (Fig. 4a). In addition, using Q_{air} as a bifurcation parameter, it is possible to increase zinc leaching with $Q_{air} = 0$, 0.00012m3/min, and with $Q_{air} > 0.00012$ m^3/min, a minimum concentration of ZnS is maintained ($C_{ZnS} = 13.84 mol/m^3$) (Fig. 4c). Regarding F_2 as a bifurcation parameter, with $F_2 = [0, 0.0004]$, it is possible to decrease the concentration of ZnS ($C_{ZnS} = 14.22 mol/m^3$) and from $F_2 > 0.0004$ m^3/min, there is no longer a considerable decrease (Fig. 4e). The results agree with what is established in the reactions that describe the zinc leaching process (Coelho et al., 2018; Haakana et al., 2007; Lampinen et al., 2015; Sadegui et al., 2017a, 2017b; Xie et al., 2018), (Eqs. (1)–(3)). For these reactions, there are two cases of direct leaching (Eqs. (1) and (3)) since the presence of oxygen and sulfuric acid favor the production of Fe^{3+} ions (Eq. (2)), which together (Fe^{3+}, O_2 and H_2SO_4) favor zinc leaching (Eqs. (1) and (2)). As shown in Fig. 4c, 4d, 4e, and 4f, leaching benefits from increased air flows (Q_{air}) and sulfuric acid flow (F_2) under certain intervals.

Fig. 5 shows the results of the eigenvalues obtained for the ranges of the chosen bifurcation parameters. In this case, when the state variables depend directly on oxygen to react, the eigenvalues obtained were close to zero ($\forall\, \lambda_{Fe^{2+}}, \lambda(Q_{air})_{O_2}, \lambda(Q_{air})_{H_2SO_4} \rightarrow Q_{air} \cong 0$) (Table 3). The central variety theorem indicates that the existence of null real eigenvalues corresponds to a reduction of the state space, which indicates that the dynamic behavior of the state variable of $C_{Fe^{2+}}$ for the three cases of bifurcation parameters, no longer provides inferences about the

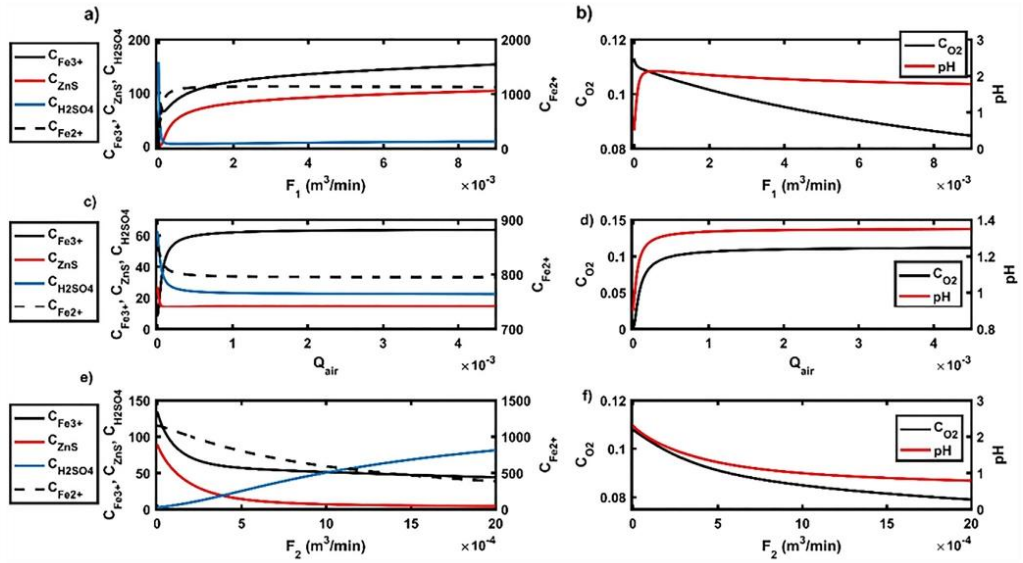

Fig. 4. Bifurcation analysis. a), b) state variables with F_1 as the bifurcation parameter; c), d) state variables with Q_{air} as the bifurcation parameter; and e), f) state variables with F_2 as the bifurcation parameter.

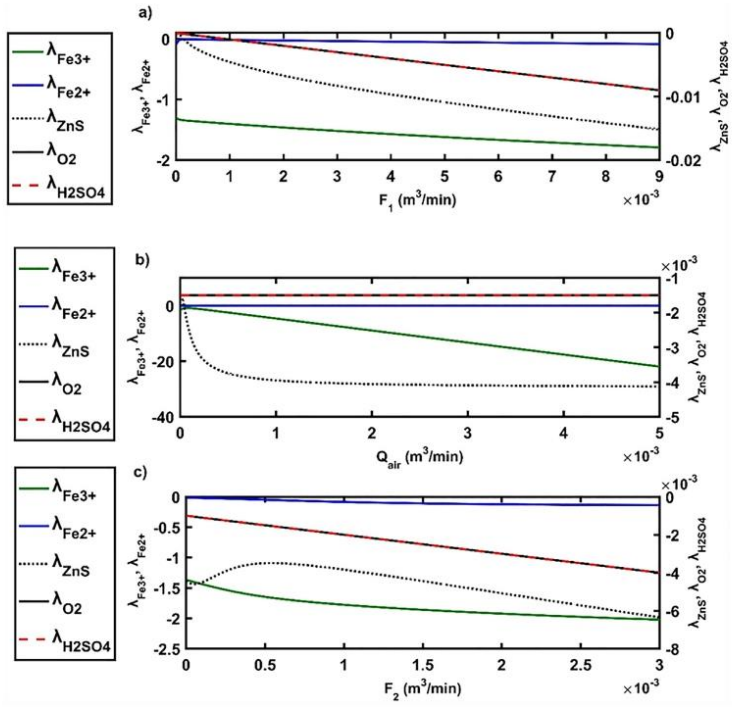

Fig. 5. Eigenvalues. a) F_1 as a bifurcation parameter, b) Q_{air} as a bifurcation parameter, and c) F_2 as a bifurcation parameter, where, λ is the eigenvalue of each state variable.

Table 3
Eigenvalues and dimensions and dimensions of the state space.

State variable	Bifurcation parameter		
	F_1	Q_{air}	F_2
$C_{Fe^{3+}}$	$\lambda < 0, \lambda \in \mathbb{R}$	$\lambda < 0, \lambda \in \mathbb{R}$	$\lambda < 0, \lambda \in \mathbb{R}$
$C_{Fe^{2+}}$	$\lambda \cong 0$	$\lambda \cong 0$	$\lambda \cong 0$
C_{ZnS}	$\lambda < 0, \lambda \in \mathbb{R}$	$\lambda < 0, \lambda \in \mathbb{R}$	$\lambda < 0, \lambda \in \mathbb{R}$
C_{O_2}	$\lambda < 0, \lambda \in \mathbb{R}$	$\lambda \cong 0$	$\lambda < 0, \lambda \in \mathbb{R}$
$C_{H_2SO_4}$	$\lambda < 0, \lambda \in \mathbb{R}$	$\lambda \cong 0$	$\lambda < 0, \lambda \in \mathbb{R}$
State space dimension	4	2	4

dynamics of the rest of the variables. In addition, when Q_{air} is used as a bifurcation parameter, the same situation occurs with the state variables C_{O_2}, $C_{H_2SO_4}$, which indicates the loss of one to three dimensions of the state space when its variables depend directly on C_{O_2}. Eqs. (2) and (3) correspond to oxidation reactions by O_2 of ferrous iron and sphalerite in which Fe^{2+} and H_2SO_4 are consumed. This result can be expected since oxidation by molecular oxygen occurs very slowly, especially since, at these conditions, there are difficulties in dissolving oxygen in the liquid phase (Haakana et al., 2007).

4.2. Relative gain array analysis (RGA)

The RGA is applied in an adequate operational steady-state point which is selected via the bifurcation analysis, where is observed the steady-state response of the state variables under variation of bifurcation parameters. For this particular case, steady state gains were calculated using the following control input values chosen with the aid of bifurcation analysis (Figs. 4 and 5): $F_1 = 0.001m^3/min$, $Q_{air} = 0.0003m^3/min$, and $F_2 = 0.00005m^3/min$, where, the steady-state gain for each control input was around of 15%.

The selected operating steady state point is [1007.8 158.6 102.12 0.135 10.2] for the ferric ion Fe^{2+}, ferrous ion Fe^{3+}, sphalerite, oxygen, and sulfuric acid concentrations, respectively. The numerical result of the RGA matrix (Eq. (15)) is:

$$\Lambda = \begin{bmatrix} 0.69 & 0.03 & 0.27 \\ -0.01 & 1.06 & -0.04 \\ 0.32 & -0.09 & 0.77 \end{bmatrix} \quad (28)$$

With the values of the RGA matrix (Eq. (28)), it was determined that the best pairs (manipulated variable-measurable input) are $C_{ZnS} - F_1$, $C_{O_2} - Q_{air}$, and $pH - F_2$. However, for this case, it was not feasible to use any on-line sensor for measuring the ZnS concentration. The values of the $C_{ZnS} - Q_{air}$ and $C_{ZnS} - F_2$ pairs were 0.03 and 0.27, respectively, which indicates that manipulating the airflow and the flow of acid can maintain the concentration of ZnS. In addition, it is consistent that the value of the $C_{ZnS} - Q_{air}$ pair is lower than $C_{ZnS} - F_2$ because the oxygen transfer from the air flow to the reactor volume is limited by the oxygen saturation concentration in the reactor volume ($C_{O_{2sat}} = 0.113mol/m^3$).

4.3. Controllability analysis

The stability of the zero dynamics was studied using numerical simulations. Fig. 6 shows the time-derivative of uncontrolled variables, i.e., iron ions and zinc concentrations. It can be observed that during the first 5 min, ferrous iron presented a transient dynamic, but finally it converges to an equilibrium point in finite time. All uncontrolled variables tend to stabilize, i.e., $\frac{dC_{Fe^{3+}}}{dt}, \frac{dC_{Fe^{2+}}}{dt}, \frac{dC_{ZnS}}{dt} \to 0$.

4.4. Control performance

With the values of the RGA matrix (Eq. (28)), it was determined that the best pairs (manipulated inputs - measurable variables) are $C_{O_2} - Q_{air}$ and $pH - F_2$.

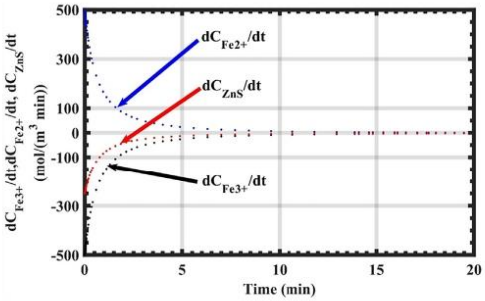

Fig. 6. Zero dynamic performance of the uncontrolled variables.

The proposed control strategy is related with the regulation of dissolved oxygen and sulfuric acid concentrations to the selected set-points. In accordance with the bifurcation analysis, when the two above referenced set-points are reached, the sphalerite concentration tends to diminish, improving the leaching process. The bounds that determine the control gains $\mathscr{F}_{O_2}$ and $\mathscr{F}_{H_2SO_4}$ are defined by the Eqs.(29) and (30):

$$\mathscr{F}_{O_2} \cong -0.25r_2 - 0.5r_3 \quad (29)$$

$$\mathscr{F}_{H_2SO_4} \cong -r_2 - r_3 \quad (30)$$

From this, the gain values (g_{2i}) were estimated numerically according to equation (A11) (see Appendix A): $g_{2_{O_2}} \cong -0.0285\text{mol}/m^3min$ and $g_{2_{H_2SO_4}} \cong -0.0569\text{mol}/m^3min$. Subsequently, considering that one difficult associated to the implementation of HOSM controllers is the lack of constructive tuning procedures of gains (Kada et al., 2017), and taking into account the highly non-linear nature of the proposed controller, the g_i gains were empirically determined by numerical simulation tests. The values of g_{1i} were estimated as: $g_{1_{O_2}} = -2.2x10^6(mol/m^3)^m$ and $g_{1_{H_2SO_4}} = 1.8x10^6(mol/m^3)^m$.

Based on the bifurcation analysis, (Figs. 4 and 5) convenient concentration values were chosen to test the efficiency of the proposed control law, the set points chosen were: $C_{O_2} = 0.091mol/m^3$ and $pH = 1.3$, and the corresponding nominal flows were $F_1 = 0.007m^3/\text{min}$, $Q_{air} = 0.003m^3/min$, and $F_2 = 0.0001m^3/\text{min}$. After 300 min, the controllers were turned-on, using an interval for $Q_{air} = [0, 0.005m^3/\text{min}]$ and $F_2 = [0, 0.002m^3/\text{min}]$. Fig. 7 shows the corresponding effort of the manipulated inputs. For both flows, the proposed control law showed more control effort than that of STSM, so the controller is expected to be more efficient to reach the selected set-points.

Fig. 8a,c shows the closed-loop trajectories of the oxygen concentration and pH, respectively, with the SSTSM controller. In both cases, the controller was able to satisfactorily force the trajectories to the proposed setpoints. In addition, in open loop, the trajectory of the concentration of ZnS reached $102.07mol/m^3$ and in closed loop, $C_{ZnS} = 46.24mol/m^3$ (Fig. 8e). Therefore, in open loop, the maximum Zn leaching was 75.13% and in closed loop, 88.73% was obtained; which indicates that closed loop with the SSTSM controller was able to improve the Zn leaching by 13.6%. In the case of the STSM controller (Fig. 8b, d, f), the control law was not able to force the trajectories of the oxygen concentration and pH to reach the proposed setpoints, so it was not possible to increase the Zn leaching.

To compare the resilience of the simulated controllers, ITSE was considered. The proposed controller (SSTSM) was able to stabilize the system in a short time, while the STSM controller caused this error to increase in an unlimited way. This result is due to the ability of the proposed controller to eliminate the compensation properties, which was not presented by the STSM controller. In accordance with Fig. 9, the proposed controller has a better response that STSM controller with a minimum values of the performance index ITSE.

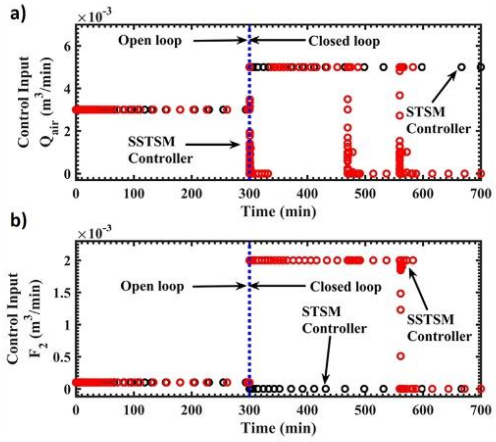

Fig. 7. Comparison of controllers and control inputs. a) Airflow (Q_{air}) and b) Acid solution flow (F_2).

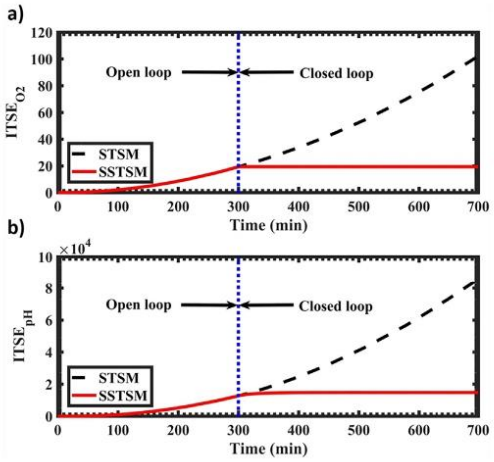

Fig. 9. Comparison of the performance index of the controlled variables with the SSTSM and STSM control laws. a) ITSE referring to O_2 and b) ITSE referring to pH.

5. Conclusions

The RGA analysis determined that the flow of aeration and acid solution are the system inputs that have the greatest effect on the concentration of oxygen and pH, respectively, so it is consistent to use them as pairs of measurable variables and manipulated inputs for the control laws. The bifurcation analysis showed that the system does not present multiplicity of stationary states, and in addition, all the states were determined as stable. From this, adequate operating regions were selected. However, the null eigenvalues showed a reduction of the state space dimension related to the low solubility of oxygen in the liquid phase. The control law proposed in this paper (SSTSM), had the capacity to force the trajectories of the controllable variables to reach the setpoints proposed, in comparison with the STSM control law, which under the same conditions was not able to achieve it. In addition, with the ITSE analysis showed that the SSTSM controller could stabilize the system in a short time compared to the STSM controller. The variables not controlled in finite time also remain stable. Finally, under the conditions proposed in this paper and in closed-loop with the SSTSM control law, it is possible to leach 13.6% more zinc compared to the open-loop system. Consequently, the proposed controller provided better overall system results.

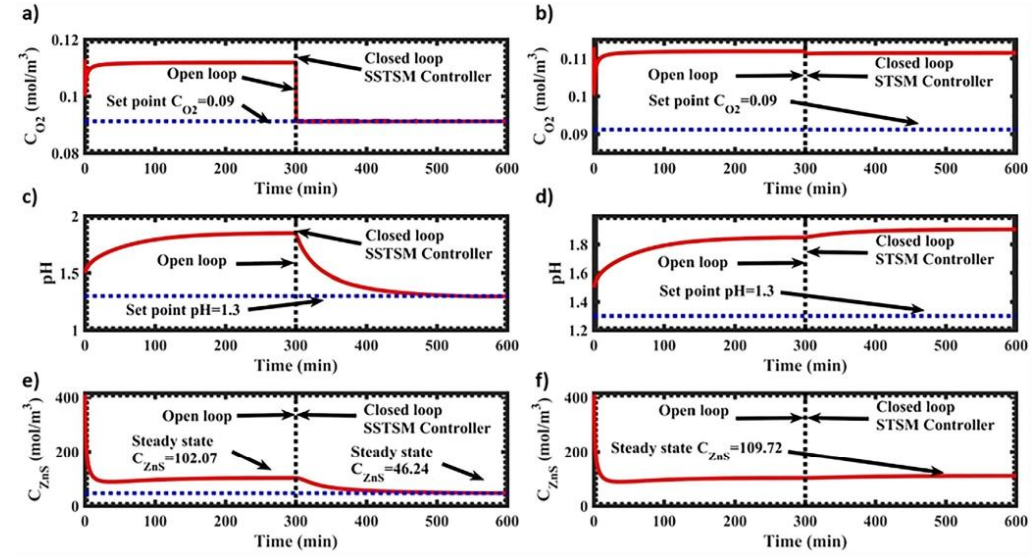

Fig. 8. Closed-loop dynamics of controllable variables and ZnS concentration. a), c) and e) concentration of oxygen, pH and concentration of zinc sulfide, respectively, with the SSTSM control law. b), d) and f) concentration of oxygen, pH and concentration of zinc sulfide, respectively, with the STSM control law.

CRediT authorship contribution statement

J.C. Figueroa-Estrada: Software, Writing - original draft. **M.I. Neria-González:** Writing - review & editing. **R. Rodríguez Vázquez:** Resources, Writing - review & editing. **E.N. Tec-Caamal:** Methodology, Investigation. **R. Aguilar-López:** Conceptualization, Project administration.

Declaration of Competing Interest

The authors declare that they have no known competing financial interests or personal relationships that could have appeared to influence the work reported in this paper.

Acknowledgments

Juan Carlos Figueroa-Estrada thanks CONACyT for support via a graduate scholarship (No. 230859, CONACYT). The financial support of CINVESTAV-IPN and TecNM (No. 502.17-PD) is recognized.

Appendix A

Controller design

Let us consider the following state-space representation of a nonlinear system class with affine control input:

$$\dot{x} = f(x) + g(x)u \tag{A.1}$$

and linear measured output:

$$y = Cx \tag{A.2}$$

where $x \in \mathbb{R}^n$ is the state variable vector, $f(x)$: $\mathbb{R}^n \to \mathbb{R}^n$ is a nonlinear vector function, $f(x) \subset \Sigma \in C^\infty$, Σ is a compact set, $g(x)$ is a smooth and invertible bounded function, $u \in \mathbb{R}^p$ is the exogenous control input vector, and $y \in \mathbb{R}^q$ is the measured output vector.

Now, let us propose the following feedback control:

$$u = g_1 \|e\|^{\frac{1}{m}} \tanh(e) + g_2 u_1 \tag{A.3}$$

$$\dot{u}_1 = -\frac{1}{e^2 + 1} \tag{A.4}$$

where $e = x - x_{ref}$, x_{ref} is the reference signal, and g_1 and g_2 are the design parameters of the controller.

To analyze the closed-loop performance of the system (Eq. (A.1)) under feedback (Eqs. (A.3) and (A.4)), let us construct the dynamic equations of the control error for the regulation case, *i. e.* x_{ref} is constant, as:

$$\dot{e} = f(x) + g(x)\left(g_1 \|e\|^{\frac{1}{m}} \tanh(e) - g_2 \int_0^t \frac{1}{e(\sigma)^2 + 1} d\sigma\right) \tag{A.5}$$

considering the following assumptions:

$$\|f(x)\| \leq \mathscr{F} < \infty \ \forall \ x \in \mathbb{R}^n \tag{A.6}$$

$$\|g(x)\| \leq \mathscr{G} < \infty \ \forall \ x \in \mathbb{R}^n \tag{A.7}$$

and the following properties:

$$\|\tanh(e)\| \leq 1 \tag{A.8}$$

$$\| \int_0^t \frac{1}{e(\sigma)^2 + 1} d\sigma \| \leq 1 (\text{Property of the } arctan \text{ function. }) \tag{A.9}$$

By including the assumptions (Eqs. (A.6) and (A.7)) and properties (Eqs. (A.8) and (A.9)) in Eq. (A.5) and applying the Cauchy-Schwarz inequality, inequality (Eq. (A.10)) is obtained as follows:

$$\|\dot{e}\| \leq \mathscr{F} - g_2 + g_1 \mathscr{G} \|e\|^{\frac{1}{m}} \tag{A.10}$$

Now, considering that the parameter g_2 is selected as:

$$g_2 \cong \mathscr{F} \tag{A.11}$$

Then:

$$\|\dot{e}\| \leq g_1 \mathscr{G} \|e\|^{-\frac{1}{m}} \tag{A.12}$$

The above inequality induces a finite time convergence of the regulation error, where parameter $m > 1$ is considered an odd integer. Then the solution of inequality (Eq. (A.12)) is,

$$\|e\| \leq sign(e_0)\left(\|e_0\| - \mathscr{G} g_1 \frac{t}{m}\right)^m \tag{A.13}$$

At steady state ($e(t) = 0$),

$$t \geq m \frac{\|e_0\|^{\frac{1}{m}}}{\mathscr{G} g_1} \tag{A.14}$$

Then, finite-time convergence is given by,

$$t_{ft} = m\frac{\|e_0\|^{\frac{1}{m}}}{\wp g_1} \tag{A.15}$$

For the tracking trajectory case, including the assumption $\|f(x) - f(x_{ref})\| \leq \mathscr{F}_r < \infty$, the convergence characteristics of the proposed methodology are similar to the regulation case.

References

Aguilar-Lopez, R., López-Pérez, P.A., Neria-González, M.I., Domínguez-Bocanegra, A.R., 2010a. Observer based adaptive model for a class of aerobic batch bioreactor. Rev. Mex. Ing. Quim. 1, 29–35.

Aguilar-López, R., Martínez-Guerra, R., Puebla, H., Hernández-Suárez, R., 2010b. High order sliding-mode dynamic control for chaotic intracellular calcium oscillations. Nonlinear Anal. Real World Appl. 11, 217–231. https://doi.org/10.1016/j.nonrwa.2008.10.054.

Ali Reza, Z., Mehdi, R., 2017. Fuzzy optimization approach for the synthesis of polyesters and their nanocomposites in in-situ polycondensation reactors. Ind. Eng. Chem. Res. 56, 11245–11256. https://doi.org/10.1021/acs.iecr.7b02307.

Çelik, C., 2012. In: Numerical Simulation - From Theory to Industry. InTech. https://doi.org/10.5772/50075.

Coelho, F.E.B., Balarini, J.C., Araújo, E.M.R., Miranda, T.L.S., Peres, A.E.C., Martins, A.H., Salum, A., 2018. Roasted zinc concentrate leaching: population balance modeling and validation. Hydrometallurgy 175, 208–217. https://doi.org/10.1016/j.hydromet.2017.11.013.

Crawford, J.D., 1991. Introduction to bifurcation theory. Rev. Mod. Phys. 63, 991–1037. https://doi.org/10.1103/RevModPhys.63.991.

Flores-Hernández, A.A., Reyes-Reyes, J., Astorga-Zaragoza, C.M., Osorio-Gordillo, G.L., García-Beltrán, C.D., 2018. Temperature control of an alcoholic fermentation process through the Takagi-Sugeno modeling. Chem. Eng. Res. Des. 140, 320–330. https://doi.org/10.1016/j.cherd.2018.10.021.

Garhyan, P., Elnashaie, S.S.E.H., Al-Haddad, S.M., Ibrahim, G., Elshishini, S.S., 2003. Exploration and exploitation of bifurcation/chaotic behavior of a continuous fermentor for the production of ethanol. Chem. Eng. Sci. 58, 1479–1496. https://doi.org/10.1016/S0009-2509(02)00681-4.

Gomez-Acata, R.V., Lopez-Perez, P.A., Maya-Yescas, R., Aguilar-Lopez, R., 2012. Bifurcation analysis of continuous aerobic nonisothermal bioreactor for wastewater treatment. IFAC Proc. 45, 24–29. https://doi.org/10.3182/20120620-3-MX-3012.00054.

Goodwin, G.C., Salgado, M.E., Silva, E.I., 2005. Time-domain performance limitations arising from decentralized architectures and their relationship to the RGA. Int. J. Control 78, 1045–1062. https://doi.org/10.1080/00207170500226016.

Haakana, T., Lahtinen, M., Takala, H., Ruonala, M., Turunen, I., 2007. Development and modelling of a novel reactor for direct leaching of zinc sulphide concentrates. Chem. Eng. Sci. 62, 5648–5654. https://doi.org/10.1016/j.ces.2006.12.075.

Hassard, B., Wan, Y.H., 1978. Bifurcation formulae derived from center manifold theory. J. Math. Anal Appl. 63, 297–312. https://doi.org/10.1016/0022-247X(78)90120-8.

Jain, A., Babu, B.V., 2015. Relative response array: a new tool for control configuration selection. Int. J. Chem. Eng. Appl. 6, 356–362. https://doi.org/10.7763/IJCEA.2015.V6.509.

Kada, B., Juhany, K.A.T., Balamesh, A.S.A., 2017. Hybrid high-order sliding mode-based control for multivariable cross-coupling systems: Scale-laboratory helicopter system application. Aeronaut. J. 121, 1319–1341. https://doi.org/10.1017/aer.2017.57.

Kravaris, C., Savoglidis, G., 2012. Tracking the singular arc of a continuous bioreactor using sliding mode control. J. Franklin Inst. 349, 1583–1601. https://doi.org/10.1016/j.jfranklin.2011.06.011.

Lampinen, M., Laari, A., Turunen, I., 2015. Kinetic model for direct leaching of zinc sulfide concentrates at high slurry and solute concentration. Hydrometallurgy 153, 160–169. https://doi.org/10.1016/j.hydromet.2015.02.012.

Lara-Cisneros, G., Femat, R., Dochain, D., 2017. Robust sliding mode-based extremum-seeking controller for reaction systems via uncertainty estimation approach. Int. J. Robust Nonlinear Control 27, 3218–3235. https://doi.org/10.1002/rnc.3736.

Levant, A., 2005. Homogeneity approach to high-order sliding mode design. Automatica. 41, 823–830. https://doi.org/10.1016/j.automatica.2004.11.029.

Liu, W., Granata, G., 2018. Temperature control in copper heap bioleaching. Hydrometallurgy 176, 26–32. https://doi.org/10.1016/j.hydromet.2018.01.001.

Luís, R., Rodrigues, E., 2017. Local stability in 3D discrete dynamical systems: application to a ricker competition model. Discrete Dyn. Nat. Soc. 6186354. https://doi.org/10.1155/2017/6186354.

Moreno, J.A., Osorio, M., 2008. A Lyapunov approach to second-order sliding mode controllers and observers. In: 2008 47th IEEE Conference on Decision and Control. IEEE, pp. 2856–2861. https://doi.org/10.1109/CDC.2008.4739356.

Muntean, I., Both, R., Crisan, R., Nascu, I., 2015. RGA analysis and decentralized control for a wastewater treatment plant. In: 2015 IEEE International Conference on Industrial Technology (ICIT). IEEE, pp. 453–458. https://doi.org/10.1109/ICIT.2015.7125140.

Musmade, B., Patre, B., 2015. Sliding mode control design for robust regulation of time-delay processes. Trans. Inst. Meas. Control 37, 699–707. https://doi.org/10.1177/0142331214536201.

Nemati, H., Bando, M., Hokamoto, S., 2017. Chattering attenuation sliding mode approach for nonlinear systems. Asian J. Control 19, 1519–1531. https://doi.org/10.1002/asjc.1477.

Ozberk, E., Jankola, W.A., Vecchiarelli, M., Krysa, B.D., 1995. Commercial operations of the Sherritt zinc pressure leach process. Hydrometallurgy 39, 49–52. https://doi.org/10.1016/0304-386X(95)00047-K.

Perko, L., 2001. Differential equations and dynamical systems, third ed. Springer-Verlag, New York.

Rivera, J., Garcia, L., Mora, C., J., J., Orteg, S., 2011. In: Sliding Mode Control. InTech. https://doi.org/10.5772/14532.

Sadegui, N., Moghaddam, J., Ojaghi Iilkhchi, M., 2017a. Kinetics of zinc sulfide concentrate direct leaching in pilot plant scale and development of semi-empirical model. Trans. Nonferrous Met. Soc. China 27, 2272–2281. https://doi.org/10.1016/S1003-6326(17)60253-X.

Sadegui, N., Moghaddam, J., Ojaghi Ilkhchi, M., 2017b. Determination of effective parameters in pilot plant scale direct leaching of a zinc sulfide concentrate. Physicochem. Probl. Miner. Process. 53, 601–616. https://doi.org/10.5277/ppmp170147.

Vaidyanathan, S., Lien, C.-H. (Eds.), 2017. Applications of Sliding Mode Control in Science and Engineering, Studies in Computational Intelligence. Springer International Publishing, Cham. https://doi.org/10.1007/978-3-319-55598-0.

Valverde-Pérez, B., Mauricio-Iglesias, M., Sin, G., 2016. Systematic design of an optimal control system for the SHARON-Anammox process. J. Process Control 39, 1–10. https://doi.org/10.1016/j.jprocont.2015.12.009.

Velázquez-Sánchez, H.I., Aguilar-López, R., 2018. Novel kinetic model for the simulation analysis of the butanol productivity of Clostridium acetobutylicum ATCC 824 under different reactor configurations. Chinese J. Chem. Eng. 26, 812–821. https://doi.org/10.1016/j.cjche.2017.07.018.

Velázquez-Sánchez, H.I., Domínguez-Bocanegra, A.R., Aguilar-López, R., 2019. Modelling of the pH dynamic and its effect over the Isopropanol-Butanol-Ethanol fermentation by Clostridium acetobutylicum pIPA3-Cm2. Fuel 235, 558–566. https://doi.org/10.1016/j.fuel.2018.08.034.

Xie, S., Xie, Y., Yang, C., Gui, W., Wang, Y., 2018. Distributed parameter modeling and optimal control of the oxidation rate in the iron removal process. J. Process Control 61, 47–57. https://doi.org/10.1016/j.jprocont.2017.11.009.

Yin, X., Liu, J., 2017. Input-output pairing accounting for both structure and strength in coupling. AIChE J. 63, 1226–1235. https://doi.org/10.1002/aic.15511.

Zhang, Y., Henson, M.A., 2001. Bifurcation analysis of continuous biochemical reactor models. Biotechnol. Prog. 17, 647–660. https://doi.org/10.1021/bp010048w.

Zhao, D., Zhu, Q., Dubbeldam, J., 2015. Terminal sliding mode control for continuous stirred tank reactor. Chem. Eng. Res. Des. 94, 266–274. https://doi.org/10.1016/j.cherd.2014.08.005.

Zhou, M., Cai, Y., Su, H., Wozny, G., Pan, H., 2018. A survey on applications of optimization-based integrating process design and control for chemical processes. Chem. Eng. Commun. 205, 1365–1383. https://doi.org/10.1080/00986445.2018.1451991.

7. CONCLUSIONES.

El metabolismo quimiolitotrófico no está claro en el género Brevibacillus. Sin embargo, la cepa LR-1 crece en condiciones quimiolitoautotróficas a bajo pH, utilizando Fe^{2+} y $S_2O_3^{2-}$ como donadores de electrones. La capacidad oxidativa del hierro por la cepa LR-1 acelera la lixiviación de los minerales de sulfuro por la regeneración y el poder oxidativo del Fe^{3+}. Así, los iones Fe^{3+} oxidan los compuestos de azufre y Fe^{2+} del mineral y provocan la liberación de metales. La oxidación del Fe^{2+} por la cepa LR-1 aumentó el porcentaje de liberación de Ag (18,66% a 29,85%), Cu (60,90% a 73,66%) y Cr (11,71% a 15,04%) del mineral de Remedios. Por lo tanto, la cepa LR-1 podría contribuir al proceso de biolixiviación indirecta de los metales de los minerales sulfurados y del hierro. Este es el primer reporte de una bacteria acidófila oxidante de hierro del género Brevibacillus en la biolixiviación de metales. Por lo tanto, estos datos contribuyen al conocimiento de la microbiología hidrometalúrgica.

En el caso del estudio mediante simulaciones numéricas, el análisis RGA determinó que el flujo de aireación y la solución ácida son las entradas del sistema que tienen mayor efecto sobre la concentración de oxígeno y el pH, respectivamente, por lo que es coherente utilizarlas como pares de variables medibles y entradas manipuladas para las leyes de control. El análisis de bifurcación mostró que el sistema no presenta multiplicidad de estados estacionarios, y además se determinaron todos los estados como estables. A partir de ello, se seleccionaron las regiones de funcionamiento adecuadas. Sin embargo, los valores propios nulos mostraron una reducción de la

dimensión del espacio de estados relacionada con la baja solubilidad del oxígeno en la fase líquida.

Las leyes de control propuestas en este trabajo tuvieron la capacidad de forzar las trayectorias de las variables controlables para alcanzar los puntos de consigna propuestos, en comparación con las versiones clásicas de las leyes de control STSM, que en las mismas condiciones no fue capaz de lograrlo. Además, con el análisis ITSE se demostró que el controlador SSTSM podía estabilizar el sistema en un tiempo corto en comparación con el controlador STSM. Las variables no controladas en tiempo finito también permanecen estables. Finalmente, bajo las condiciones propuestas en este trabajo y en lazo cerrado con la ley de control SSTSM, es posible lixiviar un 13,6% más de zinc en comparación con el sistema en lazo abierto. En consecuencia, el controlador propuesto proporcionó mejores resultados globales del sistema.

8. RECOMENDACIONES

- Propuesta de los modelos cinéticos y estimación de los parámetros cinéticos de la experimentación correspondiente a la biolixiviación de metales.
- Validar los modelos cinéticos bajo diferentes condiciones.
- Estudiar la estabilidad del sistema de biolixiviación en operación en continuo
- Validar las leyes de control propuestas en este trabajo para este sistema de biolixiviación.

9. CONTRIBUCIONES Y PARTICIPACIONES INDIRECTAS DEL PROYECTO

Capítulos de libros:

Fernando Grijalva-Hernández, Hugo Iván Velázquez-Sánchez, Juan Carlos Figueroa-Estrada, and Ricardo Aguilar-López, (2017). Biohydrogen Production by Sulphate-Reducing Bacteria: *The Importance of Mathematical Analysis Based on System Modelling* (pp. 69-98).

Hugo Iván Velázquez-Sánchez, Juan Carlos Figueroa-Estrada, Pablo Antonio López-Pérez, Ricardo Aguilar-López. (2017). Uncertainty observer based I/O linearizing control for the regulation of a continuous wastewater bioreactor for Cd removal, *Condition Monitoring and Dynamic Control Systems*. Hauppauge: Nova Science Publishers, Inc. (pp 39-69)

Congresos internacionales:

J. C. Figueroa-Estrada, H. I. Velázquez-Sánchez, H. F. Puebla-Nuñez and R. Aguilar-López, (2017). Increasing the biodiesel concentration in an heterotrophic culture via a super-twisting controller, Congreso Internacional de Energía 2017 (CIE 2017)/International Energy Conference 2017 (IEC 2017)

Jesús Soto-Bartolo, Juan Carlos Figueroa Estrada, Ricardo Aguilar López, (2017). Unstructural kinetic modeling for butanol and ethanol batch fermentation from by clostridium acetobutylicum atcc 824 using modificated posgate c medium, Congreso Internacional de Energía 2017 (CIE 2017)/International Energy Conference 2017 (IEC 2017).

10. REFERENCIAS

Anjum, F., Shahid, M., & Akcil, A. (2012). Biohydrometallurgy techniques of low grade ores: A review on black shale. *Hydrometallurgy*, *117-118*, 1-12. https://doi.org/10.1016/j.hydromet.2012.01.007

Beolchini, F., Fonti, V., Ferella, F., & Vegliò, F. (2010). Metal recovery from spent refinery catalysts by means of biotechnological strategies. *Journal Of Hazardous Materials*, *178*(1-3), 529-534. https://doi.org/10.1016/j.jhazmat.2010.01.114

Bergh, L., Jämsä-Jounela, S., & Hodouin, D. (2001). State of the art in copper hydrometallurgic processes control. *Control Engineering Practice*, *9*(9), 1007-1012. https://doi.org/10.1016/s0967-0661(01)00093-4

Biagiola, S., Solsona, J., & Milocco, R. (2000). Estimation of kinetic rates in batch Thiobacillus ferrooxidans cultures. *Journal Of Biotechnology*, *84*(1), 13-25. https://doi.org/10.1016/s0168-1656(00)00337-0

Bosecker, K. (1997). Bioleaching: metal solubilization by microorganisms. *FEMS Microbiology Reviews*, *20*(3-4), 591-604. https://doi.org/10.1111/j.1574-6976.1997.tb00340.x

Brierley, C., & Brierley, J. (2013). Progress in bioleaching: part B: applications of microbial processes by the minerals industries. *Applied Microbiology And Biotechnology*, *97*(17), 7543-7552. https://doi.org/10.1007/s00253-013-5095-3

Edwards, K., Bond, P., Gihring, T., & Banfield, J. (2000). An Archaeal Iron-Oxidizing Extreme Acidophile Important in Acid Mine Drainage. *Science*, *287*(5459), 1796-1799. https://doi.org/10.1126/science.287.5459.1796

Gentina, J., & Acevedo, F. (2016). Copper Bioleaching in Chile. *Minerals*, *6*(1), 23. https://doi.org/10.3390/min6010023

Gilligan, R., & Nikoloski, A. (2015). The extraction of uranium from brannerite – A literature review. *Minerals Engineering*, *71*, 34-48. https://doi.org/10.1016/j.mineng.2014.10.007

Golyshina, O., & Timmis, K. (2005). Ferroplasma and relatives, recently discovered cell wall-lacking archaea making a living in extremely acid, heavy metal-rich environments. *Environmental Microbiology*, *7*(9), 1277-1288. https://doi.org/10.1111/j.1462-2920.2005.00861.x

Golyshina, O., Pivovarova, T., Karavaiko, G., Kondratéva, T., Moore, E., & Abraham, W. et al. (2000). Ferroplasma acidiphilum gen. nov., sp. nov., an acidophilic, autotrophic, ferrous-iron-oxidizing, cell-wall-lacking, mesophilic member of the Ferroplasmaceae fam. nov., comprising a distinct lineage of the Archaea. *International Journal Of Systematic And Evolutionary Microbiology*, *50*(3), 997-1006. https://doi.org/10.1099/00207713-50-3-997

Gumulya, Y., Boxall, N., Khaleque, H., Santala, V., Carlson, R., & Kaksonen, A. (2018). In a quest for engineering acidophiles for biomining applications: challenges and opportunities. *Genes*, *9*(2), 116. https://doi.org/10.3390/genes9020116

Haakana, T., Lahtinen, M., Takala, H., Ruonala, M., & Turunen, I. (2007). Development and modelling of a novel reactor for direct leaching of zinc sulphide concentrates. *Chemical Engineering Science*, *62*(18-20), 5648-5654. https://doi.org/10.1016/j.ces.2006.12.075

Hidalgo R., Y. (2014). *Aislamiento e Identificación Molecular de Bacterias Quimiolitótrofas Asociadas a la Movilización de Metales*. Maestría. Tecnológico de Estudios Superiores de Ecatepec.

Jalali, F., Fakhari, J., & Zolfaghari, A. (2019). Response surface modeling for lab-scale column bioleaching of low-grade uranium ore using a new isolated strain of Acidithiobacillus Ferridurans. *Hydrometallurgy*, *185*, 194-203. https://doi.org/10.1016/j.hydromet.2019.02.014

Jia, Y., Tan, Q., Sun, H., Zhang, Y., Gao, H., & Ruan, R. (2019). Sulfide mineral dissolution microbes: Community structure and function in industrial bioleaching heaps. *Green Energy &Amp; Environment*, *4*(1), 29-37. https://doi.org/10.1016/j.gee.2018.04.001

JOHNSON, D. (2008). Biodiversity and interactions of acidophiles: Key to understanding and optimizing microbial processing of ores and concentrates. *Transactions Of Nonferrous Metals Society Of China*, *18*(6), 1367-1373. https://doi.org/10.1016/s1003-6326(09)60010-8

Komulainen, T., Doyle III, F., Rantala, A., & Jämsä-Jounela, S. (2009). Control of an industrial copper solvent extraction process. *Journal Of Process Control*, *19*(1), 2-15. https://doi.org/10.1016/j.jprocont.2008.04.019

Komulainen, T., Doyle III, F., Rantala, A., & Jämsä-Jounela, S. (2009). Control of an industrial copper solvent extraction process. *Journal Of Process Control*, *19*(1), 2-15. https://doi.org/10.1016/j.jprocont.2008.04.019

Kutschke, S., Guézennec, A., Hedrich, S., Schippers, A., Borg, G., & Kamradt, A. et al. (2015). Bioleaching of Kupferschiefer blackshale – A review including perspectives of the Ecometals project. *Minerals Engineering*, *75*, 116-125. https://doi.org/10.1016/j.mineng.2014.09.015

Kutschke, S., Guézennec, A., Hedrich, S., Schippers, A., Borg, G., & Kamradt, A. et al. (2015). Bioleaching of Kupferschiefer blackshale – A review including perspectives of the Ecometals project. *Minerals Engineering*, *75*, 116-125. https://doi.org/10.1016/j.mineng.2014.09.015

Li, Y., Kawashima, N., Li, J., Chandra, A., & Gerson, A. (2013). A review of the structure, and fundamental mechanisms and kinetics of the leaching of chalcopyrite. *Advances In Colloid And Interface Science*, *197-198*, 1-32. https://doi.org/10.1016/j.cis.2013.03.004

Mahmoud, A., Cézac, P., Hoadley, A., Contamine, F., & D'Hugues, P. (2017). A review of sulfide minerals microbially assisted leaching in stirred tank reactors. *International Biodeterioration &Amp; Biodegradation*, *119*, 118-146. https://doi.org/10.1016/j.ibiod.2016.09.015

Meruane, G., Salhe, C., Wiertz, J., & Vargas, T. (2002). Novel electrochemical-enzymatic model which quantifies the effect of the solution Eh on the kinetics of

ferrous iron oxidation withAcidithiobacillus ferrooxidans. *Biotechnology And Bioengineering*, *80*(3), 280-288. https://doi.org/10.1002/bit.10371

Ojumu, T., Petersen, J., Searby, G. and Hansford, G. (2006). A review of rate equations proposed for microbial ferrous-iron oxidation with a view to application to heap bioleaching. *Hydrometallurgy*, 83(1-4), pp.21-28.

Sand, W., Gehrke, T., Jozsa, P., & Schippers, A. (2001). (Bio)chemistry of bacterial leaching—direct vs. indirect bioleaching. *Hydrometallurgy*, *59*(2-3), 159-175. https://doi.org/10.1016/s0304-386x(00)00180-8

Santini, J., Sly, L., Schnagl, R. and Macy, J. (2000). A New Chemolithoautotrophic Arsenite-Oxidizing Bacterium Isolated from a Gold Mine: Phylogenetic, Physiological, and Preliminary Biochemical Studies. *Applied and Environmental Microbiology*, 66(1), pp.92-97.

Schippers A., Hedrich S., Vasters J., Drobe M., Sand W., Willscher S. (2013) Biomining: Metal Recovery from Ores with Microorganisms. In: Schippers A., Glombitza F., Sand W. (eds) Geobiotechnology I. Advances in *Biochemical Engineering/Biotechnology*, vol 141. Springer, Berlin, Heidelberg

Watling, H. (2006). The bioleaching of sulphide minerals with emphasis on copper sulphides — A review. *Hydrometallurgy*, *84*(1-2), 81-108. https://doi.org/10.1016/j.hydromet.2006.05.001

Wu, M., She, J., Nakano, M., & Gui, W. (2002). Expert control and fault diagnosis of the leaching process in a zinc hydrometallurgy plant. *Control Engineering Practice*, *10*(4), 433-442. https://doi.org/10.1016/s0967-0661(01)00122-8

Xie, S., Xie, Y., Yang, C., Gui, W., & Wang, Y. (2018). Distributed parameter modeling and optimal control of the oxidation rate in the iron removal process. *Journal Of Process Control*, *61*, 47-57. https://doi.org/10.1016/j.jprocont.2017.11.009

Xie, Y., Xie, S., Li, Y., Yang, C., & Gui, W. (2017). Dynamic modeling and optimal control of goethite process based on the rate-controlling step. *Control Engineering Practice*, *58*, 54-65. https://doi.org/10.1016/j.conengprac.2016.10.001